PPARγ: New insights into its role in urothelial differentiation and regeneration

Zhen Liu (Edgar)

Doctor of Philosophy

University of York

Biology

September 2021

Abstract

Urothelium functions as a urinary barrier against toxic materials in the urine. In urothelium, the cells are mitotically-quiescent, but remain able to proliferate in response to damage, or when cultured *in vitro*. The nuclear receptor, peroxisome proliferator activated receptor gamma (PPARγ), is implicated in urothelial differentiation and cancer, but underlying mechanism remains unclear.

Firstly, the analysis of the human urothelial transcriptome revealed that *PPARG*1 encoding protein isoform 1 is expressed by urothelial cells and regulates the differentiation process. Subcellular extraction results verified that PPARγ acts as a nuclear DNA-bound nuclear receptor during early stages after initiation of differentiation, but shows an alternative non-chromatin bound role in differentiated NHU cells. The research then investigated the role for PPARγ in differentiated urothelial cells and found inhibition of PPARγ negatively regulates the regeneration process by attenuating the nuclear localization of pSMAD3.

In conclusion, PPARγ protein isoform 1 was identified to act as nuclear receptor to regulate NHU cell differentiation but obtains an alternative non-chromatin-bound role for NHU cell regeneration. The switch of its compartmentalization in the nucleus might helps to maintain the balance of proliferation and differentiation in NHU cells.

Table of contents

List of Figures

List of Tables

Acknowledge

I would like to thank all of the following people for their help and contributions in helping achieve this PhD research.

First, I would like to thank my supervisor, Professor Jennifer Southgate for not only giving me the opportunity to achieve this exciting project but also provide her patient, intelligence, encouragement, and enthusiastic conversations that helps me to finish my research. I would also like to thank my co-supervisor Professor Dawn Coverley for her warmly words and continuously assistance on my writing and experimental techniques.

Thanks also goes to the members of my training advisory panel, Dr. Paul Genever and Dr. Robert White, for their ideas and stimulating conversations in my training meetings.

I would also like to thank the lovely friends and fantastic colleagues in the Jack Birch Unit who gives me support on my studies. Especially thanks for Ros Duke who kindly invite me to celebrate Christmas with

her family. Also, special thanks for Simon and Andrew for their supports on my project.

Most of all, I would like to thank my parents for their unconditional love and support throughout my studies.

Author's Declaration

I declare that this thesis is a presentation of original work and I am the sole author. This work has not previously been presented for an award at this, or any other, University. All sources are acknowledged as References.

Zhen Liu (Edgar)

Nov. 2021

Chapter 1: Introduction

1. Introduction

1.1 Peroxisome proliferator-activated receptor

Peroxisome proliferator-activated receptor (PPAR) was first discovered in rodents as a regulator of peroxisome proliferation (Dreyer et al., 1992). This protein was found to be capable to binds to peroxisome proliferators structurally(Lalwani ND et al., 1987). It is a member of the steroid hormone receptor superfamily and is activated by a variety of non-genotoxic rodent hepatocarcinogens termed peroxisome proliferators (Issemann et al., 1993). Because the expression of its mRNA shows a similar pattern to the tissue-specific effects of perocisome proliferators and it was suggested to mediate the peroxisome proliferative response, this protein was then named peroxisome proliferator-activated receptor (PPAR). There are three isotypes of PPAR belongs to the PPARs family: PPARα, PPARδ (or β), and PPARγ. In human beings, PPARs was participate in serial of biological processes such as adipogenesis, inflammation, and lipid metabolism. Literature has verified that they were lipid sensitive and activation by natural fatty acids was required to initiate their regulation role (Dussault and Forman, 2000; Evans et al., 2004; Forman et al., 1997).

In human tissues, PPARs are differently distributed and show different functions. PPARα is mainly expressed in muscles, heart, kidney, and liver

where it is considered to play a role in the metabolism of lipids and lipoproteins (Fruchart, 2009). PPARβ/δ was expressed ubiquitously but with relatively low expression in the liver. It functions to regulate the energy balance and lipid metabolism in adipose tissue, skeletal muscle, and the heart (Seedorf and Aberle, 2007). Despite its role causing insulin sensitization and enhances glucose metabolism, PPARγ is abundantly expressed in adipose tissue and was discovered to be the master regulator of adipogenesis (Mota de Sa et al., 2017; Tontonoz et al., 1994c). The systemic deletion of PPARγ disrupt the fluid metabolism which lead to severe polydipsia and polyuria (Li Zhou et al., 2015). A more recent study also conduct the whole body knockdown of PPARγ found the mice showing significant metabolic inflexibility, massive loss of urinary energy, increasing in lean mass , activation of the urea cycle, and also developed severe type-2 diabetes (Federica Gilardi et al., 2019).

Both of PPARs are grouped as nuclear receptor 1C subfamily (PPARα–NR1C1; PPARβ/δ–NR1C2; PPARγ–NR1C3) (Nuclear Receptors Nomenclature, 1999). Although the expression of PPARs in human body was different, they share similar gene transcription process. The ligand binding activates PPARs and then forms a heterodimer with another nuclear receptor RXRα. The heterodimer will further bind to a specific region on the chromatin called peroxisome proliferation response

elements (PPREs) in the promoter region of downstream targets. The recruitment of different transcription cofactors is needed for the next stage of the transcription process (Gearing et al., 1993; Lemberger et al., 1996; Yu and Reddy, 2007).

As a nuclear receptor, activation of PPARγ requires the ligand binding (Figure 1.1). Because the size of PPARγ ligand binding pocket was 3-4 times larger than that of the other nuclear receptors, it is capable to accommodate and bind serials of natural and synthetic lipophilic acids. Natural ligands such as essential fatty acids and prostaglandin PGJ_2 or synthetic ligands like thiazolidinediones (TZD) acts as PPARγ agonist (Grygiel-Gorniak, 2014). However, the physiological role of fatty acids as PPARγ agonist remain unclear. TZDs was applied as a treatment of type 2 diabetes but the adverse effects such as increased risk of bone fracture and exacerbated congestive heart failure restricting its use. The available PPARγ ligands were illustrated in the table 1.1. After ligand binding activation, PPARγ exerts its gene regulatory potential by forming the heterodimer complex with RXRα (Tontonoz et al., 1994a). The heterodimer will further bind to the PPRE region to regulate the transcription machinery. It is been reviewed that the binding of PPARγ: RXRα heterodimer to the PPRE is crucial to induce the expression of adipogenic makers during adipogenesis (Lefterova and Lazar, 2009). The
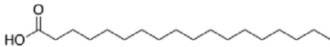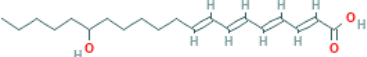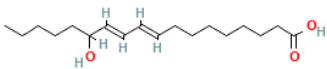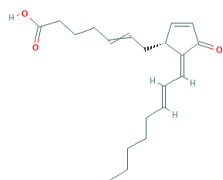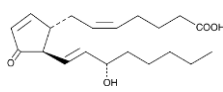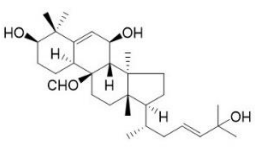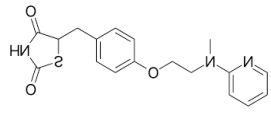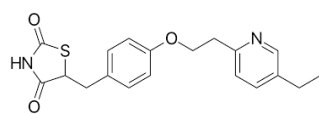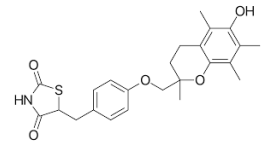
transcription activity of the heterodimer was regulated by association of its coactivators and corepressors in different tissues and cell types (Lefterova and Lazar, 2009). Recent study also identified that PPARγ: RXRα heterodimer functions as a nuclear receptor regulates the expression of leptin and in turn regulates the lipid-sensing system of adipocytes (Zhang et al., 2018). Thus, PPARγ requires activation by ligand binding to regulate adipogenesis as a nuclear receptor and suggested to plays a role post-adipogenesis in adipocyte cells.
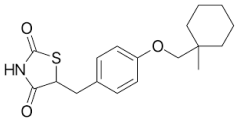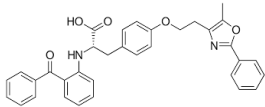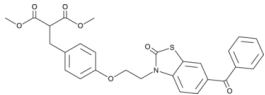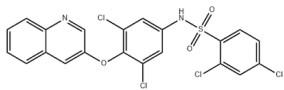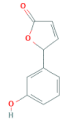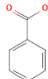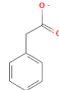
Figure 1. 1: Regulatory mechanism of PPARγ as a nuclear receptor.
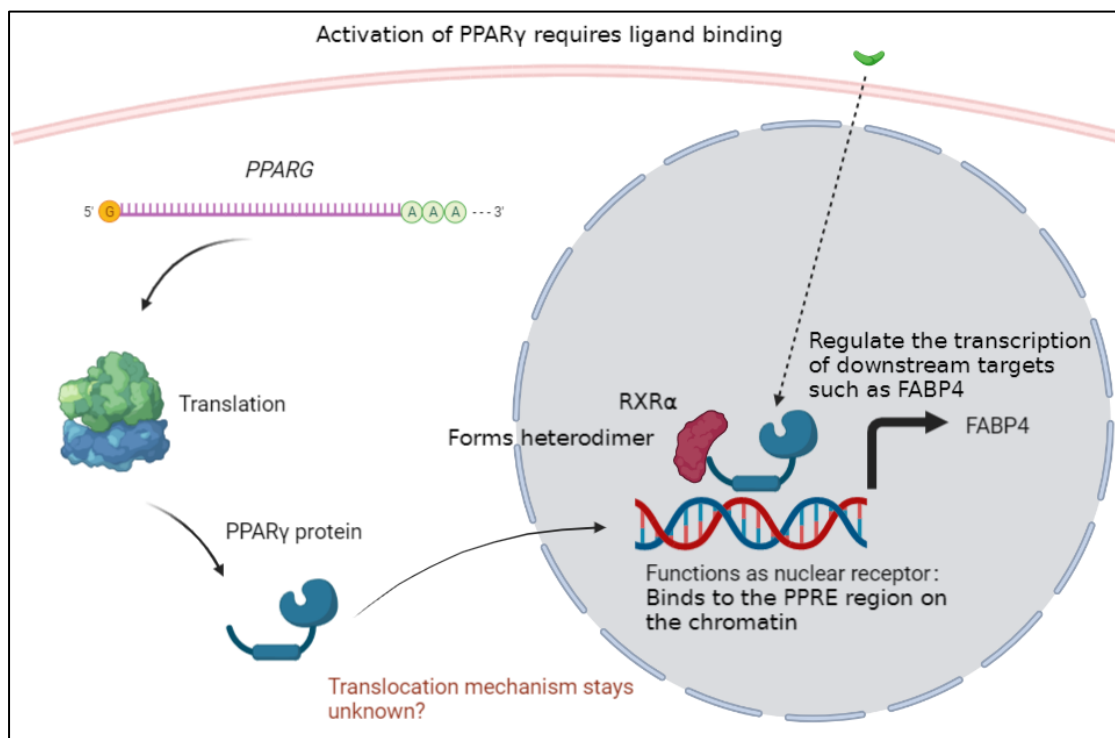
The mRNA represent *PPARG* gene. Red protein represents RXRα and blue protein represents PPARγ. Green particle represents PPARγ binding ligand functions to activate PPARγ and induce it to forms a heterodimer with RXRα.

Table 1. 1: PPARγ ligands.

Natural ligands	Unsaturated fatty acids	
	15-hydroxy eicosatetraenoic acid	
	9- and 13- hydroxy octadecadienoic acid	
	15-deoxy△12,14-prostaglandin J$_2$	
	Prostaglandin PGJ$_2$	
	3β,7β,25-trihydroxycucurbita-5,23(E)-dien-19-al (THCB)	
Synthetic ligands	Rosiglitazone	
	Pioglitazone	
	Troglitazone	

	Ciglitazone	
	Farglitazar	
	S26948	
	INT131	
	5-hydroxy-4-phenylbutenolide	
	Benzoate	
	Phenylacetate	

Data about PPARγ ligands was review in the papers (Grygiel-Gorniak, 2014; Noruddin et al., 2021; Takada and Makishima, 2020)

1.2 Adipogenesis

Adipose tissue is a dispersed organ involved in several important physiological processes: lipid metabolism, systemic energy homeostasis, and whole-body insulin sensitivity. Adipose tissue is comprised of white adipose tissue (WAT) and brown adipose tissue (BAT). WAT is responsible for energy homeostasis, insulin signaling, and endocrine action and accounts for the majority of fat present in human beings. By contrast, BAT is reported to be involved in non-shivering thermogenesis which is mediated by uncoupling protein-1 (UCP1) in the mitochondria (Farmer, 2008). No matter WAT or BAT, adipose tissue is comprised of many cell types including adipocytes, endothelial cells, blood cells, fibroblasts, pericytes, and preadipocytes. However, it is mainly adipocytes that make up the adipose tissue. To better understand the cell origin of these fat cells, *in vitro* cell model was then being built. Various immortal cell lines such as 3T3-L1, 3T3-F442A, OP9, 1246, Ob1771, TA1, and 30A5 preadipocytes were established to study adipogenesis which are capable to differentiating into mature adipocytes. Among these, 3T3-L1 derived from mouse embryonic fibroblasts is the most commonly used cell line. Based on the studies of *in vitro* adipocytes, it has been found that adipocyte maturation from preadipocytes requires cell cycle exit reviewed by Berry (Berry et al., 2016). Thus, adipogenesis is the process of cell differentiation by which

preadipocytes differentiate into mature adipocytes and is the most intensively studied model of cellular differentiation.

1.3 PPARγ: Master regulator of adipogenesis

The transcriptional machinery regulating adipogenesis has been extensively studied in 3T3-L1 preadipocytes. Early studies showed that 3T3-L1 cells can be induced to undergo adipocyte differentiation using a cocktail of insulin, dexamethasone, and cholera toxin (Green and Kehinde, 1975; Green and Meuth, 1974). It is further demonstrated that PPARγ protein is induced during adipogenesis (Chawla et al., 1994; Tontonoz et al., 1994b). Moreover, activation of PPARγ was found necessary to induce the adipocyte differentiation which suggested it might be the master regulator of adipogenesis (Tontonoz et al., 1994a). The knockout of *pparg* in mice is embryonically lethal due to placental defects (Barak et al., 1999). Specific knockout of PPARγ in mice myf5 brown fat cells results in various abnormalities including mammary gland, bone marrow, and skin (Wang et al., 2013).

At the transcriptional level, adipogenesis is now recognized as proceeding through activation of at least two waves of transcription factors. The first wave is induced *in vitro* by the adipogenic cocktail, and includes transcription factors C/EBPβ, C/EBPδ, glucocorticoid receptor (GR), signal transducer, and activator 5A (STAT5A). These transcription

factors in turn activate the second wave which initiates the adipocyte gene programme (Siersbaek et al., 2012; Steger et al., 2010). PPARγ and C/EBPα are considered to play the most prominent roles in this second wave (Siersbaek et al., 2010). It has been demonstrated that it is PPARγ protein isoform 2 that is specifically expressed in adipose tissue while PPARγ protein isoform 1 shows low abundance expression in multiple tissues (Barbatelli et al., 2010). However, exogenous expression of PPARγ2 restored adipogenesis at day 7 but exogenous expression of PPARγ1 show no effect (Ren et al., 2002). Recent studies also demonstrate that suppressing of PPARγ expression and attenuation of PPARγ activity significantly downregulates adipogenesis both *in vivo* and *in vitro* (Dean et al., 2020; Xue et al., 2020; Zhang et al., 2020).

These studies demonstrate that PPARγ was the master regulator of adipogenesis, but it is PPARγ2 rather than PPARγ1 dominantly regulating the adipogenesis process.

1.3.1 Transcription variants of *PPARG*

PPARγ was verified to be essential regulating the adipogenesis in human beings and the transcription of its gene *PPARG* draws interest of researchers. It is found *PPARG* consist of nine exons and localized in human chromosome 3. Due to differential promoter usage and

alternative splicing, the *PPARG* gene can produce multiple transcript variants. Previously four distinct PPARG transcript variants has been reported. They share exons 1 to 6 which encode the PPARγ protein but differ in their 5' terminal region (Fajas et al., 1997; Fajas et al., 1998). *PPARG1* has exons A1 and A2 at the 5' terminal end while *PPARG2* consist of exon B at the 5' terminal end. *PPARG3* consists of exon A2 at 5' terminal while *PPARG4* was only consist of exons 1 to 6 (Takenaka et al., 2013). Till now, 16 transcription variants of PPARG have been identified in human being (Data from NCIB gene database) (Figure 1.1).

Figure 1. 2: Human *PPARG* mRNA.
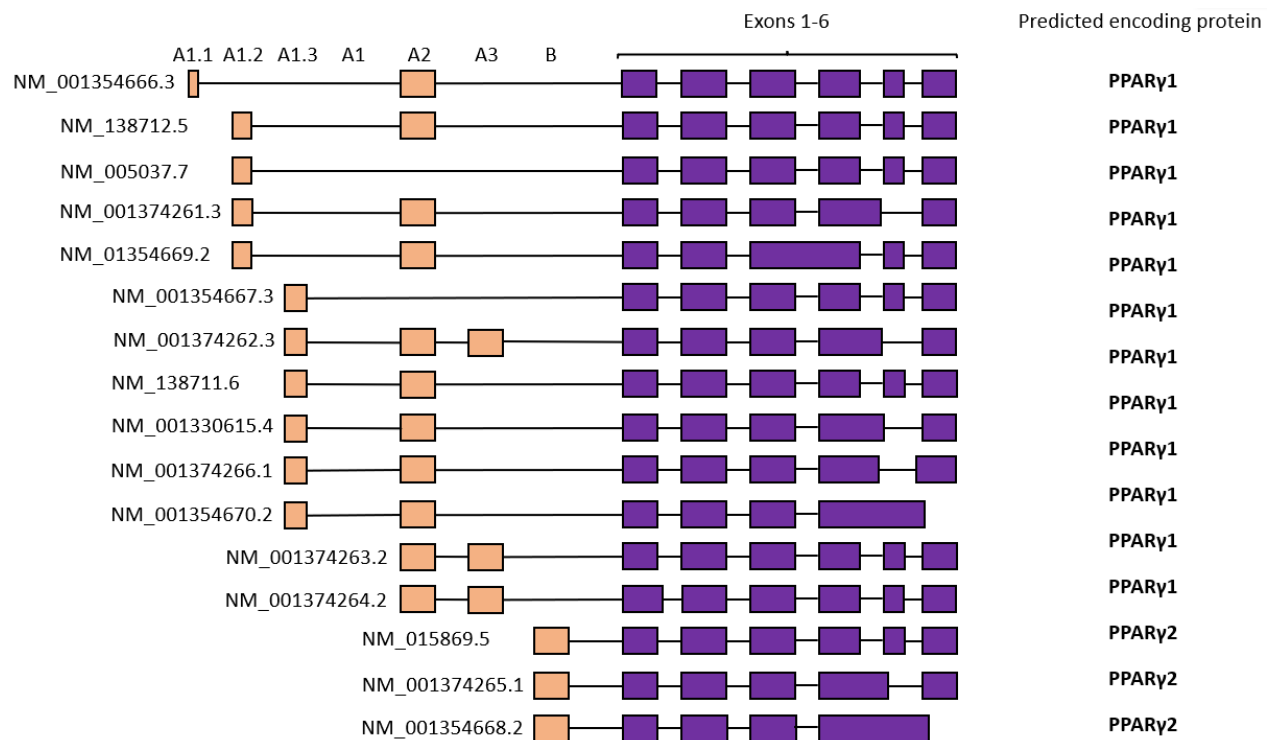
PPARG exons structure from 5' to 3'. Exons 1-6 are the conserved exons encoding PPARγ1. Exons on the 5' end were named A1.1, A1.2, A1.3, A1, A2, A3, and B from left to right. All data adapted from NCIB gene database.

1.3.2 Structure of PPARγ protein

Although various of *PPARG* transcript variants exist in human beings, there are only two PPARγ protein isoforms: PPARγ protein isoform 1 and PPARγ protein isoform 2. PPARγ protein has a conserved structure which consist of 5 domains named A to E from NH_2-terminal to COOH terminal (Chandra et al., 2008). However, the B exon of the *PPARG* transcription variant encodes 28 amino acids which contribute to the additional NH_2-teminal region of PPARγ2 (Figure 1.2). The conserved 5 domains of PPARγ protein contributes to its regulating role as a nuclear receptor. Domain A and B together construct the regulatory domain of PPARγ protein. The regulatory domain contains the intrinsically disordered activation function 1 (AF1) which contributes to the ligand-independent coregulator binding to enhance its binding capability (Hummasti and Tontonoz, 2006). The C domain of PPARγ was the DNA binding domain and consist of two highly conserved zinc fingers. They were responsible for the recognition of PPARγ DNA binding site peroxisome proliferator response elements (PPRE) allow for chromatin binding of PPARγ (A et al., 1997). The presence of zinc finger was nuclear receptor specific and differs to other DNA binding proteins. The binding of DNA domain to the

PPRE also allowing for the activation and recruitment of downstream DNA transcription machinery or the repression of transcription. The D domain of PPARγ functions as a flexible hinge which contributes to the rotation between the DNA binding domain and ligand binding domain. It also contains a nuclear localization signal (Kroker and Bruning, 2015). The E domain which was the ligand binding domain was the largest domain in the PPARγ protein. The ligand domain was formed of four essential compartments: a dimerization interface, the ligand binding pocket, a coregulatory binding surface, and activation function 2 (AF2). The ligand binding domain will stabilized immediately when ligand binds and facilities the interaction with co-activators to remodel the chromatin and recruit the transcriptional machinery (Helsen and Claessens, 2014).

Figure 1. 3: PPARγ protein structure.
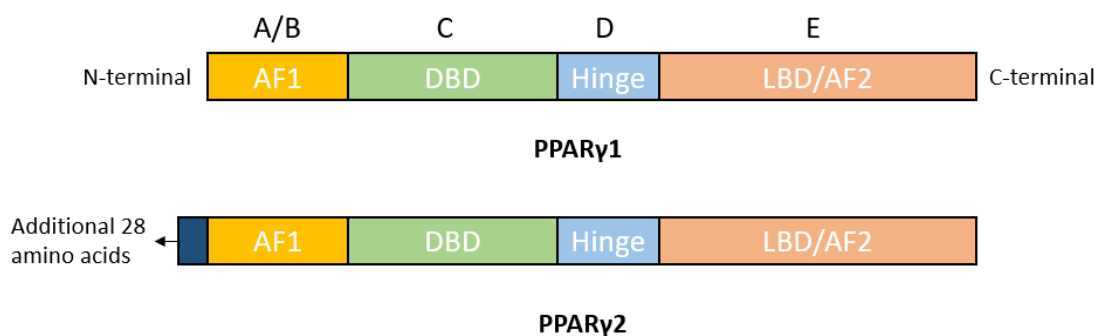
Primary structure of PPARγ protein. DBD was short for DNA binding domain. LBD was short for ligand binding domain.

1.3.3 Post-translation modification of PPARγ in adipogenesis

To better understand the role of PPARγ protein in human beings, post-translation modification of PPARγ was studied in adipogenesis over the past decades.These covalent modifications include phosphorylation, ubiquitylation, and SUMOylation. Phosphorylation of PPARγ was discovered by the observation that growth factors such as epithelial growth factor (EGF), fibroblast growth factor, and platelet-derived growth factor, had inhibitory effects on adipogenesis. Studies demonstrated that mitogen activated kinase (MAPK) which mediated by growth factors can phosphorylate PPARγ1 at N-terminal AF-1 domain at serine[82] and PPARγ2 at serine[112] (Adams et al., 1997; Camp et al., 1999; Hu et al., 1996). Moreover, the unphosphorylated Ser[112] Ala PPARγ mutant is significantly more active than wild-type PPARγ in the presence of PPARγ ligand in cultured adipocytes (Hu et al., 1996). It was also found that MAPK-mediated phosphorylation of PPARγ2 at serine[112] also inhibits PPARγ activity by modulating ligand binding within the C-terminal ligand-binding domain (Shao et al., 1998). The results revealed that MAPK-mediates phosphorylation of PPARγ at site serine112 to affect PPARγ transcriptional activity. Studies further found MEK1 interacts with the C-terminal AF-2 domain of PPARγ to regulate the movement of PPARγ proteins between the cytosol and nucleus by phosphorylation at serine 46 and serine51 (Shao et al., 1998).

Ubiquitylation is a process attaching ubiquitin to a protein and this modification serves as a signal for degradation via proteasome, alter subcellular localization, modulate protein activity, and promote or prevent protein interactions. PPARγ protein was shown to be regulated by the ubiquitin proteasome pathway (UPP) and have very short half-life in adipocytes (Floyd and Stephens, 2002; Hauser et al., 2000; Waite et al., 2001). Studies also observed that inhibition of proteasome activity increases PPARγ activity in adipocytes (Kilroy et al., 2009). Siah2 and MKRN1, which are ligases of E3 ubiquitin protein, regulate the ubiquitylation and proteasome-mediated degradation of PPARγ in adipocytes (Kilroy et al., 2015; Kilroy et al., 2012; Kim et al., 2014). Collectively, these evidence demonstrates that ubiquitin modification of PPARγ regulates the abundance and transcriptional activity of PPARγ proteins.

SUMOylation is a post-translational modification identified in 1995 and involved in various cellular processes including nuclear cytosolic transport, protein stability, stress responses, and progression through cell cycle. Several studies have shown that SUMO1 can modify the AF-1 domain of PPARγ and the SUMOlyation of PPARγ is strongly associated with a repression of transcriptional activity (Diezko and Suske, 2013; Yamashita et al., 2004). SUMOylation can be reversed by a family of

Sentrin/SUMO specific proteases (SENPs). It has been revealed that knock down of SENP2 result in a significant attenuation of adipogenesis accompanied by a marked decrease in PPARγ (Chung et al., 2010). It provides additional evidence that SUMOylation of PPARγ modulates adipogenesis. In conclusion, post-translation modification of PPARγ has been shown to regulate the expression, subcellular localization, and its transcriptional regulatory role on its downstream targets in adipogenesis.

1.4 Urothelium

Urinary system in human being was consists of kidney, ureter, bladder, and urethra. The urinary system was functions to eliminate wastes and surplus water, regulate blood volume and pressure, and control levels of electrolytes and metabolites. Urothelium was the specific epithelium tissue lines on the surface of renal pelvis, ureters, bladder, and upper portion of the urethra. Urothelium acts as a permeable barrier to protect the underlying tissue from the toxins present in the urine and prevent them from re-entering the body. It has been reviewed that urothelium was derived from the embryonic endoderm layer in the bladder and urethra and the embryonic mesoderm layer in the renal pelvis and ureters (Staack et al., 2005). Studies discovered that

urothelium was consist of three morphologically-different layers of cells: the basal, intermediate and superficial cells (Jost et al., 1989).

Superficial cells are terminally differentiated cell and forms identical tight junctions and adherens junctions. The superficial cells (refers as umbrella cells) in human beings covers multiple underlying intermediate cells and are commonly binucleate (Wang et al., 2018). They also characterized by the presence of an asymmetric unit membrane (AUM) in the plaque regions of its apical membrane (Porter et al., 1967). Dr. Tung-Tien Sun and colleagues originally identified that uroplakins are the chief components of the AUM particles in the superficial cells (Wu et al., 2009). Uroplakin proteins are a small family of transmembrane proteins that highly conserved in mammals and considered to be restricted to urothelial cell differentiation (Garcia-Espana et al., 2006; Wu et al., 1994). The cell layer directly underneath the superficial cell layer is so called the intermediate cell layer. Intermediate cells are smaller than superficial cells and commonly are mononucleate. They express tight junction-associate proteins such as claudins and the cell-cell adhesion protein CDH1 but they do not form morphologically identifiable tight junctions or adherens junctions (Acharya et al., 2004; Wang et al., 2018). The basal layer was positioned at the interface of the intermediate layer and the underlying lamina propria. They attach directly to the basement

membrane via hemidesmosomes and attach to the intermediate cells via desmosomes (Alroy and Gould, 1980; Jones, 2001).

Moreover, urothelium was identified to be mitotically quiescent with significant low cell turnover rate (Limas, 1993; Walker, 1960). Previous study has found Ki67 (Proliferating marker) is either absent or limited express to a few cells in the urothelium (Varley et al., 2005). However, urothelium was able to regenerated and can gain proliferation ability when response to damage, injury or infection (Hicks, 1975; Pust et al., 1976).

Figure 1. 4: Haematoxylin and Eosin stain of normal human ureteric urothelium.
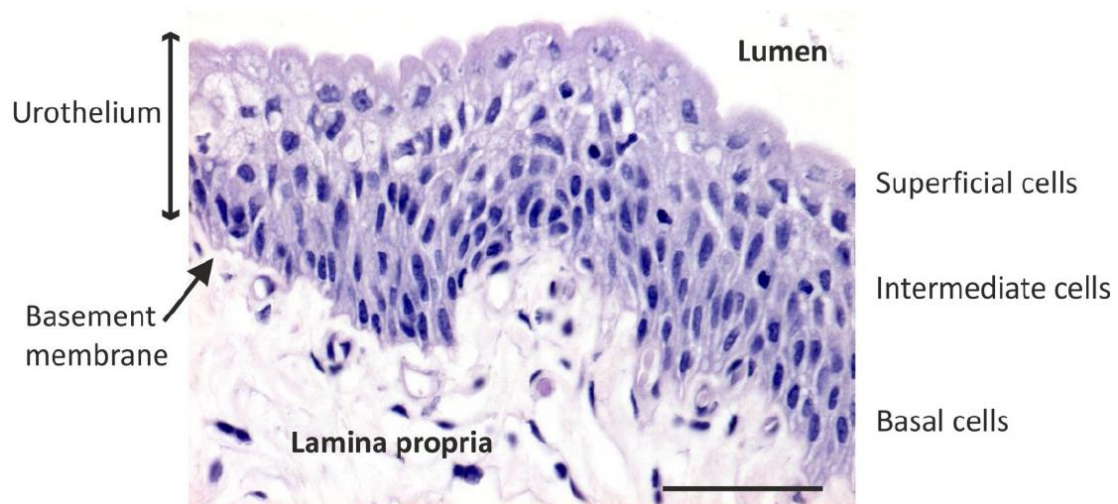
Scale Bar=50 μm, Graph adapted from Jennifer Hinley's thesis.

1.4.1 Urothelium barrier function

It is known that urothelium forms a barrier to pathogens and to the excess water, metabolic waste products, and other solutes present in urine. It is thought to be the tightest and most impermeable epithelium in the human body (Powell, 1981). The barrier function of urothelium was normally measured by the transepithelial electrical resistance (TER) which is thought to be the result of a complex network of interlocking tight junctons (Negrete et al., 1996). It has been reviewed that two groups of proteins, the uroplakin proteins and tight junction-associated proteins, contributes to the formation of tight barrier of the urothelium (Khandelwal et al., 2009).

1.4.2 Uroplakins: Urothelial cells differentiation marker

The uroplakins including UPK1A, UPK1B, UPK2, UPK3A, UPK3B, and UPK3C. The major uroplakins in the urothelium are UPK1A, UPK1B, UPK2, and UPK3A. UPK1A and UPK1B are members of the tetraspanin family of proteins, while UPK2 and UPK3A are single-pass, type-1 membrane proteins (Deng et al., 2002; Wu and Sun, 1993; Yu et al., 1994). Knockout mice lacking expression of UPK1B, UPK2, or UPK3A result in small, poorly differentiated umbrella cells, vesicoureteral reflux, and an attendant hydronephrosis (Aboushwareb et al., 2009; Carpenter et al., 2016; Hu et

al., 2001). Interestingly, the UPK3A knock out mice form small number of plaques but UPK3B knock out mice display no abnormalities in urothelium or plaque formation (Rudat et al., 2014). Recent studies also found UPK1b promote the structural integrity of the renal when damaged or injured (Jackson et al., 2018). The evidence illustrated that UPK2 and UPK3A was essential for the barrier function of the urothelium while UPK3B appears to have a non-essential role

1.4.3 Tight junction proteins in urothelium

Tight junction proteins are found at the apical surface of two adjacent epithelial cells and forms a continuous ring that completely circumscribes the apex of adjacent umbrella cells. They function to separate the apical and basolateral membrane domains as well as regulate the paracellular passage of ions, water, and molecules through the lateral interstitial space (Lewis and Diamond, 1976; Lewis et al., 1976). Study demonstrate that the chief components of tight junction proteins are claudin (CLDN) proteins, occluding, and zonula occluden (ZO) proteins (Van Itallie and Anderson, 2014).

Claudin proteins are transmembrane proteins which act to form the tight junction between two cells. Claudins forms tight junctions by two types of interactions: cis-interactions and trans-interactions. The cis-

interactions link adjacent claudins on the same membrane while trans-interaction take place when claudins on opposing cell membranes bind to each other (Blasig et al., 2006). It is shown that claudin 3, 4, 5, and 7 was expressed in human urothelium (Varley et al., 2006). Claudin 3, as a barrier forming protein, is restricted to the apico-lateral surface of the umbrella cell layer in human urothelium (Nakanishi et al., 2008). It has been found knock down of claudin 3 expression caused a complete lack of barrier function measured by TER (Smith et al., 2015). Claudin 4 was detected in the umbrella cell tight junctions and at regions of cell-cell contact in the intermediate and basal cell layers of the urothelium (Acharya et al., 2004; Fujita et al., 2012). Studies found overexpression of Claudin 4 increase the barrier function and decrease of claudin 4 expression impairs the barrier function of porcine intestine (Michikawa et al., 2008; Pinton et al., 2010). The results suggested claudin 4 to be the barrier forming proteins.

ZO proteins functions as the main intracellular component of tight junctions. Literature identified that both ZO1, ZO2, and ZO3 bind the C-terminal domain of claudin and occluding proteins to act as a link to the actin cytoskeleton in the cell (Li et al., 2005). Studies demonstrate that knockout of ZO1 and ZO2 result in embryonically lethal in mice while ZO3 knockout mice are viable (Xu et al., 2008). It suggests ZO1 and ZO3

might play a more essential role than ZO3.

Our lab further verified that overexpression of claudin 3 did not improve the barrier function when cells were induced to stratify (Smith et al., 2015). ZO-1$^{\alpha+}$, an alternative ZO-1 isoform, is identified to be a result of urothelial cell differentiation. The evidence illustrated that the barrier function of urothelium was not solely dependent on the expression of single claudin protein but requires combination expression of several tight junction proteins.

1.4.4 Urothelium regeneration

Under normal conditions of homeostasis, the urothelium is mitotically quiescent with very low turnover rate. Previous literatures labeling BrdU or Ki67 reveal that almost no cells in the urothelium were undergoing mitosis (Colopy et al., 2014; Kullmann et al., 2017). However, the urothelium has a high capacity to regenerated in response to acute injuries caused by exposure to chemicals, mechanical overdistention, bacteria infections, Interstitial Cystitis (IC), and Ketamine-induced Cystitis. Regeneration of urothelium was extremely efficient and often associated with urothelial proliferation and migration (Kreft et al., 2005; Robino et al., 2014). But the mechanism underlying the urothelium regeneration remains unknown.

In vitro experiments have been done by previous study and discovered that the initiating signal for repair is in the form of an ATP-driven calcium response. The calcium wave immediately initiates after damage and followed with migration of cells into the denuded space (Shabir and Southgate, 2008). However, the signaling pathways involved in the migration of cells in response to urothelium injury was unknown. Our lab further demonstrated that TGF-β signaling is activated when differentiated NHU cells was wounded *in vitro* and it is responsible for the migration and repairing during the regeneration process (Fleming et al., 2012).

In vivo study identified that rat bladder damaged by protamine sulphate results in loss of superficial cells but repaired by a maturation of intermediate cells which expressing uroplakins and tight junction proteins after terminally differentiated (Lavelle et al., 2002). Mouse bladder explant further identified that restoration of tight junctions happens before expression of uroplakins and suggested to be one of the earliest events in the urothelium regeneration (Kreft et al., 2005). Moreover, another group repeat the mouse bladder explant experiment and reveal that basal cells mainly distribute to the proliferation and migration of cells in urothelium regeneration. The basally derived NHU cells have a higher capacity for proliferation compared to suprabasal-

derived cells but shares similar characteristics after a short adaptation period in culture (Wezel et al., 2014).

These results illustrated that urothelium was able to immediately regenerate when injured or damaged. Previously study suggested that 10% of rat bladder basal cells are potential stem cell population in the urothelium based on long term BrdU label retention (Kurzrock et al., 2008). However, it has been demonstrated that both basal and intermediate/superficial cells have the capacity to differentiated into a multi-layer organized urothelium (Wezel et al., 2014). Bushman's group reported that KRT-, uroplakin+ intermediate cells were highly proliferated when exposed to E.coli for 24 hours (Colopy et al., 2014). Gandi et al also found KRT-, uroplakin+ intermediate cells serve as progenitors of superficial cells when faced to acute injury (Gandhi et al., 2013). More recently a paper identified that the generation of umbrella cells depends on the formation of TP63+, KRT5-, uroplakin+ intermediate cells in response to E.coli or acute injury (Wang et al., 2018). Till recent, no studies supporting the pluripotency in urothelial cells nor identify a subpopulation of stem cells from the basal cell population. Thus, it is uncertain whether a population of stem cells was available in urothelium and plays a role in the regeneration process. Based on the current studies, it is more possible that all NHU cells in urothelium retains the

capacity to form a functional multi-layer urothelium in response to injury and damage.

1.5 Urothelial cell proliferation and differentiation *in vitro*

Subculturing of human urothelial cells *in vitro* has been proved to be an important tool to study the cell biology of normal human urothelial (NHU) cells. Southgate has developed the method to isolate NHU cells from patient biopsies of bladder, ureter or renal pelvis tissue (Southgate et al., 1994). According to the literature, the tissue was placed into a "stripping" solution to disassociate the urothelial cell sheet from the basement membrane. The sheet will be further break into single cell and cultured in a serum free, low calcium (0.09 mM) keratinocyte serum-free medium (KSFM) supplemented with recombinant human epidermal growth factor, bovine pituitary extract and choleratoxin (Southgate et al., 1994). The supplemented KSFM is referred as KSFMc. Under this condition, NHU cells are highly proliferative and adopted a basal-like phenotype. The typical markers of differentiated NHU cells were lost in this condition including the expression of tight junction proteins, CK13, CK20 and several uroplakin genes. It has been identified that proliferating NHU cells *in vitro* became squamous and expressing the squamous epithelial cell-assocaited cytokeratin CK14. It is further

discovered that the NHU cells maintaining the basal-like, proliferative phenotype even after reaching confluence and activation of epidermal growth factor receptor (EGFR) signaling contributes to the *in vitro* growth of NHU cells (Southgate et al., 1994; Varley et al., 2005).

Although NHU cells shows the proliferating phenotype in the serum free, low calcium condition but it can differentiate *in vitro*. The first method to drive the differentiation of NHU cells was called "TZPD" differentiation. It requires the treatment of NHU cells using troglitazone (TZ) to activate PPARγ and inhibit the EGFR signaling using the EGF tyrosine kinase inhibitor PD153035 (PD) (Varley et al., 2005). TZ was demonstrated to initiate the urothelial gene transcription program and results in the expression of uroplakin, CK13, and tight junction proteins (Varley et al., 2006; Varley et al., 2004). But the TZPD differentiated NHU cells are unable to form a barrier epithelium thus not producing an integrated functional epithelium. The second differentiation method refers as ABS/Ca^{2+} which relies on the culturing of NHU cells in adult bovine serum (ABS) with near physiological concentration of calcium to 2mM. The ABS/Ca^{2+} differentiated NHU cells shares similar differentiation markers compared to the TZPD differentiated NHU cells. On the contrary, ABS/Ca^{2+} differentiation allow NHU cells to self-organize into a multilayered urothelium with barrier function as

demonstrated by high TER value of >3000Ω.cm2 (Cross et al., 2005). Previous study also found that increased calcium concentration alone fails to induce the differentiation of NHU cells suggested that ABS was essential for the differentiation process (Sugasi et al., 2000). However, there are so many factors in the serum including fatty acids and retinoids which can activate PPARγ and other pathways crucial to urothelial tissue development. So, it is unclear about the exact components of adult bovine serum that contributes to the differentiation of NHU cells but PPARγ might plays the major role. In conclusion, our lab can isolate NHU cells from clinical tissue biopsies and proliferate them *in vitro*. We can further differentiate the NHU cells to an end point which shares similarities of in situ differentiated NHU cells at cellular level.

1.5.1 Role of PPARγ in urothelial cell cytodifferentiation

Differentiation of NHU cells *in vitro* was regulated by a group of transcription factors. Several key factors were shown to involved in this process and the hierarchical transcription factor profile of NHU cell differentiation stays unknown. Activation of PPARγ and blocking of EGFR signaling has proved to reverse the squamous phenotype and result in the expression of CK13, UPK2, UPK1a, UPK1b, and tight junction proteins

which all associate with terminal differentiation (Varley et al., 2006; Varley et al., 2004).It is illustrated that the promoter region of claudin 3 encloses a consensus PPRE and the expression reaches a maximum in 3 days post treatment (Varley et al., 2006). Moreover, posttranslational effects of PPARγ on claudin 4/5 was also identified in NHU cells and mediated through proteosome inhibition. Varley also found that activation of PPARγ shown to upregulating transcription factors ELF3, FOXA1, and IRF1 (Bock et al., 2014; Varley et al., 2009). It is found that indirect upregulating transcription of UPK gene possess via two intermediate transcription factors, FOXA1 and IRF1 (Varley et al., 2009). ELF3 which suggested to be activated by PPARγ acts directly and activate downstream urothelial regulating transcription factors and urothelial marker genes (Bock et al., 2014). Thus, PPARγ might be the master regulator of NHU cell differentiation.

1.5.2 Urothelial cell differentiation associate transcription factors

FOXA1 is a transcription factor shown to play essential role in many cells types especially in particular cells of endodermal origin (Bernardo and Keri, 2012). Previous study found FOXA1 is expressed during the embryonic development and in the mature adult murine urothelium (Oottamasathien et al., 2007). Study also demonstrates that urothelium-

specific knockout of FOXA1 in mice results in changes to the urothelium (Reddy et al., 2015). The change is gender-specific which male mice show increasing expression of CK14 in areas of hyperplastic urothelium while female mice on the contrast developed areas of keratinizing squamous metaplasia. Instead of shown that FOXA1 acts downstream of PPARγ in NHU cell differentiation, Varley also illustrated that knockdown of FOXA1 expressing in NHU cells result in downregulating of urothelial differentiation genes including CLDN3, CK13, UPK1A, UPK2, and UPK3A. These evidences suggest FOXA1 plays an essential role in urothelium and functions as a key regulator of NHU cell differentiation.

E74-like transcription factor-3 (ELF3) is a member of the E26 transformation-specific (ETS) family of transcription factors. This family is characterized by its helix turn helix DNA binding domain and they bind to a GGAA/T conserved sequence within the regulatory region of responsive genes (Oettgen et al., 1997). Study found ELF3 can regulate the transcription of urothelial terminal differentiation associate genes CK8 and SPRR2A in several epithelial cancer cell lines (Brembeck et al., 2000). Literature also identified that ELF3 modulate the transcription of Grhl-3, FOXA1, UPK3a and CLDN7 genes (Bock et al., 2014). It indicates ELF3 might be a key regulator of NHU cell differentiation and barrier

formation. Thus, ELF3 was a transcription factor that regulate the differentiation process of NHU cells.

1.6 PPARγ: Potential therapy target of bladder cancer

Nowadays bladder cancer has become one of the most prevalent malignant tumors in the urinary system (Siegel et al., 2016). Patients suffering from bladder cancer with its high recurrence rate and limited therapeutic methods. Radical cystectomy is still the most effective treatment of bladder cancer but accompany with unfavorable outcomes. It is urgent to find a new target for the treatment of bladder cancer. Previous study using the Oncomine database discovered amplified transcription of *PPARG* in bladder cancer tissues (Cheng et al., 2019). Another study also found despite the mutation of its heterodimer parter RXRα, the recurrent mutation of *PPARG* also contributes to activate the transcriptional activity of PPARγ/RXRα pathway (Rochel et al., 2019). It is also verified that the expression of PPARγ protein was upregulated in tumors compared with normal tissues (Yang et al., 2013). Thus, PPARγ and its mutation was highly detected in bladder cancer tissue. Study also verified that inhibition of PPARγ by either pharmacologic inhibition or genetic ablation attenuates the proliferation of *PPARG*-activated bladder

cancer cells (Goldstein et al., 2017). All the results suggests PPARγ plays an essential role in bladder cancer cells.

Previous research also focused to identify the molecular mechanism of PPARγ in bladder cancer cells. Applying gene ontology (GO) enrichment analysis and Kyoto Encyclopedia of Genes and Genomes (KEGG) pathway analysis has suggest PPARγ might involve in the cell proliferation, cell death, cell migration and the PI3K-AKT signaling pathways of bladder cancer cells (Cheng et al., 2019). There are also studies identified that reducing expression of PPARγ inhibits the cell viability of bladder cancer lines showing gain or enhancement of PPARγ (Biton et al., 2014; Goldstein et al., 2017). Thus, inhibition of PPARγ might be a potential treatment of bladder cancer. However, these results were generated from several bladder cancer cell lines and insufficient to reveal the general function of PPARγ in bladder cancer. Despite of its potential role in bladder cancer, PPARγ also reported to regulate the differentiation of PPARγ in normal urothelial cells previously in our lab and bladder cancer was evolved from normal urothelial cells (Varley et al., 2004). It is highly possible that bladder cancer cells hijack the function of PPARγ to escape from cell cycle arrest or promote its migration in the human body. Comprehensive understanding about the mechanism of PPARγ in normal

urothelial cells will contributes to discover its functional role in bladder cancer cells.

1.7 Thesis Hypothesis and Aims

Urothelium is a tissue in human body functions to provide the barrier against toxic materials in the urine. Urothelial cells in the urothelium stays mitotically-quiescent. In order to maintain the barrier function, the urothelial cells in the urothelium were required to immediately response to damage and injury which they will proliferates and differentiated to re-build the tight-barrier.

Previously in the lab using *in vitro* urothelial cell system has identified that activation of a nuclear receptor PPARγ was essential to initiate the differentiation process of normal human urothelial (NHU) cells. Studies have detected a series of PPARγ protein isoforms and suggested differentially distribution and function of PPARγ protein isoforms in different human tissues. However, the transcription variants of *PPARG* and its encoding protein isoforms in human urothelium stays unknown. Moreover, although PPARγ was well known to functions as a nuclear receptor regulating adipogenesis, the regulatory mechanism of PPARγ protein in NHU cells differentiation haven't been revealed. PPARγ was believed to be the upstream regulator of NHU cells differentiation and

several transcription factors was suggested to be NHU cells differentiation-associated while the downstream target of PPARγ in NHU cells stays unknown.

Despite its initiation role in NHU cells differentiation, PPARγ protein was shown to be highly expressed in *in vivo* differentiated urothelial cells. The repair mechanism of NHU cells in response to damage and injury was important to maintain the barrier function. However, it is not reported that whether PPARγ was involved in the regeneration process of differentiated NHU cells.

The working hypothesis for this project is PPARγ protein regulates the differentiation process of NHU cells as nuclear receptor through differentiation-associated transcription factors.

The overall aims of this works were to characterize the expression of PPARγ in NHU cells using the *in vitro* cell system and identify the regulation role of PPARγ in NHU cells differentiation and regeneration. Specific objectives were to:

● Characterize the expression of PPARγ protein isoforms in NHU cells and its expression during NHU cells differentiation.

- Determine whether PPARγ protein regulates the differentiation of NHU cells as nuclear receptor.

- Identify the downstream target of PPARγ protein in NHU cells differentiation.

- To study whether PPARγ protein participate in the regeneration process of NHU cells.

Chapter 2: Materials and methods

2. Materials and methods

2.1 Ethical Approval

Urological (renal pelvis and ureter) samples were collected with the approval from National Health Service (NHS) Research Ethics Committee (REC). Only the patients' age and gender were collected for the purpose of the research. Samples were sent unlinked and anonymized to the lab. The research received the local ethical approval from the University of York Biology Ethics Committee. The received urological tissue samples were given a unique 'Y' number (eg. Y1236). The epithelial cells were isolated from the tissue sample and cultured *in vitro*. Each urothelial cell line was marked with its distinct Y number as well as its passage number during its culturing.

2.2 General

All laboratory work was carried out in the Department of Biology at the University of York in York, UK. Day to day work was done in the Jack Birch Unit under the supervision of Professor Jennifer Southgate. Bioinformatics analyzing was performed by Dr. Andrew Mason in the Jack Birch Unit.

2.2.1 H₂O and buffers

All water used for experiments and making buffers was ultrapure water (ELGA purified water) generated from the type 1 ultrapure water purification system (ELGA, PURELAB® Ultra) with water purify of 18.2 MΩ-cm.

All water used for the tissue culture experiments was ELGA purified water further autoclaved at 121 °C for 20 minutes (Priorclave, 60L compact Priorclave) prior to use.

For molecular experiments where it was important to exclude RNAse activity, including RNA extraction, DNase treatment, cDNA synthesis, and PCR, the ELGA purified water was treated with 0.1% diethylprocarbonate (DEPC supplied by Sigma-Aldrich, D5758) overnight and then autoclaved at 121 °C for 20 minutes (Priorclave, 60L compact Priorclave). The DEPC treated water is referred to as DEPC-H₂O.

The recipes of general used buffers and solutions (eg. TBS & TBST) can be found in Appendix 8.2.1. All the buffers and solutions were prepared using the ELGA-purified water.

2.2.2 Lab glassware, disposable plastic ware and accessories

For all experiments, the pipette tips (Starlab), Pasteur pipettes (Fisher Scientific), glass multispot slides (C A Hendley), and disposable microfuge tubes (Sarstedt) were autoclaved at 121 °C for 20 minutes (Priorclave,

60L compact Priorclave). Plastic Pasteur pipettes (SLS), Universal tubes (Sarstedt) and serological pipettes (Sarstedt) were supplied sterile. Coverslips used for all microscopy work were supplied by SLS.

2.2.3 Antibodies

The detailed information of all primary antibodies is listed in Table 2.1. The optimized concentration of primary antibodies was obtained by titration on known positive and negative control samples. Most antibodies were aliquoted and stored at -80 $^{\circ}$C to avoid freeze-thaw cycles. Some antibodies (eg. 81B8 & D69) were stored at -20 $^{\circ}$C in 50% (v:v) glycerol and stay liquid. Once thawed, all stock aliquots were diluted to the working stock concentration in TBS (Appendix) with 0.1 % (w/v) BSA as a protective protein and 0.1 % (w/v) sodium azide and stored at 4 $^{\circ}$C.

Information on secondary antibodies is provided in Table 2.2. All secondary antibodies purchased were cross absorbed against human serum and human IgG. The concentration of the secondary antibody was optimized using the primary antibody controls for each batch. Background and non-specific binding of the secondary antibody was also tested by exclusion of primary antibody from the reaction for each batch. The secondary antibodies were stored in a light protective box at 4 $^{\circ}$C and were diluted immediately before use.

Table 2. 1: Primary antibody list.

Antigen	Supplier ref	Molecular weight	Host	Supplier	Application
PPARγ	81B8	50 kD	Rb	Cell signaling	IF:1/100, WB:1/500
PPARγ	D69	50 kD	Rb	Cell signaling	IF:1/100, WB:1/500
ELF3	HPA330049	42 kD	Rb	Altas Antibodies	IF:1/200, WB:1/1,000
FOXA1	C-20	49 kD	Gt	Santa Cruz	IF:1/250, WB:1/1,000
GATA3	D13C9	48 kD	Rb	Cell signaling	IF:1/400, WB:1/1,000
Claudin4	3E2C1	22 kD	M	Invitrogen	IF:1/500, WB:1/1,000
Ki67	MM1	395 kD	M	Leica	IF:1/800
ZO1	1A12	220 kD	M	ThermoFisher	IF:1/400
ZO2	2874	150 kD	Rb	Cell signaling	IF:1/400
ZO3	D57G7	140 kD	Rb	Cell signaling	IF:1/400
LDS14	LDS14	ND	M	In house	IF:1/800
P-Smad3	EP823Y	48 kD	Rb	Abcam	IF:1/400
β-actin	AC-15	42 kD	M	Sigma	WB:1/10,000
FABP4/5	2120s	15 kD	Rb	CST	IF:1/250, WB:1/1,000
FABP4	HPA002188	15 kD	Rb	Altas Antibodies	WB:1/1,000
ERK	610123	42/44 kD	Rb	Becton-Dickinson	WB:1/1,000
MEK	L38C12	45 kD	M	Cell signaling	WB:1/1,000
P-ERK	9101	42/44 kD	Rb	Cell signaling	WB:1/1,000
P-MEK	41G9	45 kD	Rb	Cell signaling	WB:1/1,000
Histone 3	Ab1791	17 kD	Rb	Abcam	WB:1/1,000

| RARγ | HPA053883 | 47 kD | Rb | Altas Antibodies | IF:1/200 |
| RXRα | D-20 | 50 kD | Rb | Santa Cruz | IF:1/400, WB:1/1,000 |

M=Mouse, Rb=Rabbit, Gt=Goat

Table 2. 2: Secondary antibody list.

Antigen	Supplier ref	Host	Supplier	Ref	Application
Mouse IgG	Alexa 488	Goat	Life Technologies	A11001	IF: 1/1,000
Mouse IgG	Alexa 555	Goat	Life Technologies	A21424	IF: 1/1,000
Mouse IgG	Alexa 594	Goat	Life Technologies	A11005	IF: 1/1,000
Rabbit IgG	Alexa 488	Goat	Life Technologies	A11008	IF: 1/1,000
Rabbit IgG	Alexa 555	Goat	Life Technologies	A21428	IF: 1/1,000
Rabbit IgG	Alexa 594	Goat	Life Technologies	A11012	IF: 1/1,000
Mouse IgG	Alexa 680	Goat	Life Technologies	A21057	WB:1/10,000
Rabbit IgG	IR dye 800	Goat	Tebu Bio	611-132-122	WB:1/10,000

IF: Immunofluorescence WB: Western blot

2.2.4 Agonist and inhibitors

Agonist and inhibitors used in experiments were all dissolved in fresh cell culture grade dimethyl sulphoxide (DMSO). The agonist and inhibitors were aliquoted and stored in light protective boxes at -20 ºC. Agonist and inhibitors which had been previously optimised for NHU cell treatments were used at the published concentrations. New batches of agonist and inhibitor or untested agonist and inhibitors were tested over

a concentration range to determine the effective dosage. Working concentration of used agonist and inhibitors are described in Table 2.3.

Table 2. 3: Agonists and inhibitors list.

Drug name	Target	Supplier	Vehicle	Working concentration	Published Concentration
Troglitazone	PPARγ ligand	R&D	DMSO	1 µM	1 µM (Varley et al., 2004)
PD153035	Inhibitor of EGF tyrosine kinase	Merck	DMSO	1 µM	1 µM (Varley et al., 2004)
T0070907	PPARγ antagonist	Cambridge bioscience	DMSO	1 µM	1 µM (Varley et al., 2006)
UO126	MEK inhibitor		DMSO	5 µM	2 µM (Varley et al., 2004)
LY294002	PI3K inhibitor		DMSO	2 µM	2 µM (Varley et al., 2004)
FR180204	ERK inhibitor		DMSO	1 µM	1 µM (Varley et al., 2004)

2.2.5 Statistical analysis

The data from all the experiments were collected and recorded in the Microsoft Excel (2010). Data were presented with mean of all replicates and standard deviation (SD) calculated using Microsoft Excel or Prism GraphPad. Data were tested for normality and confirmed to be drawn from normal distributions. Two-sample T-tests were used to comparing two sample means. If there are more than two sample means, one-way

analysis of variance (ANOVA) was applied with appropriate post-test selected. Statistical analysis of immunoblot results were calculated using the image J software. The statistical quantification of immunofluorescence results was analyzed using image J software or using the TissueQuest software with help from technician Dr. Karen Hogg from the York Bioscience Technology Facility. Details of the data including replicates number, statistical test, p-values, and levels of significance are indicated in the text or figure caption.

2.3 Tissue Culture

2.3.1 General

All cell culture work was conducted in the class II laminar air flow safety cabinets with HEPA (High-efficiency particulate absorbing) filters. The workspace of the safety cabinet was cleaned using UV light everyday. The surface of the safety cabinet was cleaned using 70% (v/v) ethanol before and after use. All cells were cultured in Heracell™ 240 Incubators (Heraeus®) at 37 °C in a humidified atmosphere of 5 % CO_2 in air (NHU cells cultured in KSFMc) or 10% CO_2 in air (established cell lines). Culture medium was changed every 2 days unless special treatment was required. The spent medium was vacuum aspired into a glass pot containing 10% (w/v) Virkon for decontamination.

Centrifugation was performed in the Sigma 2-6E compact centrifuge (SLS). Cell suspensions were centrifuged at 400 x g for 5 minutes to get the cell pellet. Cell counting was conducted by pipetting 10 µl of a single cell suspension into a chamber of the "improved Neubauer" hemocytometer (VWR). The number of cells was counted in the outer four grids with the mean cell count multiplied by 10^4 to get the accurate cell number per ml of cell suspension. Adherent urothelial cells were cultured in Primaria (BD Biosciences) or Cell+ plastic-ware (Sarstedt) which surface was treated to enhance the attachment and growth of normal cells. All digital photos of cultured cells were taken by phase-contrast microscopy on an EVOS XL Core microscope in the tissue culture room.

2.3.2 Primary Urothelial cells isolation and sub-culture

2.3.2.1 Tissue samples

Tissue samples of normal human ureter were collected under the approval of relevant local NHS Research Ethics Committee and the University of York Department of Biology Ethics Committee. No patient identifiable information was collected. Ureter tissue samples were provided by surgeons at St. James's University Hospital Leeds and Pinderfields Hospital in Wakefield. Samples were collected into 15 ml

sterile Transport Medium (Appendix) in sterile disposable Universal tubes and stored at 4 $^{\circ}$C fridge in the main lab when delivered. The samples were processed within the week. The list of used tissue samples and derived NHU cell lines in the thesis is listed in Table 2.4.

Table 2. 4: NHU tissue samples.

Sample ID	NHU No	Operation	Tissue Type
Y1236	NHU1		Ureter
Y2080	NHU2		Ureter
Y2244	NHU3		Ureter
Y2527	NHU4		Ureter
Y2567	NHU5		Ureter
Y2607	NHU6		Ureter

2.3.2.2 Normal Human Urothelial (NHU) cells isolation

It has been previously described in the introduction that our lab developed the method to isolate urothelial cells from patients' biopsies and cultured *in vitro* (Southgate et al., 1994). Samples were dissected in sterile Petri-dishes (Sterilin) in the safety cabinet. Sterilized scissors and forceps were used to remove extra excess fat and connective tissue. A 1 cm long tissue was cut off by the scissor and fixed using 10% (v/v) formalin for 48 hours for histological experiments. Remaining tissue was

cut in 2-3 cm long and opened with the scissor. They were further incubated in 10 ml Stripper Medium (Appendix) for 4 hours at 37 $^{\circ}$C or overnight incubation at 4 $^{\circ}$C. The urothelial sheet can be separated from the underlying stromal tissue using sterile forceps after incubation. Separated sheet will be centrifuged and resuspend in 2 ml collagenase IV (Appendix) for 20 min at 37 $^{\circ}$C. Treated sheet will be further gentle pipette into single cell suspension and seed at 4 X 10^4 cells/cm^2 in Keratinocyte Serum-free Medium (KSFM, Invitrogen) supplemented with 5 ng/ml recombinant human-EGF (Invitrogen), 50 µg/ml Bovine Pituitary Extract (Invitrogen) and 30 ng/ml cholera toxin (Sigma). NHU cells will be further cultured in the completed KSFM unless special treatment was needed.

2.3.2.3 Subculture of NHU cells

When reaching visual confluence, NHU cell cultures were passaged by incubating in 37 $^{\circ}$C pre-warmed 0.1% (w/v) Ethylenediaminetetra-acetic acid (EDTA) diluted in PBS for around 5 minutes at 37 $^{\circ}$C. The morphology of NHU cells was monitored under microscope until the cell contacts were separated and cells began to round up. Then the EDTA was replaced with 0.25% (w/v) trypsin versine solution in Hank's balanced salt solution (HBSS; Life Technologies) containing 0.02% (w/v)

EDTA to detach NHU cells from the plastic by incubating at 37 $^\circ$C for another 3 minutes. Completed KSFM (KSFMc) medium containing 1.5 mg/ml trypsin inhibitor (from soybean) was added to stop the trypsin. The suspension was counted, centrifuged and the supernatant aspirated. NHU cells were resuspended in KSFMc and plated at the desired density. Normally NHU cultures were split at a ratio of 1:3 for maintenance. Only passage 1 to 5 NHU cells were used in experiments.

2.3.2.4 Freezing and thawing of NHU cells

NHU cells were harvested as described in Methods section 2.2.4 but the cell pellet after centrifuge was resuspended in appropriate 'Freeze medium' composed of KSFMc with 10% (v/v) FBS and 10% (v/v) DMSO (Sigma-Aldrich, D2650).

The freeze medium with NHU cells was transferred into 2ml cryovials (Sarstedt, 73.380.992). The vials were slowly frozen at a rate of -1 $^\circ$C per min by placed in a Mr. Frosty™ Freezing Container (Thermo Scientific, 5100-0001) in the -80 $^\circ$C freezer for 24 hours. Frozen vials were transferred to liquid nitrogen-containing dewars for long-term storage.

Thawing NHU cells started by removing stored vials of NHU cells from the liquid nitrogen and then thawed rapidly in the 37 $^\circ$C water bath to recover from frozen. The contents of the vial were suspended in 10 ml of

37 $^{\circ}$C pre-warmed KSFMc and centrifuged to pellet. The supernatant was aspirated and cells resuspended in KSFMc medium to be seeded in culture vessels as required.

2.3.3 NHU cell differentiation *in vitro*

NHU cells were differentiated *in vitro* by two different differentiation methods. The TZPD differentiation requires the adding of drug Troglitazone (TZ) and PD153035 (PD). The ABS/Ca^{2+} differentiation requires the adding of adult bovine serum (ABS) and increase the calcium concentration.

2.3.3.1 Differentiation of NHU cells using PPARγ activator and EGFR signaling inhibitor

In TZPD differentiation, NHU cells were cultured to 70-80% confluence (Figure 2.4). Then the NHU cells were treated with 1 µM Troglitazone (TZ) (Tocris, 3114) and 1 µM PD153035 (PD) (Merck Millipore, 234490) in KSFMc for 24 hours (Varley et al., 2004). The medium was changed the next day to remove Troglitazone but still contain 1 µM PD153035 (PD). After that, the culture was maintained for up to 6 days with medium changed every two days. NHU cells cultured with KSFMc containing 0.1% dimethyl sulphoxide (DMSO) were used as the vehicle control. The

amount of DMSO was always kept constant at 0.1% (v/v).

2.3.3.2 Differentiation of NHU cells using 5% Adult bovine serum (ABS) and physiological calcium

In ABS/Ca^{2+} differentiation adapted from (Cross et al., 2005), NHU cells were cultured to 80% confluent (Figure 2.4). Then the medium was changed to KSFMC containing 5% (v/v) Adult Bovine Serum (ABS) (Harlan Sera lab) for 3 days at 37 °C. Then NHU cells will be cultured in KSFMc containing 5% ABS and 2mM CaCl$_2$. Cultures were continued for further 6 days with medium change every two days. NHU cells cultured in KSFMc alone were used as the control.

Figure 2. 1: Differentiation of NHU cells *in vitro*.
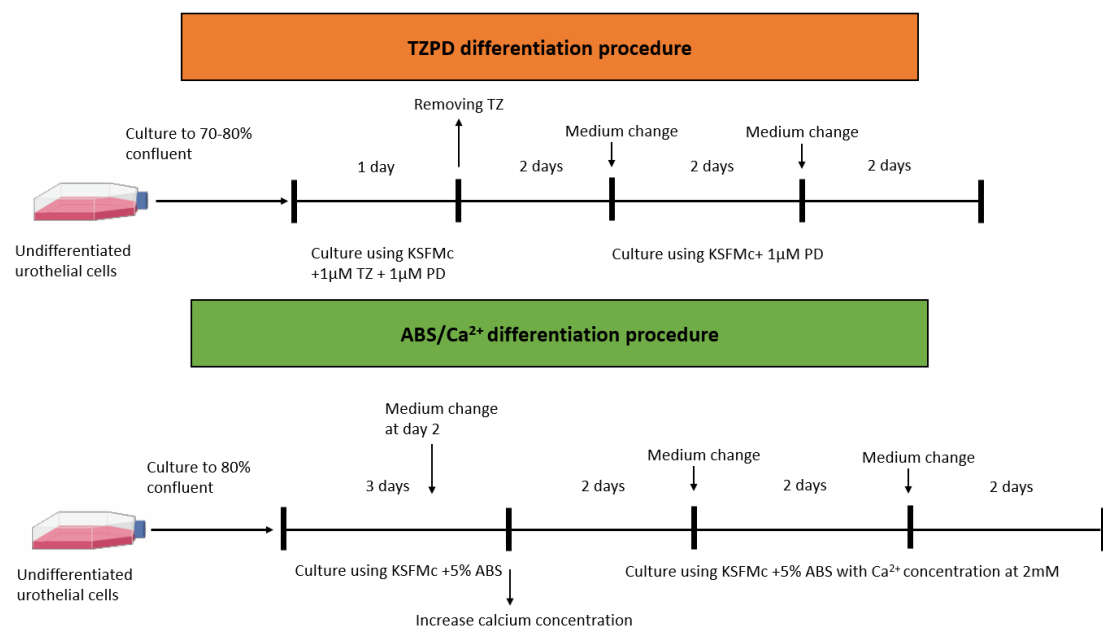
PD=PD153035 (EGFR inhibitor), TZ=troglitazone (PPARγ agonist), ABS= Adult Bovine

Serum.

2.3.4 Subculturing of carcinoma-derived cell lines

Six carcinoma-derived cell lines (MCF-7, 5637, SCaBER, RT4, RT112, and UMUC9) were cultured, and used for experiments in this thesis; MCF-7 cells are a breast carcinoma-derived cell line, rest cell lines (5637, SCaBER, RT4, RT112, UMUC9) are bladder carcinoma-derived cell lines. Cells were cultured in Dulbecco's Modified Eagle's Medium (DMEM) (Gibco®, 21969-035) with 10 % Fetal Bovine Serum (FBS) (SeraLab, EU-000) supplemented with 1% L-glutamine (LG) (Gibco®, 25030-024) referred as DMEM 10% medium or DMEM:RPMI (Roswell Park Memorial Institute) 1640 (Gibco®, 21875-034) (50:50, v/v) supplement with10 % Fetal Bovine Serum (FBS) (SeraLab, EU-000) and 1% L-glutamine (LG) (Gibco®, 25030-024) refers as DR 10%FBS medium. Carcinoma-derived cell lines were cultured in Corning® cell culture plasticware (Sigma-Aldrich) at 37 °C in a humidified atmosphere of 10 % CO_2 in air.

For the passage of carcinoma-derived cell lines, the same protocol was applied as described in Method section 2.2.4 except KSFMc was changed to DMEM 10% medium. Trypsin inhibitor was not required because the presence of serum in the DMEM 10% medium was capable to inhibit the trypsin activity.

Freeze and thaw of carcinoma-derived cell lines was following the protocol described in Method section 2.2.5 except the 'Freeze mix' was made up using DMEM with 10% (v/v) FBS and 10% (v/v) DMSO (Sigma-Aldrich, D2650) or DMEM:RPMI 1640 (50:50, v/v) with 10% (v/v) FBS and 10% (v/v) DMSO (Sigma-Aldrich, D2650).

Table 2. 5: Subculturing of carcinoma-derived cell lines.

Cell line	Cell line type	Culturing Medium
MCF7	breast carcinoma-derived	DMEM+10%FBS+1%LG
5637	bladder carcinoma-derived	DMEM+10%FBS+1%LG
SCaBER	bladder carcinoma-derived	DMEM:RPMI+10%FBS+1%LG
RT4	bladder carcinoma-derived	DMEM:RPMI+10%FBS+1%LG
RT112	bladder carcinoma-derived	DMEM:RPMI+10%FBS+1%LG
UMUC9	bladder carcinoma-derived	DMEM:RPMI+10%FBS+1%LG

2.3.5 Cell viability assay

The viability of cell cultures was measured using AlamarBlue®, a reagent that undergoes a colourimetric change in response to cell metabolism and which can be used to estimate changes in population mass (based on relative change) or number (following comparison against a standard curve). The assay can detect the reduction of all elements of the electron transport chain and assumes that mitochondrial activity is

directly proportional to cell viability.

NHU cells were seeded at a density of 2×10^3 cells/well into Primaria® 96-well plates and allowed to attach for 18 hours overnight in the incubator. The next day (day 0), one plate will be used to establish initial seeding viability while the growth medium in the remaining plates was change with fresh KSFMc or treatment as appropriate. The relative number of proliferating cells was measure by replacing the growth medium with 200µl of freshly prepared 10 % (v/v) AlamarBlue® reagent (diluted in pre-warmed KSFMc) in six replicate wells, including empty (no cell) control wells. Then the plates will be incubating at 37 °C for 4 hours. he absorbance of samples was measured at 570 nm and 600 nm using a Multiskan Ascent 96-well plate spectrophotometer (Thermo Scientific). The absorbance readings were directly proportional to the mitochondrial activity within the cells and were taken to be directly proportional to viable cell number. The percentage reduction of AlamarBlue® was calculated from the absorbance values using the following equation:

Percentage Reduction = (O2 x A1) – (O1 x A2) x100

(R1 x N2) – (R2 x N1)

Where:

O1 = molar extinction coefficient (E) of oxidized AlamarBlue® (Blue) at 570 nm, a constant value of 80586

O2= E of oxidized AlamarBlue® at 630 nm, a constant value of 34798

R1 = E of reduced AlamarBlue® at 570 nm, a constant value of 155677

R2= E of reduced AlamarBlue® at 630 nm, a constant value of 5494

A1 = absorbance of test wells at 570 nm

A2 = absorbance of test wells at 630 nm

N1 = absorbance of negative control well (medium plus AlamarBlue® but no cells) at 570 nm

N2 = absorbance of negative control well (medium plus AlamarBlue® but no cells) at 630 nm

2.4 Analysis of gene transcription

2.4.1 General

All RNA work was conducted on a specific bench area pre-cleaned with RNAse*Zap*® wipes (Ambion) and only RNA-related experiments were allowed to perform on the bench to avoid any RNA contamination. All DNA work except PCR was conducted on a dedicated DNA bench which was pre-cleaned with 75% (v/v) ethanol. DNase/RNase-free filter pipette tips (Starlab) and 1.5 ml tubes (Ambion) were used for all the RNA and

DNA work. 15ml polypropylene tubes and caps (Sarstedt) were treated overnight with 0.1% (v/v) DEPC at ambient temperature to remove RNase enzymes and then autoclaved to destroy DEPC. The tubes were further dried before use.

2.4.2 RNA isolation

Cells were cultured in either 6 well plate, 25 cm^2 flask, 75 cm^2 flask, or 10 cm (diameter) dishes. The culture medium was aspirated and the cells washed once with PBS. Cells were solubilized by adding 1ml (6 well plate), 2.5 ml (25 cm^2 flask) or 5ml (75 cm^2 flask or 10 cm dish) TRIzol® Reagent (Life Technologies). Cells were collected from the culturing plate, flask, or dish by scraping using plastic cell scrapers. The lysates were frozen stored at -80 °C in 15 ml DEPC-treated polypropylene tubes if not used immediately. Fresh lysates or thawed lysates were transferred to RNase-free 1.5 ml vial and incubated at ambient temperature for 5 minutes to allow complete dissociation of nucleoprotein complexes. For every 1 ml of TRIzol® Reagent used, 0.2 ml chloroform was added and vortexed for 15 seconds followed by incubation at ambient temperature for 3-5 minutes to allow phase solubilization of RNA. The vials were centrifuged at 12,000 x g for 15 minutes at 4 °C to phase-separate the RNA. The upper RNA-containing

aqueous phase was carefully collected using a 100 µl pipette to avoid any contamination from the lower DNA containing phase or the middle protein and lipid containing interphase. The collected RNA-containing phase was further transferred to a clean RNase-free vial. RNA was precipitated by adding 0.5 ml isopropanol for every 1 ml of TRIzol® Reagent used for lysis. The vials were gently inverted several times before incubating at ambient temperature for 10 minutes, followed by centrifugation at 12,000 x g for 20 minutes at 4 °C. The supernatant was aspirated and 75% (v/v) ethanol was added to a volume equal to the original lysis volume. The vials were gently disturbed to lift the pellet to be fully washed in the 75% (vlv) ethanol and further centrifuged at 7,500 x g for 5 minutes at 4 °C. The ethanol was carefully aspirated to avoid losing the pellet as it is not firmly attached to the bottom. The ethanol wash process was repeated again and the RNA pellet was air-dried before resuspending in 30 µl nuclease-free water. The RNA was stored at -80 °C if not used immediately.

2.4.3 DNase treatment and cDNA synthesis from RNA

DNase treatment was performed to remove any contaminating DNA from isolated RNA samples using the DNA-*free*™ kit (Ambion). RNA sample was treated with 1 µl DNase enzyme and 0.1 volume of 10 x

DNase buffer followed by incubating at 37 °C for 30 minutes. The "DNase inactivation reagent" was vortexed for 1 minute during the previous incubation and 5 µl was added to each RNA sample followed by incubating at ambient temperature for 2 minutes. The RNA sample was then centrifuged at 10,000 x g for 1 minute and the DNA-free supernatant was transferred to a fresh RNase-free 1.5 ml vial. The concentration and quality of the DNase treated RNA were measured using the NanoDrop™ UV spectrophotometer as shown in Table 2.6. DNase treated RNA samples were stored in -80 °C if not used immediately.

cDNA synthesis of DNase treated RNA was performed using the SuperScript®II First-Strand Synthesis System (Life Technologies). 50 ng poly-A tail specific primers were annealed to 1 µg RNA at 65 °C for 10 minutes. Master mix containing 2.5 mM $MgCl_2$, 10 mM DTT, 1 mM dNTP mix, and 1 x 'ReverseTranscript buffer' was made on ice during the incubation before added to the RNA sample followed by incubation at 25 for 2 minutes. 50 units of SuperScript®II reverse transcriptase enzyme were added to each reaction. For 'RT negative' control of each RNA sample, equal volume of DEPC-H_2O was added to replace the SuperScript®II reverse transcriptase enzyme. The RNA samples were

incubated for 50 minutes at 42 $^{\circ}$C and then 15 minutes at 70 $^{\circ}$C to inactivate the reverse transcriptase. The cDNA was short-term stored at -20 $^{\circ}$C or long-term stored at -80 $^{\circ}$C if not used immediately.

Table 2. 6: Concentration and quality of DNase treated RNA.

Sample	Tube Label	ng/ul	260/280	260/230
Y2244	1	526.03	2.02	2.11
Y2080	2	555.38	2.02	2.07
Y1236	3	868.94	2.02	2.14
Y2244 DIF 3D	4	520.85	2.03	1.99
Y2080 DIF 3D	5	340.69	2.01	2.07
Y1236 DIF 3D	6	784.49	2.02	2.10

2.4.4 RT-PCR

T100™ Thermal Cycler (Bio-Rad) and the GoTaq® Hot Start Polymerase system (Promega) was applied to perform all the RT-PCR experiments. Master mix was pre-made containing 1 x 1 x GoTaq® Flexi Buffer, 2.5 mM MgCl2, 0.2 mM of each dNTP (Life Technologies), 10 µM forward and reverse primers. and 0.5 units of GoTaq® Hot Start Polymerase enzyme, made up to 19 µl using nuclease-free dH$_2$O. 1 µl cDNA sample was added to make up the whole RT-PCR sample. PCR reaction was performed in the PCR machine and the thermal cycle program was set up as follow: 95 $^{\circ}$C 5 minutes, followed by a suitable number of cycles at

95 °C for 30 seconds, optimum annealing temperature for 30 sec, and a 72 °C extension of optimum extension time. 72 °C extension for further 10 minutes. Optimum annealing temperature of each primer set was determined by performing the RT-PCR on a positive cDNA control. Optimum extension time was calculated by template length and the speed of the extension enzyme. Human genomic DNA (Promega) was used as the positive control if the primers were contained within an exon. Optimum temperature of each primer set was tested in a range of 55-62 °C. All RT-PCR results include the target cDNA samples, RT-negative for each target cDNA sample, a non-template (cDNA negative) control and a positive control of human genomic DNA. GAPDH was used as the house-keeping gene to demonstrate equivalent stating amount of RNA/cDNA was used.

2.4.5 RT-qPCR

Quantitative or real-time PCR was performed to measure the accumulation of the SYBR® Green I Dye. It is aiming to quantify the gene transcription between samples. The Dye binds only to the double stranded DNA and emit a fluorescent signal proportional to the accumulation of PCR product. 19 ul master mix was pre-made and comprise of 300 nM target gene primer set, 15 ul 2 x SYBR® Green PCR

master mix (Applied Biosystems) containing SYBR® Green I dye, AmpliTaq Gold® DNA polymerase, dNTPs, and buffer components (including a passive reference ROX, which did not bind to DNA). 1 ul cDNA template was added to make up the final sample. Triplicate PCR reaction of each sample was conducted into a clear optical 96-well reaction plate and sealed with an optical adhesive cover (both Applied Biosystems). The PCR reaction was performed in BI Prism® 7900HT Sequence Detection System and analysed with Sequence Detection System software v2.2 (both Applied Biosystems). The PCR reaction program was set as follow: 95 °C for 10 minutes, 40 cycles of denaturation for 15 seconds at 95 °C, and extension for 1 minute at 60 °C. The fluorescence of the SYBR® Green I dye in each cycle was detected by the ABI Prism® and normalized against the ROX fluorophore. The final stage 'melt-curve' which involved three incubations at 95 °C, 60 °C, and finally 95 °C for 15 seconds each was performed to verify that a single product was formed. All qRT-PCR experiments include triplicates of target cDNA sample, RT-negative for each target cDNA sample, a non-template (cDNA negative) control, and a positive control of human genomic DNA. GAPDH was used as the house-keeping gene to check the template cDNA is at an equivalent concentration between samples.

2.5 Protein analysis

2.5.1 Indirect Immunofluorescence Microscopy

Indirect immunofluorescence (IF) is a technique aiming to identify the expression and localization of a protein in cultured cells or tissue samples. The technique relies on the application of primary antibody to the protein with fluorescently labelled secondary antibodies binds to the primary antibody. Cells or tissue requires to fix and permeabilized by lipid extraction or detergent to allow the detection of intracellular antigens.

2.5.1.1 Slide preparation

Sterilised 12-well glass slides (C.A.Hendley Ltd, Essex) were placed in 4-slide quadriPERM culture dishes (Sarstedt). NHU cells were seeded at 5 X 10^3 cells per well of the slide and left to attach at 37 ^{o}C for 4 hours before flooding with 5 ml KSFMc and left to grow at 37 ^{o}C in the cell incubator overnight. NHU cells were cultured to desired density before further differentiation treatment or pharmacological agents' treatment. When cells were ready, they will be washed twice briefly in PBS and fixed either by:

1. Methanol acetone fixing: Slides flooded for 30 seconds in a Methanol acetone mix (50: 50, v/v) before air-drying. Slides can used

immediately for immunolabelling or wrapped in Saran Wrap™ and stored with silica gel desiccant at -20 °C.

2. 10% formalin fixing: Slides flooded in 10% formalin for 10 minutes. The slides then further washed twice in PBS for 5 minutes and used immediately for immunolabelling. Slides were permeabilized in PBS containing 0.5% (w/v) Triton X-100 before antibody labelling.

2.5.1.2 Antibody labelling

A grease pen (Cell Path) was used to circle each well of the 12-well slide to prevent antibody movement. 30 µl of primary antibody, diluted diluted (as required) in Tris Buffered Saline (TBS), pH 7.6 with 0.1 % NaN3 (Sigma-Aldrich, S8032) and 0.1% bovine serum albumin (BSA) (Thermo Fisher Scientific, 37520) were added onto the wells and incubate at 4 °C overnight in a humidified chamber. For each experiment, a negative control was included with antibody diluent added only. Primary antibody was removed by washing 4 time, 5 minutes in PBS on an orbital shaker (Jencons-PLS, R100T/W). Then 30 µl of Alexa-488, 555 or 594-conjugated Goat anti-Rabbit IgG or Goat anti-Mouse IgG secondary antibodies diluted in Tris Buffered Saline (TBS), pH 7.6 with 0.1 % NaN3 (Sigma-Aldrich, S8032) and 0.1% bovine serum albumin (BSA) (Thermo Fisher Scientific, 37520) was applied to each well for 1 hour at

ambient temperature. Chamber containing the slides were covered with aluminium foil paper to protect from light. Slides were washed in PBS containing 0.25 % (w/v) Tween®20 twice for 5 minutes to remove excess secondary antibody. The slides were further incubating with PBS, containing 0.1 µg/ml Hoechst 33258 for 5 minutes to stain the nuclei. Slides were then rinsed in PBS for 5 minutes and then in dH2O for 5 minutes before mounting. The slides will be mounted in antifade mountant (Appendix XX) or Prolong™ Gold antifade (Thermo Fisher Scientific, P36930). Since the mountant was non-setting, coverslips were sealed with clear nail varnish. Slides were also mounted with Slides were examined by epifluorescent microscopy on an Olympus BX60 microscope.

2.5.2 Immunoblotting

2.5.2.1 Protein extraction

Before protein extraction, cultures were first wash twice with ice-cold PBS. Then protein was lysis under reducing conditions in 2 X SDS sample buffer, supplemented with 0.2 % DTT and 1 x protease inhibitor cocktail set III (Sigma). Lysis buffer applied to each culture and lysates which were harvest by scraping into ice-cold microfuge tubes using rubber cell scrapers (Sarstedt). Protein lysates were sonicated for two 10 second

burst and rest on ice in-between. The sonic probe at 25 W (Jencons) was clean with 70% ethanol between samples. The samples were further incubating on ice for 30 minutes and centrifuge at 25,000 g for 30 minutes at 4 °C. The supernatant was collected into clean, ice-cold microfuge tubes and used immediately for protein quantification. The protein lysates can store at -20 °C for weeks and can long-term store at -80 °C.

2.5.2.2 Protein quantification

Coomassie® protein assay kit was applied to measure the protein concentration of the protein lysates. Samples were diluted at 1/12.5 in dH$_2$O and 10 µl of dilute sample was added in duplicate to a 96-well plate. 10 µl aliquots of known protein concentration BSA sample (Supplied at 2 mg/ml from Pierce) were also added to the 96-well plate to generate a standard curve which contributes to calculate the unknown concentration of the loaded samples. Then 200 µl of Coomassie reagent was added to each well and shaken for 30 seconds in a Multiskan Ascent® plate reader (Thermo-scientific). The light absorbance of each sample was measure at reference wavelength of 570 nm and 630 nm respectively against a blank H$_2$O control. The Ascent software (version 2.6) was used to generate the standard curve and

calculate the protein concentration of samples.

2.5.2.3 SDS-PAGE and Western Blot

SDS-PAGE is the technique to separate linear proteins in a gel based on the size of the protein. To prepare the protein lysates for SDS-PAGE, 20 µg total protein was combined with 4x LDS (Novex®, NP0007) to a final concentration of 1x, 10x Reducing Agent (Novex®, NP0005) to a final concentration of 1x, and DEPC-treated water to a final volume of 20 µl. Sample were further heated at 70 °C for 10 minutes to denature the protein and brief centrifuge to collect the samples on the tube lid. NuPAGE® 4-12 % bis-Tris or 3-8 % Tris-acetate gels were selected for SDS-PAGE, depending on the molecular weight of the protein to be probed, with Tris-acetate gels used for larger proteins (>100 kD). NuPAGE® pre-cast gels contain a "stacker" gel at the top to concentrate proteins to ensure they enter the running gel collectively. The running gel is a gradient gel to promote the separation of the bands over a wide range of molecule weights. The loading samples were added to the well at the top of the gel which set up in the XCell Surelock™ Mini-Cell Electrophoresis system (Invitrogen, EI0002). The tank of the system containing 20x MOPs SDS buffer (Novex®, NP0001) or 20x Tris-Acetate SDS buffer (Novex®, LA0041) which were diluted to 1x in ELGA-treated

water and used as the running buffer. 200 µl NuPAGE® antioxidant added to the inner chamber prior to the running. Electrophoresis was performed at 200 V (for bis-tris) or 150 V (for tris-acetate) to separate proteins for approximately 1 hour with tank surrounded with ice. 6 µl Precision Plus Protein™ ladder (BioRad) was added to the first well in each gel to allow for estimation of protein size.

The protein was then transferred to an Immobilon-FL 0.45 µm PVDF membrane (Fisher Scientific, 10113432). The membrane was trimmed before rinsing in methanol for 30 seconds, washing in dH_2O and equilibrating in western blot transfer buffer (Appendix 2). The gel-membrane "sandwich" was assembled into the XCell II™ blot module (Life Technologies) with trimmed filter paper and blotting pad wrapped outside. The inner chamber of the blot module was filled with western blot transfer buffer and tap water was filled in the outer chamber. The tank was surrounded by ice to prevent overheating during transfer. Resolved proteins were electro-transferred from gel to membrane at 30 V for 1.5 h. The protein attached membranes were incubated in a solution of 0.5 % (w/v) Ponceau red to detect the protein band for successful transfer, equal loading and any air bubbles which may have interfered with transfer. The membrane then rinsed with dH2O to remove excess Ponceau red.

2.5.2.4 Immunolabelling

The membrane was blocked for 1 hour at ambient temperature using 50:50 Odyssey® blocking buffer (LI-COR): TBS to minimize non-specific binding by secondary antibodies. Membranes were probed with rabbit or mouse primary antibodies (Table 2.1), diluted in 50 % (v/v) Odyssey® blocking buffer in TBS + 0.5 % Tween®20 (TBST) and incubated for 16 h on an orbital shaker at 4 °C. The primary antibody will be harvest after incubation and membrane was washing in TBS for 4 X 5 minutes. Fluorescent dye-labelled secondary antibodies, AlexaFluor 680 goat anti-rabbit or IRDye800-conjugated goat anti-mouse IgG (Table 2.2), diluted in 50 % (v/v) Odyssey® blocking buffer in TBS + 0.5 % Tween®20, were applied to visualize the primary antibody. The negative control membrane was incubating with fluorescent dye-labelled secondary antibody alone. To remove excess secondary antibody, membranes were further washed with TBST 4 X 5 minutes and TBS 1 X 5 minutes. Membranes were scanned and fluorescent bands directly quantified using the Odyssey infrared imaging system and associated Odyssey software (v1.1; LI-COR). Band intensities were measured using the Odyssey software by drawing boxes around each protein band to calculate densitometry following background subtraction or calculated using the image J software to draw the box of the ban and quantified using the color intensity. Densitometry analysis was complete for β-actin

or Histone 3 expression which was used as a loading control to normalize protein loading in each lane.

Figure 2. 2: Rabbit secondary antibody test.
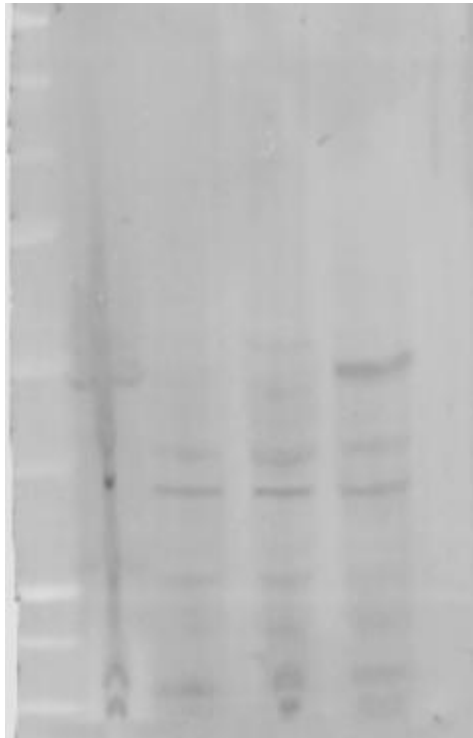
Four different NHU cell protein lysates were loaded with only secondary antibody bloted in the membrane.

2.5.2.4.1 Slide Scanner analysis of immunolabelling

Antibody-labelled 12 well slides were scanned on a Zeiss AxioScan. Z1 slide scanner. Each well was circles out automatically with immunofluorescent channels selected. The slide scanner machine will automatically adjust the focus and scanned selected wells in the slides. Analysis of the generated image was using the HistoQuest (TissueGnostics) image analysis software. The cells were automatically

selected based on the staining of the Hochest33258. The percentage of positive labelled cells (Red: 547, 555. Green:488) was calculated based on the number of Hochest33258 labelled cells.

2.5.2.4.2 Image J analysis of immunolabelling

Analysis of the image was performed in ImageJ software. Hoechst33258 stained image was firstly opened in Image J to identify the cells. Applying Process>Binary>Make Binary to generate black and white image to detect the nucleus of the cells. Then perform Process>Binary>Fill holes to filling up the blank space in the nucleus. Perform Process>Binary>Watershed to automatically separate connected or overlapping cells. Then perform Analyze>Analyze Particles to count every cell in the image. At last, open the target expression image in Image J and perform Image>Overlay>From ROI manager to overlap with the previous image. The target intensity of each cell will be present in the ROI manager window.

2.5.2.5 Striping and re-probing of membranes

To allowing for multiple labelling of antibodies in the blot, the membranes were stripped by incubating for 30 minutes in high pH western blot recycling buffer (Source Bioscience), diluted 1:10 in dH2O.

After stripping, the membrane will be incubating with secondary antibody and scanned as above to confirm the removal of primary antibodies. Then membrane will be re-probe with the primary antibody and finish the immunolabelling as described above.

2.6 Functional studies

2.6.1 TER measurement

NHU cells were seeded on the 0.45 μM permeable Snapwell^{TM} membranes (Fisher Scientific) at density of 5 X 10^5 cells per 1.1 cm^2 membrane. Three replicates were included for each group. The NHU cells then differentiated using ABS/Ca^{2+} differentiation methods as described previously. For each well, 0.5 ml medium was added to the inner chamber and 3 ml medium was added to the outer chamber. After the NHU cells were differentiated, transepithelial electrical resistance (TER) was measure every daytime points. The TER probe was sterilized in Cidex Plus®, 3.4 % (v/v) gluteraldehyde solution (Civco Medical Solutions) for 20 minutes before incubates in growth medium for 2 X 5 minutes. After wash, the electrical resistance of a blank (no cells) membrane was measured and used as the control. The experimental reading will subtract the reading of the control and record as the resistance of the cell sheet alone in the membrane.

2.6.2 Wound healing assay

NHU cells were seeded in either 12 wells slide or 24 well plate. The NHU cells then differentiated using the ABS/Ca^{2+} differentiation method as described above. After differentiated, NHU cells were culture in fresh medium 24 hours before scratch-wounded. The cultured NHU cells will be wounded using a 100 μl sterile pipette tip to generate an approximately 750-1000 μm wide horizontal scratch over the well of the plate or the slide. The wound healing process will be either observed under the microscope or analyze using the time-lapse machine.

2.6.3 Analysis of wound healing in differentiated NHU cells using time-lapse microscopy

The scratch-wounded NHU cells in the 24-well plate were places into an environmental chamber (Solent Scientific) at 37 °C with 5 % CO_2 (in air) feed for buffering of medium. The wound healing process of each well on the plate was monitored by phase-contrast microscopy using an Olympus IX81 motorised microscope. Image taken interval time was set based on the experimental design with image automatically captured using CellM image capture software over a time-course of 36-48 hours. The image analysis software was then used to measure the initial wound area and serial wound-areas during repair to calculate the percentage

wound-closure at various time points. Three replicate cultures were measured for each experimental condition and the mean percentage wound closure plotted against time.

Chapter 3: Transcription variants of *PPARG* and Expression of PPARγ protein in Normal Human Urothelial Cells

3. Transcription variants of PPARG and Expression of PPARγ protein in Normal Human Urothelial Cells

3.1 Rationale and Aim

It is known that there exist different *PPARG* transcription variants in human tissues which differentially encode PPARγ protein isoform 1 and PPARγ protein isoform 2. These PPARγ protein isoforms are involved in different biological processes in human tissues. Previously, our lab has implicated *PPARG* transcription and activation in human urothelial cell differentiation. However, it remains unknown which PPARγ protein isoform is expressed or functions during urothelial cell differentiation.

The aim of this chapter was to identify the transcription variants of *PPARG* in human urothelial cells and examine expression of PPARγ protein during urothelial cell differentiation. To achieve the aim, the objectives were to:

- Describe and quantify the transcription variants of *PPARG* expressed in human urothelial cells in situ and *in vitro*.

- Verify the transcription of *PPARG* and its potential downstream targets in during urothelial cell differentiation.

- Explore the expression of PPARγ protein isoforms in human urothelial cells.

o Explore the expression of PPARγ protein and its potential downstream targets during urothelial cell differentiation.

The hypothesis was that:

The expression of PPARγ and its potential downstream targets increases during urothelial cell differentiation to drive the differentiation process.

3.2 Experimental Approach

Urothelial cells were isolated from human ureter tissue samples and expanded as NHU cells by culture *in vitro* in KSFMc medium (section 2.3.2.3). The differentiation of NHU cells was induced *in vitro* by adding PPARγ agonist troglitazone (TZ) and EGFR inhibitor PD153035 (PD) together (section 2.3.3.1). The differentiation of NHU cells to a barrier-forming urothelium could also be achieved by pre-treating with 5% ABS for 72 hours followed by an increase of calcium concentration to 2mM (section 2.3.3.1). Based on these techniques, the RNA and protein of urothelial cells in situ, proliferating urothelial cells *in vitro*, confluent urothelial cell *in vitro* and differentiated urothelial cells *in vitro* could be collected for further analysis.

3.2.1 Explore and quantify the transcription variants of *PPARG* in human urothelial cells

Human urothelium was separated and collected from one ureter tissue sample. The RNA of the human urothelial cells was extracted (section 2.4.1) and used for Nanopore long sequencing to identify the transcript variants of *PPARG* in human urothelium. The abundance of each transcript variant of *PPARG* was calculated based on the short RNA sequencing results from three independent urothelial cell lines. Help was provided by Dr Andrew Mason.

3.2.2 NHU cell samples collecting

To verify the transcription of *PPARG* and expression of PPARγ in NHU cells, proliferating, differentiated, and in situ NHU cell samples were included. Three independent *in vitro* urothelial cell line lines Y2244, Y2080, and Y1236 were included. A time-course experiment of TZPD differentiation and ABS/Ca^{2+} differentiation was set up to collect NHU cell samples during the differentiation process. Y2249 is the NHU cell line directly isolated from the tissue which represent NHU cells in situ and immediately go through RNA extraction after isolation. The in situ NHU cells were highly differentiated and used as the positive control of differentiated NHU cells *in vitro*.

3.2.3 Identify the expression of PPARγ protein in human urothelial cells

Protein lysates generated from NHU cell samples described above (section 3.2.2) were generated, separated by polyacrylamide gel electrophoresis and electrotransferred onto membranes for western blotting (sections 2.5.2.1 to 2.5.2.3). To identify PPARγ protein in these urothelial cells, two different primary antibodies (81B8 & D69) that bind at each end of the PPARγ protein were applied (Figure 3.1). To further study expression of PPARγ protein in NHU cells, undifferentiated and differentiated NHU cells were grown and fixed on 12 well slides followed by indirect immunofluorescence microscopy analysis. The expression of PPARγ in urothelial cells was semi-quantified by using set exposures to capture images and calculating the nuclear intensity of PPARγ using Image J.

Figure 3. 1: Binding site of PPARγ antibody D69 and 81B8.
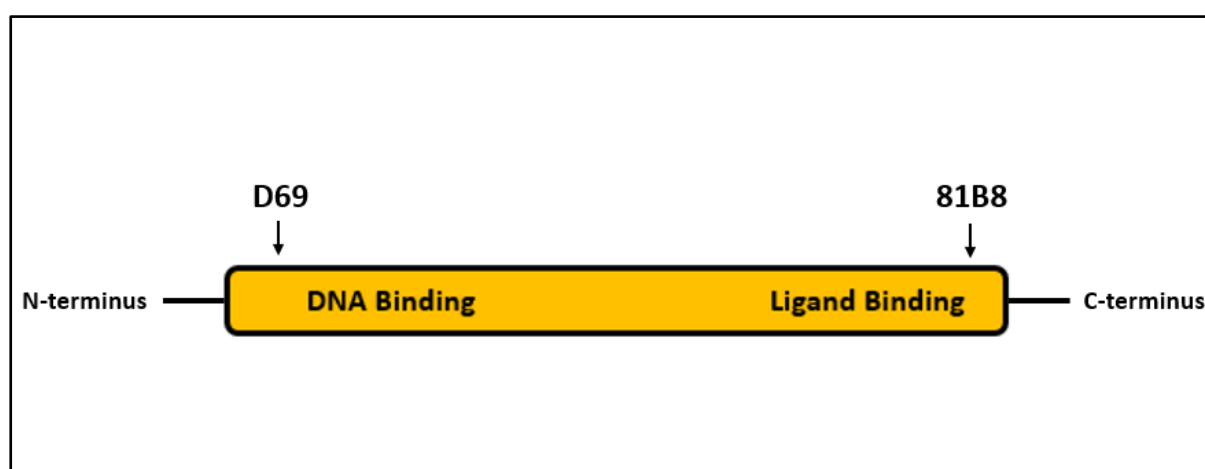
The above graph simply showed the structure of PPARγ protein which DNA binding domain on the N-terminus side and Ligand-binding domain on the C-terminus side. D69 is a rabbit polyclonal antibody binds to the N-terminus side of PPARγ. 81B8 is also a rabbit polyclonal antibody binds to the C-terminus side of PPARγ.

3.3 Results

3.3.1 Transcription of *PPARG* transcription variants in ureteric urothelium in situ

Human *PPARG* consists of nine exons but can develop into different transcript variants by differential promoter usage and alternative splicing. The transcript variants of *PPARG* display six conserved coding exons with different 5' untranslated regions (UTRs). Here, Dr Andrew Mason helped describe the transcript variants of PPARγ in urothelium in situ (sample Y2391) using nanopore long RNAseq technique. Each transcript variant was given an identical name (STRG.10532. *) (Figure 3.2). All transcript variants contained the conserved exons 1-6 which encode the PPARγ protein. Exons within the 5' UTR were different for each transcript variant. Although variable transcript variants of *PPARG* were identified, they only encoded two protein isoforms- PPARγ protein isoform 1 (PPARγ1) and PPARγ protein isoform 2 (PPARγ2). Transcripts encode PPARγ 2 contain an exon B which could translated to 28 amino acids. Thus, PPARγ 2 was 28 amino acids longer than PPARγ 1. The abundance of transcript variants of *PPARG* was quantified based on the

short RNAseq data of three independent in situ urothelial cell lines (Y1026, Y1077, and Y1108). Twelve transcript variants were selected (Transcript abundance ≥0.01%) (Figure 3.2). Among the twelve transcript variants, only transcript STRG.10532.15 encoded PPARγ 2 and rest were encoding PPARγ 1. The transcription abundance of STRG.10532.15 was 0.02% indicating transcripts encoding PPARγ 1 was highly dominant in urothelial cells.

Figure 3. 2: *PPARG* transcription variants of NHU cells in situ.
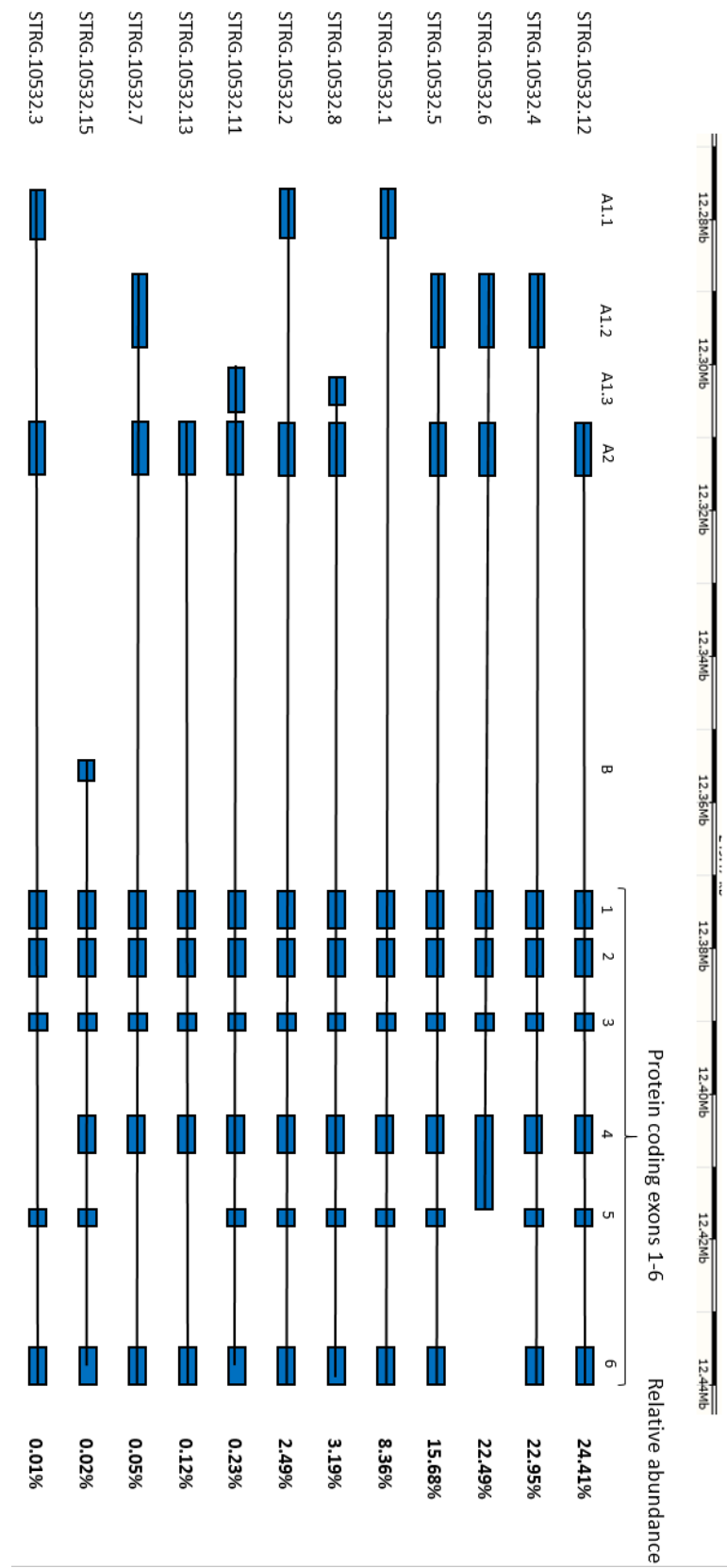
Schematic structure of *PPARG* transcript variants identified in in situ urothelial cells. Identical name (STRG.10532. *) of each transcription variants were labelled on the left. Conserved exons 1-6 encode the PPARγ protein isoform 1. Exons A1.1, A1.2, A1.3 and A2 are UTRs encoding no proteins. Exon B exon encoded 28 amino acids which contributes to the translation of PPARγ protein isoform 2. The abundance of each transcript variant quantified by short RNA sequencing was cited on the right side of each transcription variant.

3.3.2 *PPARG* transcription during NHU cells differentiation

The morphology of urothelial cells was observed during both the TZPD differentiation and ABS/Ca^{2+} differentiation. Compared to untreated NHU cells, urothelial cells formed a rosette morphology after TZPD differentiated for 7 days. However, the morphology of NHU cells shows no difference during ABS/Ca^{2+} differentiation (Figure 3.3).

From the RT-PCR results (Figure 3.3), transcription of differentiation-associated genes *FOXA1, GATA3* and differentiation-restricted gene *UPK2* were used to verify the differentiation state of urothelial cells. *FOXA1,* and *GATA3* were not or weakly transcribed in undifferentiated NHU cells but highly transcribe when the TZPD differentiation process started. *UPK2* was only transcribed at the late stage of differentiation (day 4). The results found *PPARG* was continuously transcribed in both undifferentiated and differentiated urothelial cells, indicating that transcription of *PPARG* was independent of differentiation state. During ABS/Ca^{2+} differentiation, the transcription of *PPARG* was consistent with

TZPD differentiation which is shown during the entire differentiation process. The transcription of *FOXA1, and GATA3* genes also showed a similar pattern compared to the TZPD differentiation: they were all highly transcribed after differentiation induced. The differentiation-restricted gene *UPK2* was only transcribed at late stage of ABS/Ca^{2+} differentiation (day 4).

Figure 3. 3: Morphology of NHU cells go through TZPD or ABS/Ca2+ differentiation.
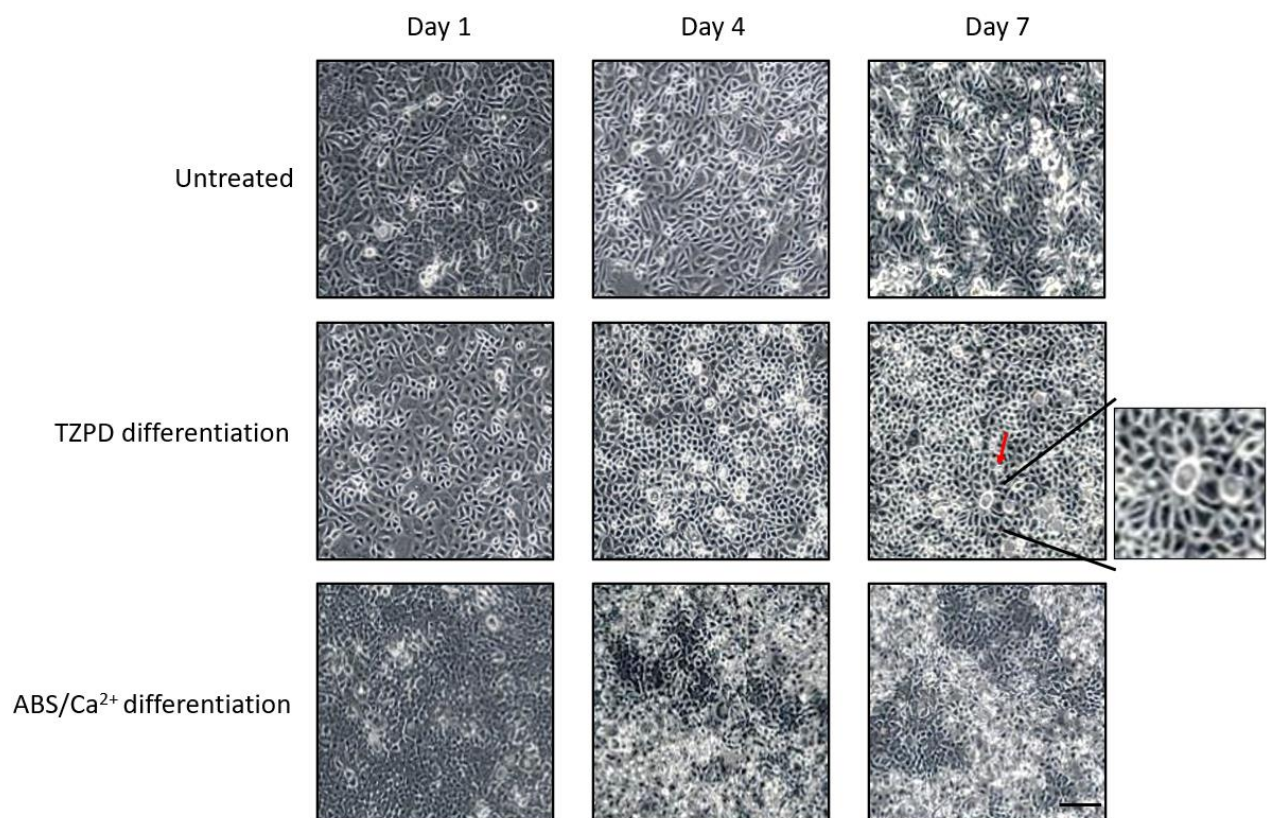
Phase contrast morphology of untreated NHU cells, TZPD differentiated NHU cells, and ABS/Ca2+ differentiated NHU cells. Images of NHU cell Y2244 were taken at time points day 1, day 4, and day 7. The red arrow points the rosette morphology of NHU cells after TZPD differentiated for 7 days. Bar, 200 μm.

Figure 3. 4: RT-PCR screen of *PPARG* transcription in urothelial cells.
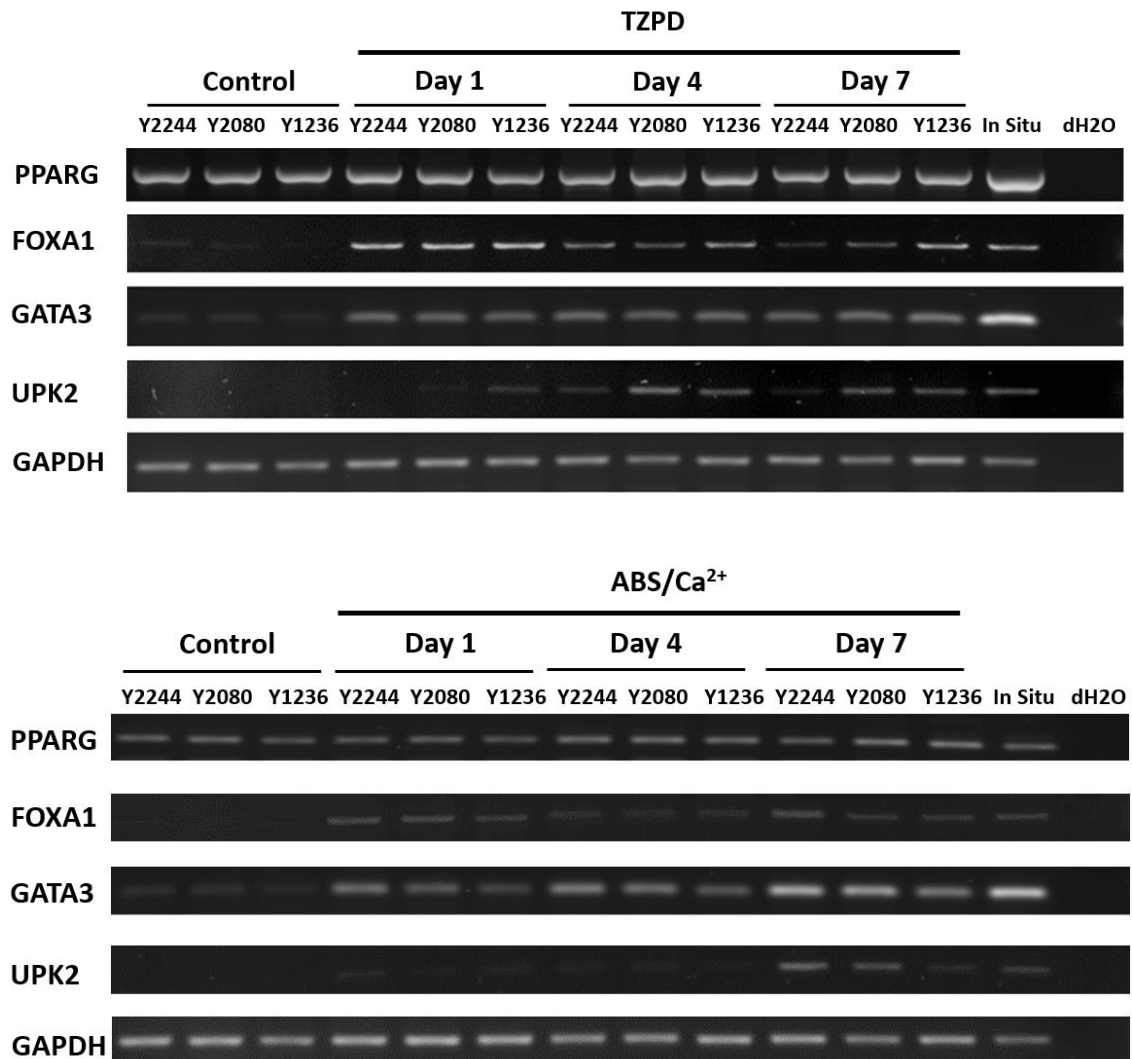
RT-PCR screen to assess transcript expression during NHU cell differentiation. Three independent NHU cell lines Y2244, Y2080, and Y1236 were used. Same amount of cDNA of each sample was loaded. The samples were electrophoresed and *GAPDH* was used as housekeeping gene. RNA was extracted from untreated NHU cells, TZPD differentiated NHU cells and ABS/Ca^{2+} differentiated NHU cells. In situ NHU cell line Y2249 was included as a positive control. DEPC-dH$_2$O was used as a negative control. Differentiation-associated genes and differentiation-restricted gene UPK2 were applied to identify the differentiation state of NHU cell lines. RT negative products which use water as template were also included to verify no contamination of DNA in each sample during RNA extraction. All product results from 25-30 PCR cycles.

3.3.3 Transcription of differentiation-associated transcription factors during NHU cell differentiation

PPARG was shown to continuously transcribed in NHU cells (section 3.3.2). RNAseq data verified that the transcription of *PPARG* shows no difference during the TZPD differentiation (P> 0.05) (Figure 3.5). FABP4, known as the PPARγ reporter in adipogenesis, was significantly higher transcribed when differentiation was initiated suggest it might be NHU cells differentiation-associated (P< 0.05). Previous results also shown that the transcription of differentiation-associated transcription factors *GATA3* and *FOXA1* during NHU differentiation (section 3.3.2). The RNAseq data here found that the transcription of *GATA3* and *FOXA1* was significantly higher transcribed in differentiated NHU cells compared to undifferentiated NHU cells(P> 0.05). Moreover, ELF3 as a recent identified differentiation-associated transcription factor is also significantly transcribed in differentiated NHU cells.

Figure 3. 5: Transcription of *PPARG*, *ELF3*, *GATA3*, *FOXA1*, and *FABP4* during NHU cell differentiation.
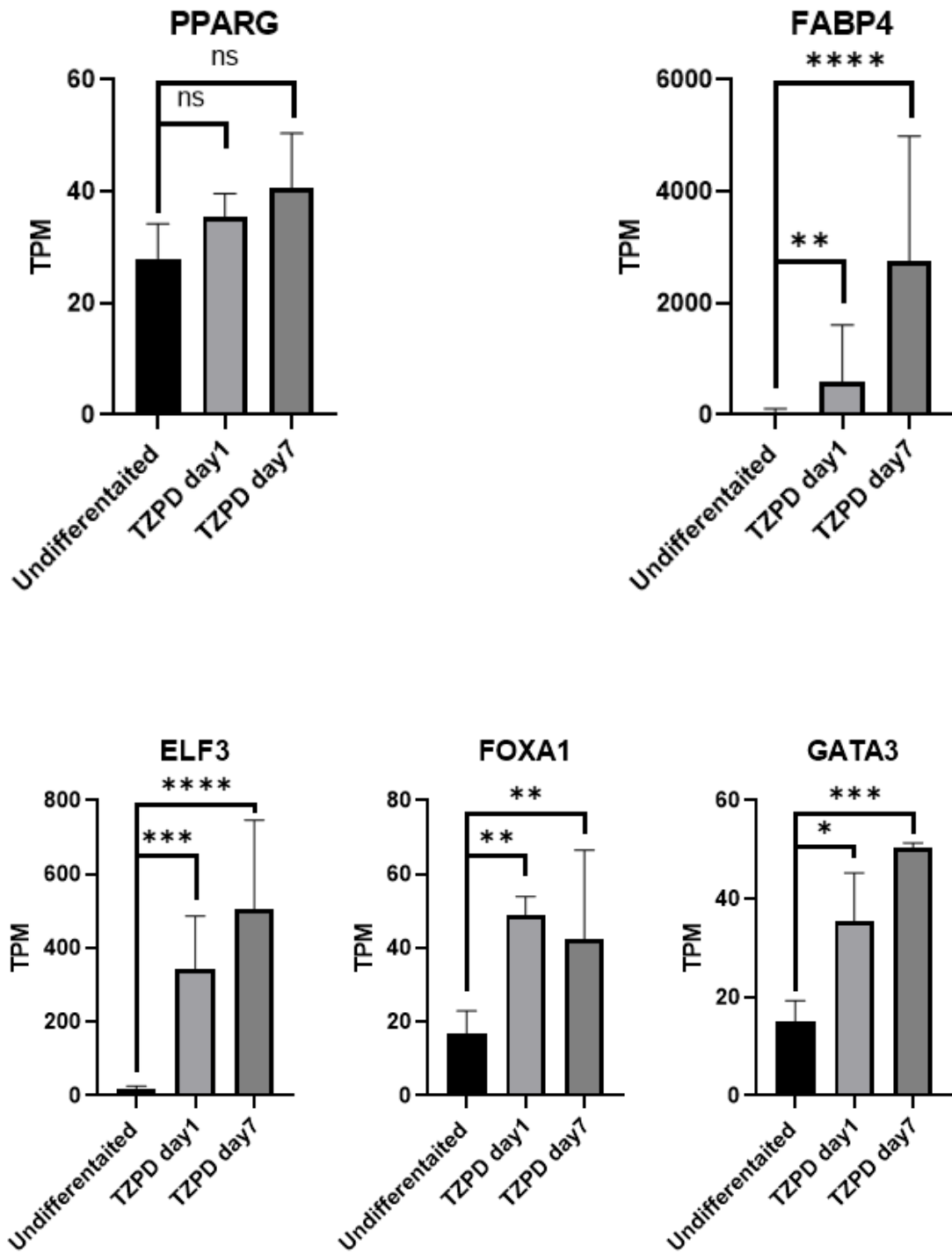
RNAseq data from NHU cell lines Y967, Y1192, and Y1214. Y axis shows the TPM of each gene. One Way ANOVA was applied to quantify the difference between groups with post-HOC test to further identify the difference between each group. NS represent p-value > 0.05. *, **, and *** represents P-value < 0.05. **** represent P-value < 0.01.

3.3.4 Expression of PPARγ protein in NHU Cells *in vitro*

Previous results (section 3.3.2) verified that *PPARG* was continuously transcribed in undifferentiated and differentiated urothelial cells while *PPARG* encode PPARγ 1 was dominantly transcribed. Up to now, the expression of PPARγ protein isoform in human urothelial cells stays unknown.

To validate the anti-PPARγ antibodies, MCF-7 cells was selected as a breast cancer cell line that show no expression of PPARγ protein. MCF-7 cells transduced with empty vector, PPARγ protein isoform 1 and PPARγ protein isoform 2 were used as negative and positive controls. The results indicate that only PPARγ1 is expressed in human urothelial cells and no expression of PPARγ2 was detected in any state (Figure 3.6). The result further verifies the transcription result identifying *PPARG1* as important in urothelial cells. Importantly, expression of PPARγ protein was not detected in proliferating urothelial cells and was only weakly detected in confluent urothelial cells. It suggested that transcription of *PPARG* is not always followed by the translation of PPARγ protein. The

PPARγ protein was highly expressed in differentiated NHU cells indicate expression of PPARγ protein was differentiation-associated.

Figure 3. 6: Expression of PPARγ in NHU cells.
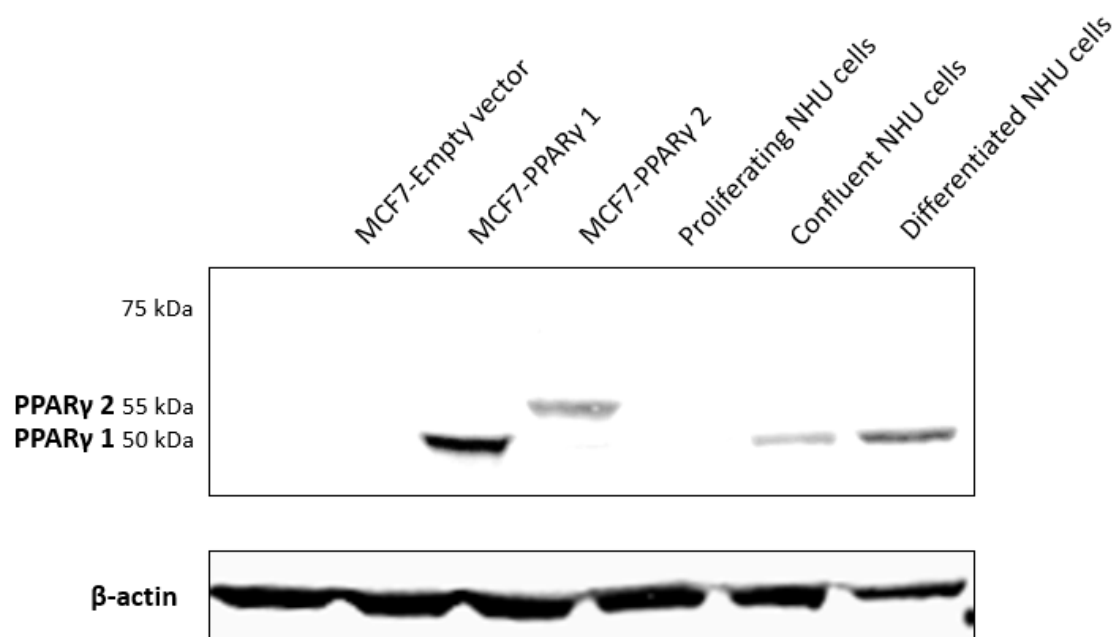
Western blot was applied to detect the expression of PPARγ protein in NHU cells. 20 µg of total protein was loaded. β-actin was used as housekeeping protein. MCF-7 breast cancer cells transduced with empty vector, PPARγ protein isoform 1, and PPARγ protein isoform2 were used as negative and positive control. Antibody 81B8 was applied to detect the PPAR protein isoform1 (PPARγ1) and PPARγ protein isoform 2 (PPARγ2) at 50 and 55 kDa.

3.3.5 Expression of PPARγ protein during NHU cells differentiation

Expression of PPARγ protein in undifferentiated and differentiated urothelial cells showed that it was dramatically increased in differentiated urothelial cells (section 3.4). Further experiment was designed to investigate the expression of PPARγ protein during the NHU

cells differentiation. Claudin 4 was a NHU cell differentiation-restrict protein, and its expression indicate both differentiation methods were successful. The expression of PPARγ protein was obviously detected when the differentiation was initiated, and the expression was increased within the differentiation in the first few days in TZPD differentiation (Figure 3.7). PPARγ protein was also obviously shown after initiation of ABS/Ca2+ differentiation but the expression of PPARγ was similar during the entire differentiation process compared to TZPD differentiation (Figure 3.8). The differentiation-associated transcription factors ELF3 was not expressed unless the differentiation was started, and its expression pattern was consistent with the expression of PPARγ in both differentiation procedures. FABP4 was identified as the reporter of PPARγ in aidpogenesis. However, it was only expressed during TZPD differentiation. MCM2 is a proliferation-associated protein. Its expression showed no significant change during TZPD differentiation but decrease with the time during ABS/Ca^{2+} differentiation.

Figure 3. 7: Expression of PPARγ during NHU differentiation.

TZPD differentiation

| | Ctrl | Day1 | Day2 | Day3 | Day4 | Day5 | Day6 | Day7 |

PPARγ

ELF3

FABP4

Claudin 4

MCM2

β-actin

5% ABS   5% ABS + 2mM Ca²⁺

| | Ctrl | Day1 | Day2 | Day3 | Day4 | Day5 | Day6 | Day7 | Day8 |

PPARγ

ELF3

FABP4

Claudin 4

MCM2
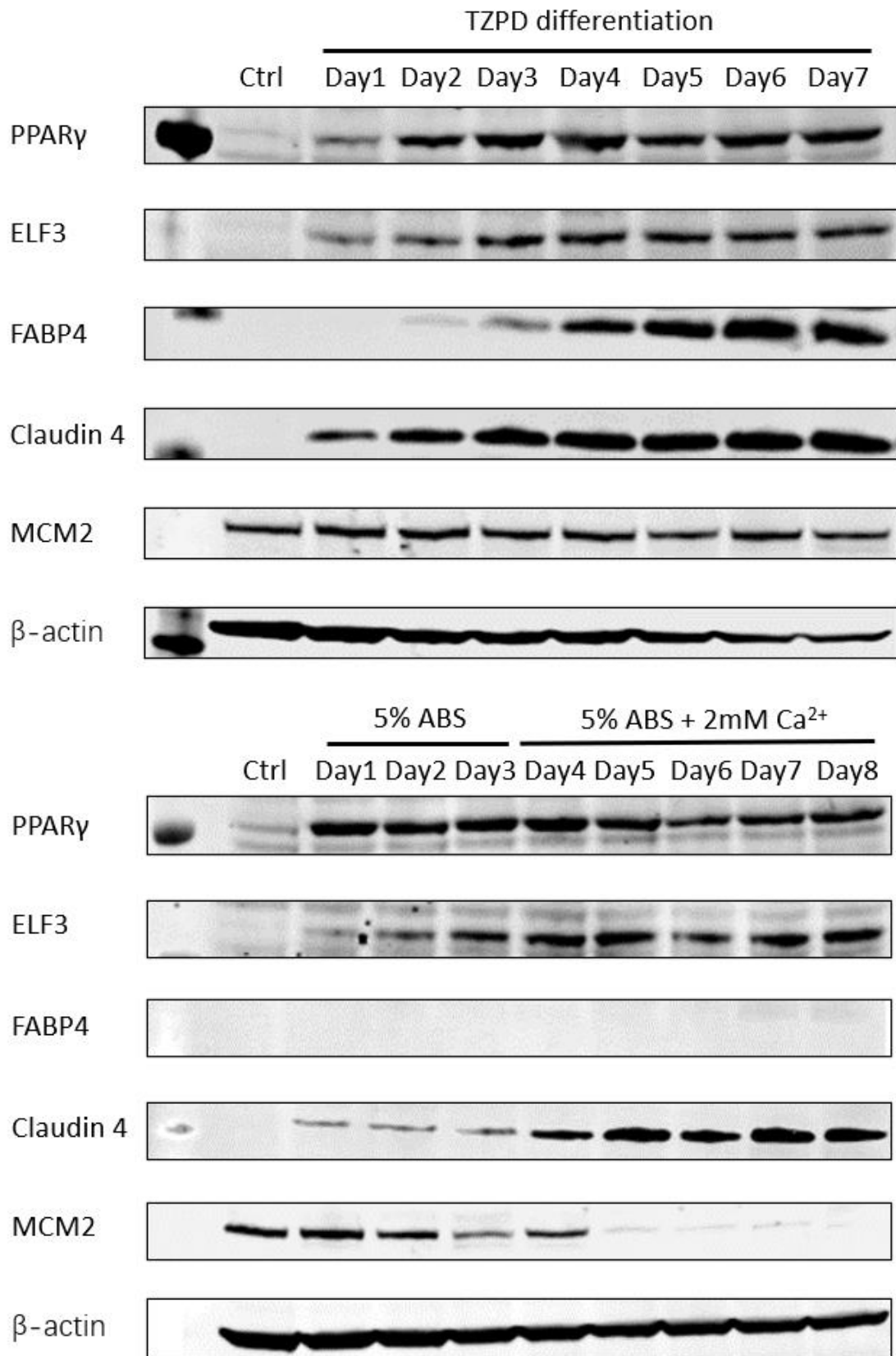
β-actin

Western blot applied to detect the expression of PPARγ during NHU differentiation. 20 μg of total protein was loaded. β-actin was used as housekeeping protein. Antibody 81B8 was used to detect PPARγ at 50 KDa. Ctrl was untreated NHU cells at day 0 before differentiation.

3.4 Discussion

3.4.1 *PPARG* transcription variants

To fully define the landscape of PPARγ protein activity in NHU cells, some relevant aspects need to be taken into account. The most relevant feature is *PPARG* gene could give rise to different transcripts which result in the translation of PPARγ1 or PPARγ2. In the chapter, it is the first investigation in which nanopore long RNA sequencing was applied to identify the existing transcription variants of *PPARG* in NHU cells. There is only one transcript of *PPARG* encoding PPARγ2 and rest were all encoding PPARγ1 (Section 3.3.1.1). RNA sequencing result of three independent NHU cell lines was included and quantify the transcribe of each transcription variants of *PPARG* in NHU cells. Opposite to adipose cells, *PPARG* transcript encoding PPARγ1 was dominantly transcribed suggest it is PPARγ1 functions in NHU cells.

3.4.2 PPARγ protein isoform 1 functions in NHU cells

In adipogenesis, PPARγ2 was demonstrated to be the main protein isoform type functions and regulate adipogenesis (Section 1.3.2). Although expression and function of PPARγ protein isoforms in NHU cells

was not studied before, recent study suggested that PPARγ2 was the isoform expressed principally in adipocyte cells, as well as in urothelial cells, whereas PPARγ1 is ubiquitously expressed (Rochel et al., 2019). Previous finding has verified *PPARG* encoding PPARγ1 was dominantly transcribed. It is further investigated the expression of PPARγ protein isoforms in NHU cells. The results clearly showed it is only PPARγ1 expressed in NHU cells (Section 3.3.3). To fill the knowledge gap about which PPARγ protein isoform functions in NHU cells, the results demonstrated that it is PPARγ1 expressed in NHU cell at protein level. The evidence suggest PPARγ1 was the protein isoform functions in NHU cells and following research in NHU cells will focused on this isoform.

3.4.3 Expression of PPARγ1 during NHU cells differentiation

RT-PCR was applied to identify the transcription of *PPARG* in different state of NHU cells. *PPARG* was transcribed in both undifferentiated and differentiated NHU cells (Section 3.3.1.2). However, limited PPARγ protein was detected in undifferentiated NHU cells but highly expressed when differentiation process was initiated (Section 3.3.3). Although there exists evidence that transcription could coupled with translation in mammalian cells (Iborra et al., 2001), it is more widely accepted that transcription happens in nucleus while translation separately occurs in cytoplasm. Study also suggested that translation becomes increasingly

114

regulated with the onset of stem cell differentiation and cell-cycle was coupled to the post-transcriptional repression in stem cells (Baser et al., 2019). Considering differentiation of NHU cells requires exit of cell cycle, the translation of PPARγ might repressed in proliferation NHU cells and initiate together with the start of differentiation. The total expression of PPARγ protein shows no significant changed during NHU cell differentiation and it is only PPARγ1 expressed during the whole differentiation process. It further verified it is PPARγ1 functions in NHU cell differentiation. The expression of several differentiation-associated transcription factors was consistent with the expression of PPARγ (Section 3.3.4). Previous study in the lab also suggested that these transcription factors were high possible PPARγ downstream signals but needs further verification.

3.5 Summary of findings

In summary, the results verified that *PPARG* encoding PPARγ protein isoform 1 was dominantly transcribed in in situ urothelial cells. Further research verified that only PPARγ protein isoform 1 was expressed in NHU cells *in vitro*. It is weakly detected in confluent NHU cells and highly expressed in differentiated NHU cells. Moreover, the expression of PPARγ was increased during TZPD differentiation but its expression during ABS/Ca^{2+} differentiation shows no significant difference. However,

it is unclear why there is transcription of *PPARG* in proliferating NHU cells but no expression of PPARγ protein was shown. Next chapter will focus on the translation of PPARγ protein in NHU cells and investigate its downstream targets during NHU cells differentiation.

Chapter 4: Protein abundance of PPARγ and its downstream targets in Normal Human Urothelial (NHU) cells

4. Protein abundance of PPARγ and its downstream targets in Normal Human Urothelial (NHU) cells

4.1 Rationale and Aim

Previous results in chapter 3 have shown the transcription of *PPARG* and expression of PPARγ in NHU cells during differentiation. The expression of PPARγ protein detected by antibody D69 or 81B8 was not consistent with the transcription of *PPARG*. However, the mechanism underlying the translation of PPARγ protein in NHU cells was unclear. In the literature it has been reported that inhibition of EGFR using PD1503035 combined with PPARγ agonist troglitazone could induce the differentiation of NHU cells (Claire, 2004). This paper indicated that inhibition of EGFR signaling helps to induce the NHU cells differentiation, but its mechanism is not fully understood. Moreover, urothelial cell differentiation-associated transcription factors were identified in previous literature published from the lab (Bock et al., 2014; Varley et al., 2009). But the relationship between PPARγ protein to the expression of those transcription factors is not fully clear. Characterizing the relationship between PPARγ protein and differentiation-associated TFs and other markers is important for understanding the role of PPARγ signalling in urothelial cell differentiation. To achieve the aim, the objectives were to:

● Investigate the relationship between inhibition of EGFR and translation of PPARγ protein in urothelial cells.

● Explore the downstream targets of PPARγ in differentiating human urothelial cells.

The hypothesis was that inhibition of EGFR was required for the translation of PPARγ protein. ELF3, as a urothelial differentiation-associate transcription factor and FABP4 were predicted as the downstream targets of PPARγ in urothelial cells.

4.2 Experimental approach

4.2.1 Inhibition of EGFR signalling pathway

EGFR signalling is a well-known signalling pathway involved in many cellular biological processes and given its previous implication in urothelial differentiation (Varley ref), is predicted to play a role in PPARγ protein translation in urothelial cells. Downstream signaling of EGFR includes PI3K-AKT signalling and RAS-RAF-MEK-ERK signaling. Different inhibitors of EGFR and its downstream targets were used as shown in Figure 4.1. DMSO was included as the vehicle solvent throughout at 0.1%. Urothelial cells were cultured with the inhibitors for 24 hours and

72 hours. Expression of PPARγ protein was evaluated by both western blot and immunofluorescence.

Figure 4. 1: Inhibitors of EGFR and its downstream targets.
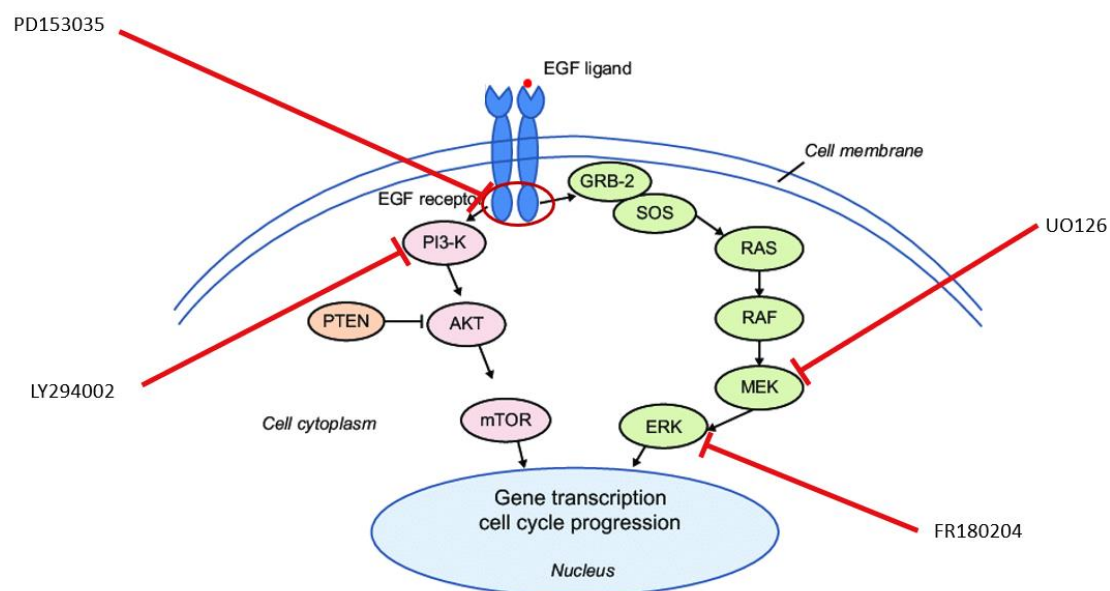
Schematic graph showing the EGFR signaling. EGFR inhibitor (PD153035), PI3K inhibitor (LY294002), MEK inhibitor (UO126), ERK inhibitor (FR180204) and their inhibiting target was shown in the figure.

4.2.2 Optimizing the concentration of MEK inhibitor UO126

MEK was the downstream target of EGFR signalling. UO126 is a drug commonly used as the MEK inhibitor. To optimize the concentration of UO126 to inhibit MEK kinase, different concentrations of UO126 was added to NHU cells. Urothelial cells were first cultured to 50% confluence to maintain its proliferating state. UO126 was then added at concentration 50 nM, 500 nM, 1 µM, and 5 µM for 30 min and 2 hours. ERK kinase was the downstream target of MEK. Inhibition of MEK results

in the loss of phosphorylation of ERK. Inhibition of EGFR using PD153035 was included as the positive control. Results verified that applying UO126 at 5 µM was sufficient to completely inhibit MEK kinase (Figure 4.2).

Figure 4. 2: Optimizing the concentration of UO126.
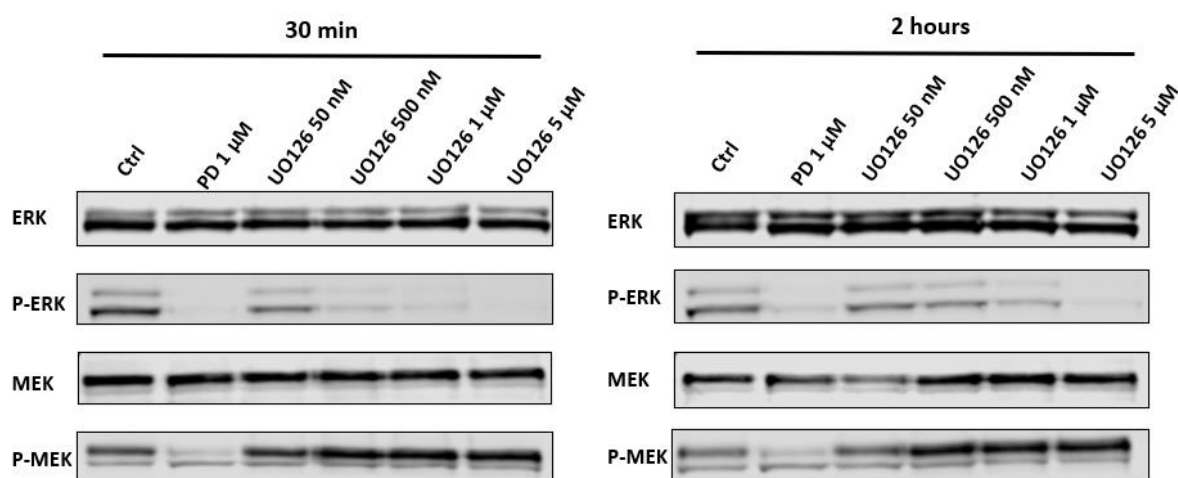
NHU cells were cultured to 50% confluence. Drugs were dissolved in 0.1% DMSO at different concentration and then added to the NHU cells for 30 min or 2 hours. NHU cells with 0.1% DMSO was used as the control. Protein lysates were harvest and western blot was used to detect the phosphorylation of ERK.

4.2.3 Activation and inhibition of PPARγ

TZPD differentiation relies on the activation of PPARγ by adding PPARγ agonist troglitazone at 1 µM. Troglitazone is an artificial ligand that competitively binds to the ligand-binding pocket of PPARγ protein to activate it (Figure 4.3). PPARγ antagonist T0070907 is a small molecule compound that irreversibly binds to the ligand-binding pocket of PPARγ

protein to inhibit activation of PPARγ. Activation and inhibition of PPARγ was applied to discover the downstream target of PPARγ in urothelial cells.

Figure 4. 3: Ligand-binding pocket of PPARγ protein.
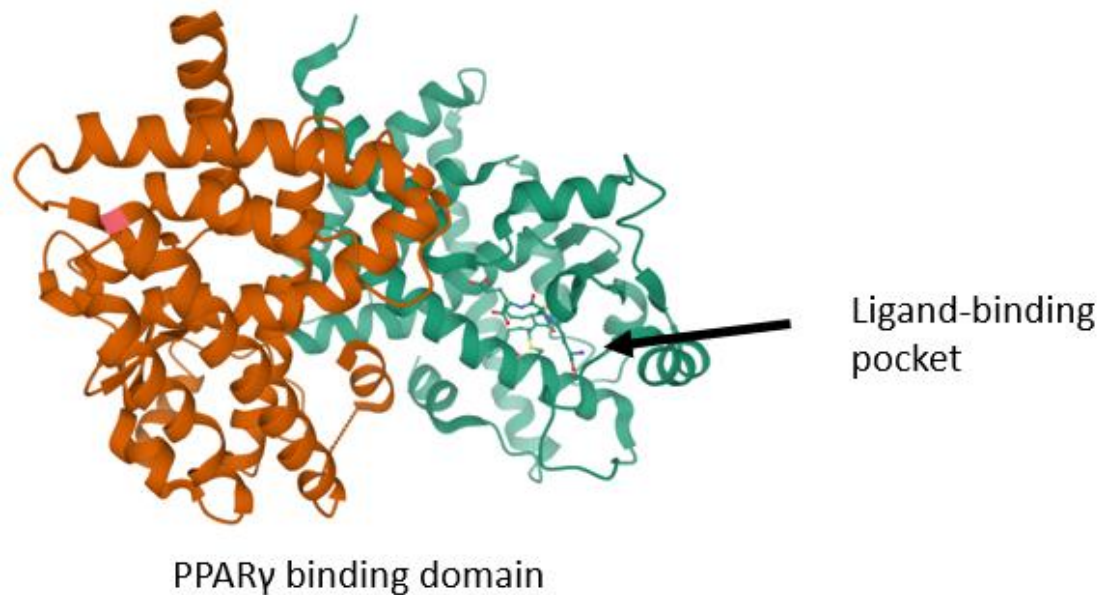
The figure was adapted from the structure of PPARγ in the Protein Data Base (PDB).

4.3 Results

4.3.1 Translation of PPARγ protein in NHU cells *in vitro*

4.3.1.1 Inhibition of EGFR induce the translation of PPARγ protein

Inhibition of EGFR using 1 μM PD153035 combined with activation of PPARγ using 1μM troglitazone (TZ) could induce the differentiation of NHU cells *in vitro*. The previous results found abundant protein expression of PPARγ protein was detected upon its activation within the

initiation of NHU cell differentiation (Section 3.5). As inhibition of EGFR was required to induce the NHU cell differentiation in the TZPD differentiation method, it might involve in PPARγ protein translation. NHU cells were either TZPD differentiated or treated with 1 µM EGFR inhibitor PD153035 or 1 µM TZ. Undifferentiated NHU cell was included as control.

The cell morphology of TZ treated NHU cells is similar to the undifferentiated NHU cells (Figure 4.4). Meanwhile the cell morphology of PD153035 treated cells show similarity with TZPD differentiated NHU cells but did not show any TZPD differentiation-associated rosette phenotype. From protein lysates of confluent NHU cells collected after culturing for 7 days, western blot results showed that inhibition of EGFR signaling alone could induce the translation of PPARγ protein (Figure 4.5). By contrast, NHU cells treated with PPARγ agonist TZ at 1 µM alone was unable to initiate the translation of PPARγ protein. The experiment was repeated in three independent NHU cell lines (Appendix , page) with expression of PPARγ quantified using Image J. The expression of PPARγ in PD153035 treated urothelial cells was weaker compared to TZPD differentiated NHU cells (Figure 4.5). Although expression of PPARγ was obviously shown in EGFR-inhibited NHU cells, the expression of differentiation-associate transcription factor ELF3 was only weakly

expressed. Moreover, the low expression of PPARγ in undifferentiated NHU cells might result by the degration of the protein. The research further applied proteasome inhibitor MG132 but did not rescue the protein expression of PPARγ (Figure 8.8).

Figure 4. 4: Morphology of troglitazone and PD153035 treated urothelial cells.
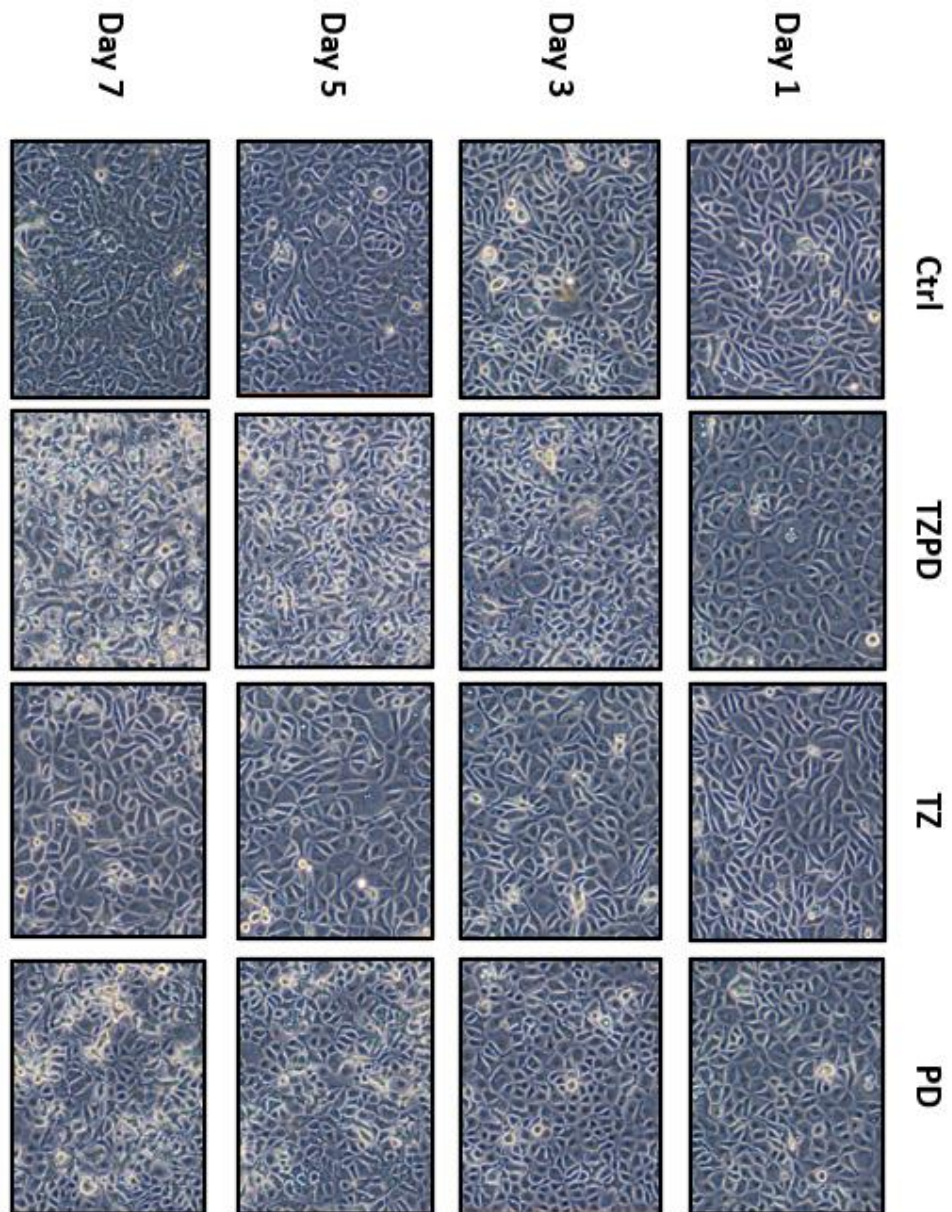
NHU cells were treated with 0.1% DMSO(Control), 1µM troglitazone and PD153035 (TZPD), 1 µM troglitzone (TZ) or 1µM PD153035 (PD) for 7 days. The morphology of the cells was captured every day.

Figure 4. 5: Expression of PPARγ in troglitazone and PD153035 treated urothelial cells.
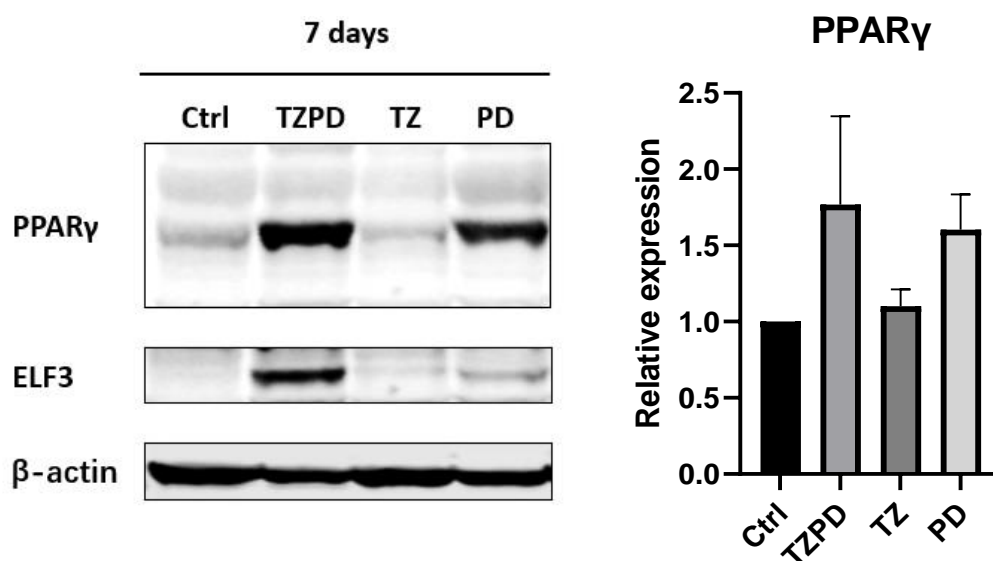
NHU cells were treated with 0.1% DMSO (Control), 1µM troglitazone and PD153035 (TZPD), 1 µM troglitzone (TZ) or 1µM PD153035 (PD) for 7 days. NHU cells were cultured to 90% confluence and started the treatment. Troglitazone was removed after 24 hours in the TZPD differentiation group. Phenotype of cells were captured every day as shown in the picture. Protein lysates were harvest at day 7. Expression of PPARγ and ELF3 was detected using western blot shown in the left graph (One of the three results). β-actin was used as housekeeping protein. Expression of PPARγ and ELF3 among the groups was calculated from 3 independent experiments (Section 8.5.1) and quantified using image J as shown on the right graph.

4.3.1.2 Inhibition of MEK kinase was responsible for the translation of PPARγ.

Based on the experimental approach, inhibitors of EGFR and its downstream targets were applied to identify which downstream of EGFR was responsible for the translation of PPARγ protein. Up to 72 hours treatment, the morphology of NHU cells was similar except TZPD differentiated NHU cells and PD153035 treated urothelial cells (Figure 4.6).

The protein lysates of treated urothelial cells were collected at 24 hours and 72 hours. Expression of PPARγ was obviously detected after TZPD differentiated for 24 hours which was consistent with previous results (section 3.5). Results further found weak expression of PPARγ in EGFR inhibited and MEK inhibited NHU cells. At 72 hours, TZPD differentiated urothelial cells showed the highest expression of PPARγ (Figure 4.7). Obviously expression of PPARγ was detected in NHU cells treated with PD153035 (EGFR inhibitor) or UO126 (MEK inhibitor). Inhibition of PI3K using Ly294002 or inhibition of ERK using FR180204 did not induce any translation of PPARγ protein. Thus. the MEK kinase could be the downstream of EGFR that responsible for the translation of PPARγ protein but still needs further verification.

Expression of ELF3, a differentiation-associated transcription factor, was used to illustrate the differentiation state of NHU cells. Although ELF3 was abundant expressed in TZPD differentiated NHU cells, it was not highly expressed in either EGFR inhibited or MEK inhibited urothelial cells. The expression of PPARγ protein alone was not enough to initiate the differentiation of urothelial cells. The activation of PPARγ was required to initiate its regulating role of urothelial cell differentiation.

Figure 4. 6: Morphology of treated NHU cells.
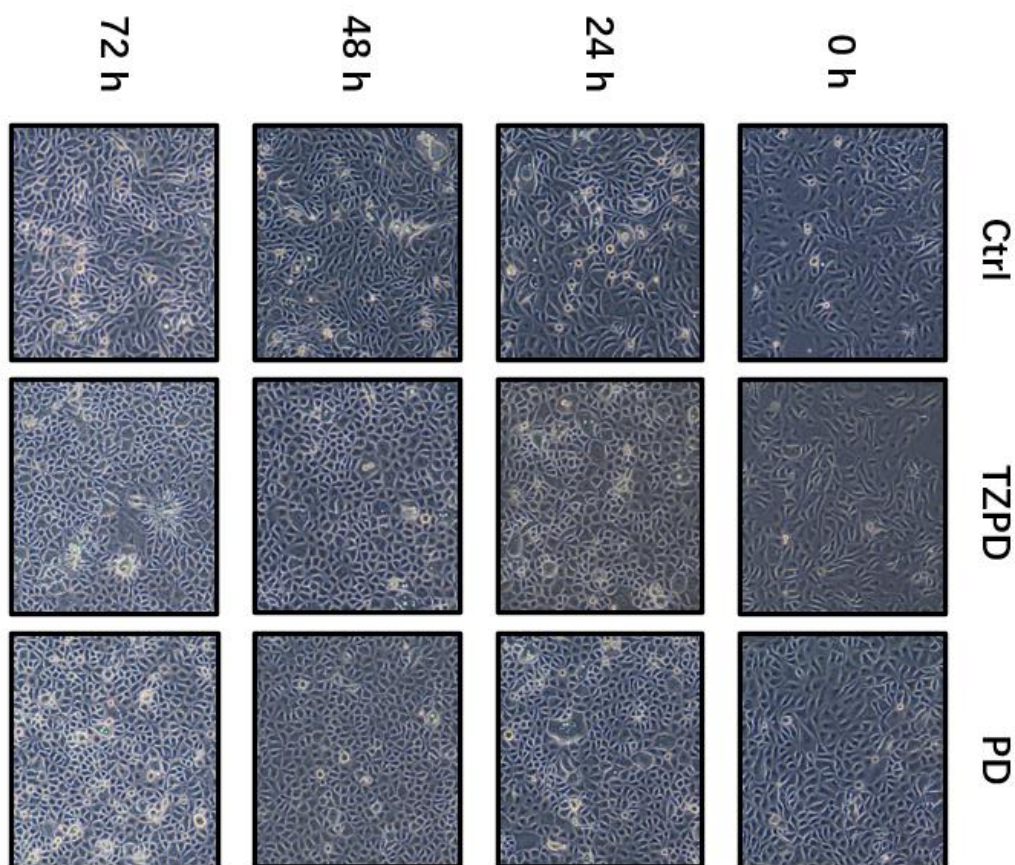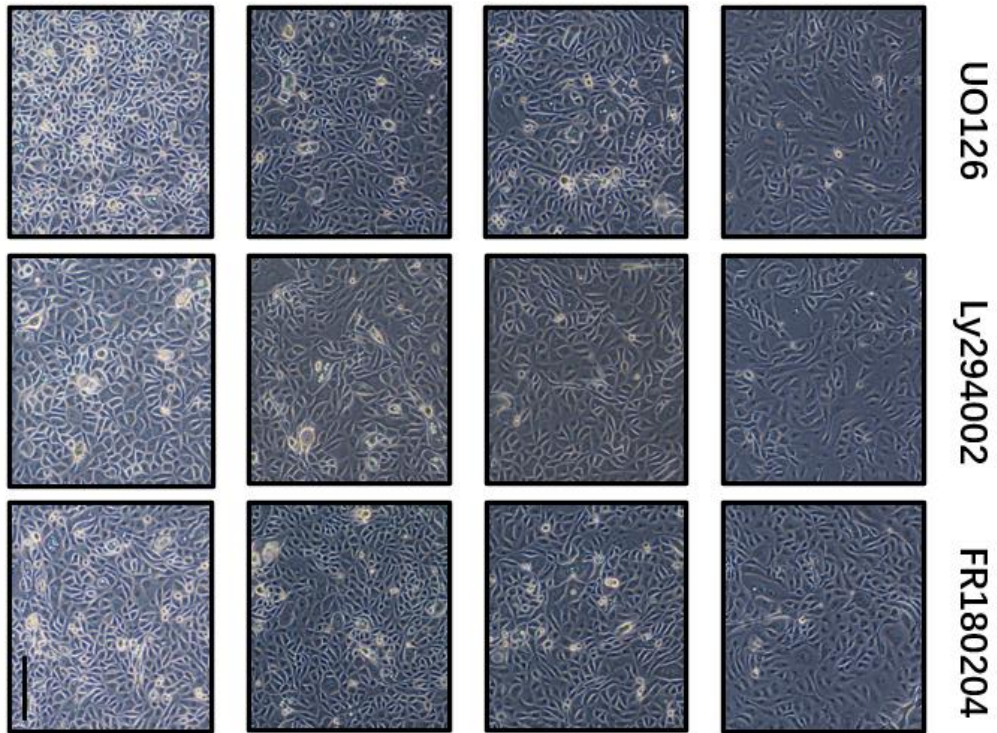
NHU cells were cultured to 90% confluence before the starting of the treatments. NHU cells treated with 0.1% DMSO was used as control. TZPD differentiated NHU cells was included with troglitazone removed after 24 hours. Inhibitors were added at different concentration which diluted in 0.1% DMSO: PD153035 (EGFR inhibitor) 1 µM, LY294002 (PI3K inhibitor) 3 µM, UO126 (MEK inhibitor) 5µM, FR180204 (ERK inhibitor) 1 µM. Bar was 200 µM.

Figure 4. 7: Inhibition of MEK induce the translation of PPARγ protein.
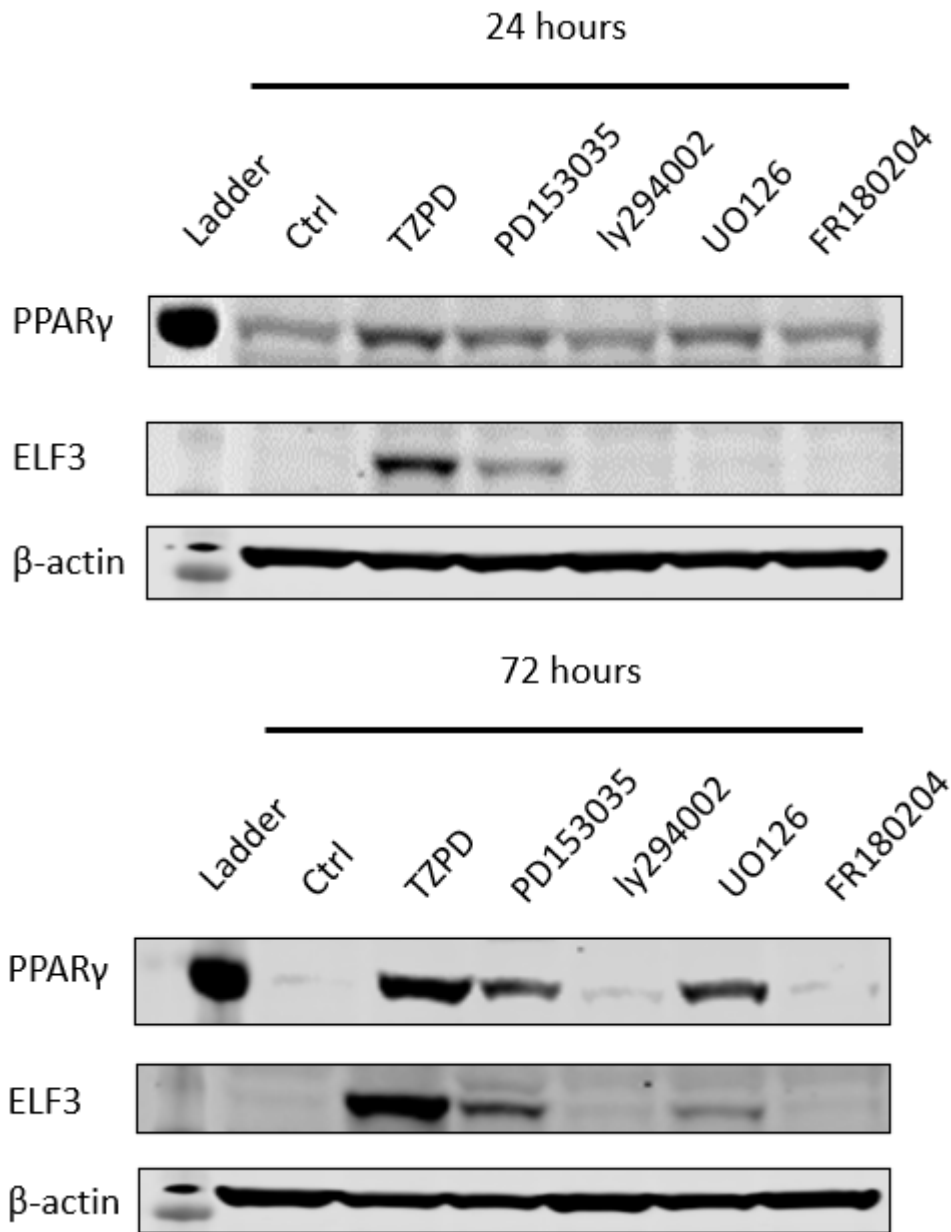
NHU cells were cultured to 90% confluence before the starting of the treatments. NHU cells treated with 0.1% DMSO was used as control. TZPD differentiated NHU cells was included with troglitazone removed after 24 hours. Inhibitors were added at different concentration which diluted in 0.1% DMSO: PD153035 (EGFR inhibitor) 1 µM, LY294002 (PI3K inhibitor) 3 µM, UO126 (MEK inhibitor) 5µM, FR180204 (ERK inhibitor) 1 µM. Protein lysates were harvest at time points 24 hours and 72 hours.

PPARγ and was detected using antibody 81B8. β-actin was used as the housekeeping protein.

4.3.1.3 EGFR downstream target MEK partially regulates the NHU cells differentiation

Previous results found that inhibition of MEK alone could induce the translation of PPARγ protein in NHU cells but unable induce the differentiation of NHU cells (section 4.3.2). Further experiment was set up to verify whether inhibition of EGFR downstream targets combined with adding of adding of PPARγ agonist could initiate the differentiation process of NHU cells. The results found that treatment of PPARγ agonist troglitazone and EGFR inhibitor PD153035 give rise to high expression of differentiation-associate ELF3 which consistent with previous results. The treatment of troglitazone with the MEK inhibitor UO126 could induce low expression of ELF3 protein. However, the inhibitor of MEK downstream target ERK was unable to induce the expression of ELF3. Although inhibition of MEK promote the translation of PPARγ protein in NHU cells. It is only partially regulating the differentiation of NHU cells *in vitro*.

Figure 4. 8: EGFR downstream target MEK partially regulates the NHU cells differentiation.

24 hours

PD153035	-	+	-	-	-	+	-	-	-
ly294002	-	-	+	-	-	-	+	-	-
UO126	-	-	-	+	-	-	-	+	-
FR180204	-	-	-	-	+	-	-	-	+
TZ	-	-	-	-	-	+	+	+	+

PPARγ

ELF3

B-actin

72 hours

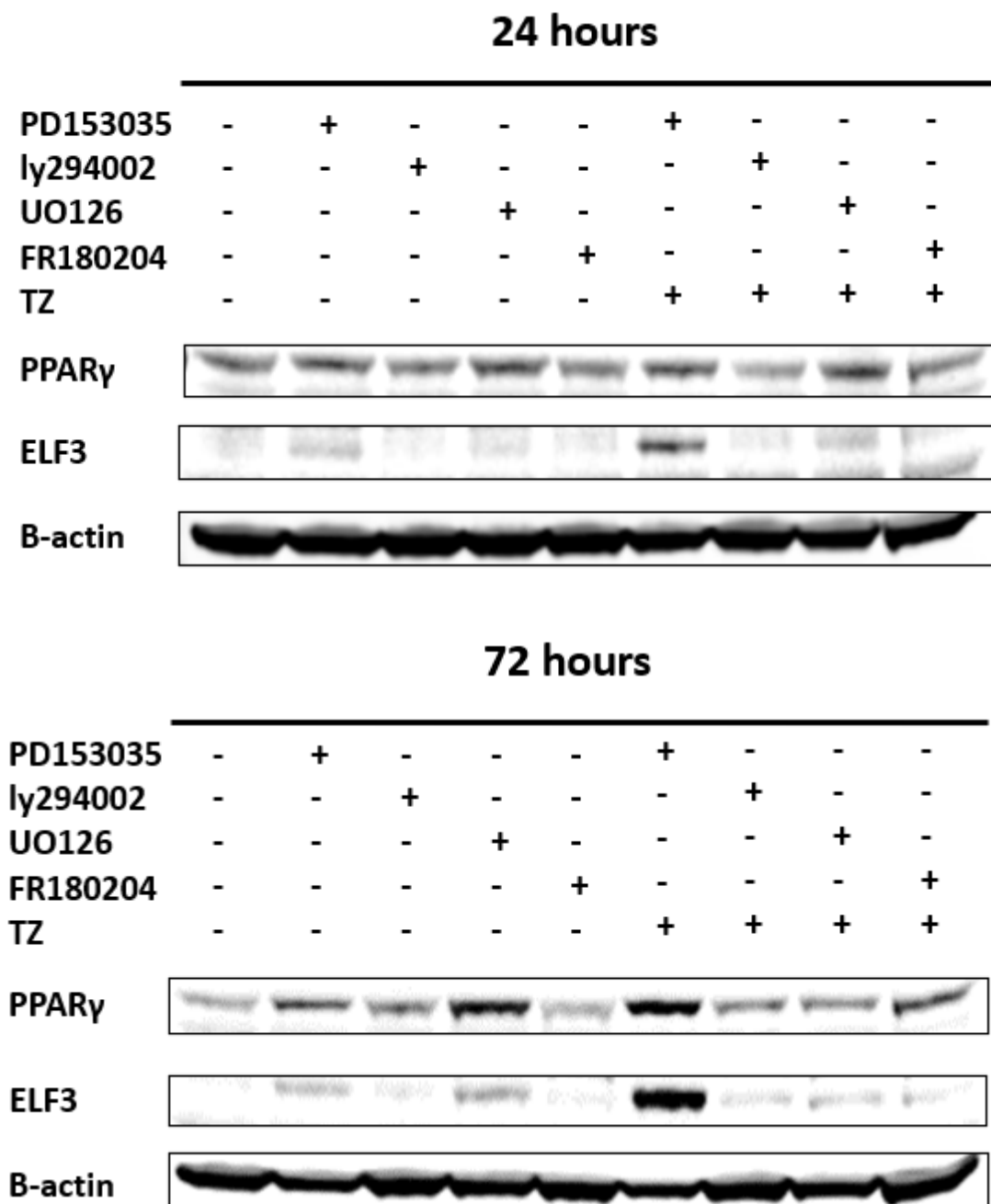|									
PD153035	-	+	-	-	-	+	-	-	-
ly294002	-	-	+	-	-	-	+	-	-
UO126	-	-	-	+	-	-	-	+	-
FR180204	-	-	-	-	+	-	-	-	+
TZ	-	-	-	-	-	+	+	+	+

PPARγ

ELF3

B-actin

NHU cells were cultured to 90% confluence before the starting of the treatments. NHU cells treated with 0.1% DMSO was used as control. Inhibitors were added at different concentration which diluted in 0.1% DMSO: PD153035 (EGFR inhibitor) 1 μM, LY294002 (PI3K inhibitor) 3 μM, UO126 (MEK inhibitor) 5μM, FR180204 (ERK inhibitor) 1 μM. PPARγ agonist troglitazone was added at 1 μM diluted in 0.1% DMSO. Protein lysates were harvest at time points 24 hours and 72 hours. PPARγ and was detected using antibody 81B8. β-actin was used as the housekeeping protein.

4.3.2 Inhibition of PPARγ attenuates the expression of FABP4 and ELF3

Activation and inhibition of PPARγ was applied to investigate the downstream target of PPARγ in urothelial cells. FABP4, commonly used as PPARγ activation marker, was detected in PD153035 treated NHU cells but the expression was disappeared when PPARγ was inhibited by T0070907 (Figure 4.9). Expression of ELF3 was also affected by the inhibition of PPARγ. ELF3 was not highly but clearly observed in PD153035 treated NHU cells. The adding of PPARγ inhibitor T0070907 in PD153035 treated NHU cells obviously attenuated the expression of ELF3. The expression of FOXA1 shows no obvious change when PPARγ was inhibited. The results suggest both FABP4 and ELF3 might be the reporter of PPARγ activation in NHU cells. However, the expression of ELF3 and FABP4 was not decrease in TZPD differentiated NHU cells treated with PPARγ inhibitor T0070907 together. It might because the NHU cells were not pretreated with T0070907 before the initiation of differentiation. The pre-binding of PPARγ agonist troglitazone might

prevent the binding of T0070907 to initiate its inhibitory role. Thus, the adding of PPARγ inhibitor T0070907 together with the adding of PPARγ agonist troglitazone was unable to effectively inhibit the activation of PPARγ. The experiment needs to be repeated with pretreatment of T0070907 to better verify the finding. However, the pandemic of COVID-19 make it impossible to repeat those experiments at the end of my PhD period.

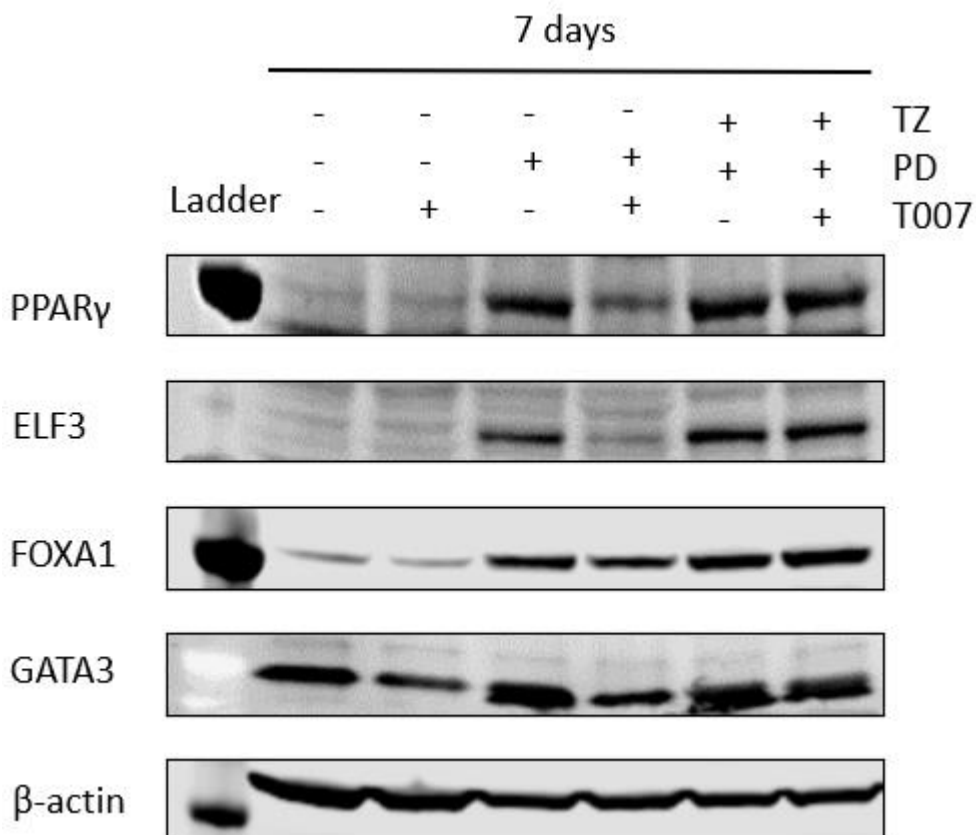**Figure 4. 9: Inhibition of PPARγ decrease the expression of ELF3 and FABP4.**

Urothelial cells were cultured to 90% confluence before the starting of the treatments. Urothelial cells treated with 0.1% DMSO was used as control. TZPD differentiated urothelial cells was included with troglitazone removed after 24 hours. PPARγ agonist troglitazone (TZ), PPARγ inhibitor T0070907 (T007), and EGFR inhibitor PD1503035 (PD) was used at concentration 1 µM and diluted in 0.1% DMSO. PPARγ was detected using antibody 81B8.

4.4 Discussion

4.4.1 Inhibition of EGFR induce the translation of PPARγ protein

EGFR is a signaling pathway known to be associated with cell proliferation. In urothelium, studies revealed that EGFR was abundantly expressed (Cheng et al., 2002; Rotterud et al., 2005). Inhibition of EGFR using PD153035 (PD) combined with activation of PPARγ using ligand troglitazone (TZ) could driving the differentiation of NHU cells refers as the TZPD differentiation in our lab (Section 3.3.3) (Varley et al., 2004). However, the mechanism underlying the differentiation method stays unclear.

Previous results have identified that PPARγ protein was not detected in undifferentiated NHU cells but highly expressed when treated with 1 µM PD153035 and troglitazone for 24 hours. It is questioned which treatment results in the translation of PPARγ protein. The results verified that it is the inhibition of EGFR give rise to the translation of PPARγ protein in NHU cells (Section 4.3.1.1). Previous literature has reported

that enhanced activation of EGFR could result in degradation of PPARγ protein in Hela human cells and SW480 clonal cancer cell line (Xu et al., 2016). Moreover, another study also demonstrates the treatment of PPARγ agonist pioglitazone could reverse the EGFR mediated degradation of PPARγ protein (Shi et al., 2016). The relationship of EGFR signaling and PPARγ was illustrated in cancer cell lines while no evidence revealed the regulation role of EGFR signaling on PPARγ protein translation in normal human tissues. The investigation suggested EGFR signaling was negatively regulating the translation of PPARγ which might through the degradation of PPARγ protein in human urothelium. The treatment of PPARγ agonist troglitazone alone was unable to reverse the degradation could because there was no PPARγ protein exist at the beginning. However, expression of PPARγ protein was only detected after long treatment of EGFR inhibitor. Considering PPARγ might participates in the early stage of NHU cell differentiation, it needs to identify the expression of PPARγ at early time points.

4.4.2 MEK as the downstream of EGFR involved in regulation of NHU cells differentiation

EGFR signaling was previously suggested to be involved in regulation of urothelial cell differentiation (Varley et al., 2004). The investigation

indicates that EGFR signalling inhibits PPARγ protein translation/stability in undifferentiated urothelial cells (4.3.1.1). Inclusion of inhibitors against EGFR downstream targets showed that inhibition of MEK resulted in the highest expression of PPARγ protein compare to the inhibition of other EGFR downstream targets (Section 4.3.1.2). Further treatment of undifferentiated urothelial cells with PPARγ ligand combined with inhibition of MEK was unable to induce the expression of differentiation-associated proteins (Section 4.3.1.3). These results agree with previous findings that EGFR signaling inhibits the initiation of NHU cells differentiation but take it a step further in implicating a translational block.

The possible regulation role of MEK on PPARγ is poorly understood. In adipocyte cells, literature reveals that activation of MEK-ERK pathway significantly upregulates the inhibitory phosphorylation of PPARγ at Ser273 which results in the deactivation of PPARγ (Das et al., 2021). An earlier paper reported that MEK1 can directly binds with PPARγ protein and result in the deactivation of PPARγ by nuclear export in cancer cells (Burgermeister and Seger, 2007). These findings illustrate that MEK could function to inhibits PPARγ activity but there is no evidence suggested MEK was inhibiting the translation of PPARγ protein or stability in adipogenesis. The observation gives insights into finding the

responsible downstream target of EGFR involved in regulating urothelial cells differentiation but the mechanism underlying it was still unclear. Future experiments focused on identify the relationship of EGFR signaling and PPARγ activity was required to better understand the role of EGFR signaling in NHU cells differentiation.

4.4.3 PPARγ signaling in NHU cells differentiation

The involvement of PPARγ signalling has been well documented in adipogenesis reviewed by previous literature and it is also found to regulate the differentiation of urothelial cells (Lefterova et al., 2014). However, the downstream signals of PPARγ regulating the differentiation process of urothelial cell stays unknown. Fatty Acid Binding Protein 4 (FABP4), an adipogenic marker, was found to be the reporter gene of PPARγ in not only adipocyte cells but also in monocytes by recent studies (Lamas Bervejillo et al., 2020; Zhang et al., 2020). But the expression of FABP4 in urothelial cells has not been identified. The results discovered that the expression of FABP4 was consistent with the expression of PPARγ during the differentiation of NHU cells (Section 4.3.2). It suggested FABP4 might also be a reporter gene of PPARγ activity in urothelial cells as its expression concurred when PPARγ was activated by the ligand and was prevented by PPARγ inhibition. Previous

research in the lab found ligand activation of PPARγ induced (gene/protein) expression of differentiation-associated transcription factor FOXA1 and IRF-1 (Varley et al., 2009). Carl Fishwick further verified Claire's finding that FOXA1 was the potential downstream target of PPARγ and identified a novel differentiation-associated transcription factor GATA3 which suggested to positively regulate the transcript of *PPARG* (Fishwick et al., 2017). ELF3 was more recently identified as a differentiation marker of NHU cells but its upregulator stays unclear (Bock et al., 2014). However, previous literatures focused on the transcription of those transcription factors and it is not clear which PPARγ protein was regulating the NHU cells differentiation process. The results revealed the expression of those transcription factors during NHU cells differentiation and the results suggested FOXA1 and ELF3 could be the potential downstream target of PPARγ in NHU cells (Section 4.3.2). Further applying of PPARγ antagonist and inhibitors discovered that translation of ELF3 protein was directly associate with PPARγ activity but FOXA1 was being affected. It suggests ELF3 might be the downstream target of PPARγ regulating the differentiation process of NHU cells (Section 4.3.2). But it needs further evidence to identify whether PPARγ was directly regulating the expression of ELF3 in urothelial cells.

4.5 Summary of findings

The results found that inhibition of EGFR signaling helps to induce the translation of PPARγ protein in NHU cells. Further investigation identified EGFR downstream target MEK was responsible for the translation of PPARγ protein. However, the inhibition of MEK combined with adding of PPARγ agonist was not able to initiate the fully differentiation of NHU cells. It suggested there might exists other mechanism controlling the differentiation of NHU cells. Moreover, the adding of PPARγ inhibitor T0070907 in EGFR inhibited NHU cells lowered PPARγ protein abundance. It also attenuate the protein expression of ELF3 and FABP4. This suggests ELF3 and FABP4 might functions as the reporter of PPARγ activation in NHU cells.

Chapter 5: Compartmentalization of PPARγ changes during NHU cell differentiation.

5. Compartmentalization of PPARγ changes during NHU cell differentiation

5.1 Rationale and Aim

PPARγ is the regulator of NHU cell differentiation. PPARγ was continuously transcribed in both undifferentiated and differentiated NHU cells. However, the expression of PPARγ protein was only detected when differentiation processes being initiated. Previously results have identified the expression of PPARγ protein increases at early stage during NHU cell differentiation. The abundant expression of its downstream target ELF3 was detected at 24 hours after the initiation of differentiation process. It is suggested that PPARγ functions early during NHU differentiation. But the time points it activated and functions to regulate the NHU cell differentiation stays unknown.

In adipogenesis, the regulatory mechanism of PPARγ was well understood and it functions as a nuclear receptor. PPARγ forms heterodimer with another nuclear receptor RXRα first and then binds to a specific region on the chromatin to regulate its downstream targets. Although the mechanism of PPARγ regulating NHU cell differentiation was unknown, the time points that PPARγ activated and functions can be identified by detecting the time points PPARγ binds with the

chromatin. Thus, the aim of the chapter was to detect the compartmentalization change of PPARγ in the nucleus during NHU cells differentiation. To achieve the aim, the objectives were to address the following questions:

- Is there difference between the compartmentalization of PPARγ in undifferentiated and differentiated NHU cells?

- Did the compartmentalization of PPARγ changes during NHU cells differentiation?

- Is PPARγ still binds with chromatin at late stage of NHU cell differentiation?

- Is the Compartmentalization of differentiation-associate transcription factors changes during NHU cells differentiation?

5.2 Experimental approach

5.2.1 Cytosekleton stabilization (CSK) extraction

All buffers were made in RNase-free water. The subcellular extraction was applied for either immunoblotting or immunofluorescence:

5.2.1.1 CSK extraction: Immunoblotting analysis

Cells were washed twice with ice-cold PBS and twice in ice-cold cytoskeletal buffer (CSK: 10 mM PIPES/KOH pH 6.8, 100 mM NaCl,

300 mM Sucrose, 1 mM EGTA, 1 mM MgCl2, 1 mM DTT, 1 cOmplete™ Protease Inhibitor Cocktail per 50 ml). Cells was harvest by scraping and supplemented with vanadyl ribonucleoside complex (VRC) to 2.5 mM (NEB) and Triton X-100 to 0.1%. Cells will be mixed by pipetting and equally aliquoted into 4 clean tubes labelled as total, detergent (Det), high salt (HS), and DNase (DN). Tubes Det, HS, and DN were centrifuge at 1,000 g for 3 minutes. Supernatant (SN) and pellet (P) of tube Det was harvest as Det SN and Det P. The supernatant of tube HS and DN was removed, and the pellet was resuspended with 0.1% Triton-X-100 and 0.5 M NaCl in CSK. The tubes were incubating on ice for 1 minute and centrifuge at 1,000 g for 3 min. The supernatant of tube HS was harvested as HS SN. The supernatant of tube DN was removed and pellets of tubes HS and DN was further washed with digestion buffer (40 mM Tris/HCl, 10 mM NaCl, 6 mM MgCl2, 1 mM CaCl2, pH 7.9, supplemented 1/500 with RNaseOUT for RNase-free samples). The supernatants of the tubes were harvest and labelled wash (w). The pellets were further resuspended in fresh digestion buffer with presence of 0.3 U/µl DNase I (Roche) in the DN tube. The tubes were further incubating at 30 °C for 1 h with gentle agitation. Before final centrifugation, reactions were supplemented to 0.5 M NaCl for 5 min, then centrifuge 1,000 g X 3 minutes to separate the supernatant and pellets. Pellets were resuspended in 1× denaturing buffer (2% SDS, 15%

glycerol, 1.7% betamercaptoethanol, 75 mM Tris pH 6.8 with bromophenol blue), and supernatants supplemented with 4× denaturing buffer and heated to 95 °C with repeated vortexing to shear remaining nucleic acid.

5.2.1.2 CSK extraction: Immunofluorescence analysis

The 12-well slides contain the cultured cells were incubated with CSK supplemented with 0.1% Triton-X-100 and 2.5 mM VRC (CSK-D) for 1 min. The CSKD treated slides were either fixed using 10% formalin or Acetone: Methanol (50:50, v/v) or further incubated with CSK-D with 0.5 M NaCl (CSK-DS) for 1 min. For slides to further treated with DNase I enzyme, the slides were washed twice for 1 min with digestion buffer before incubation for 1 h at 37 °C in digestion buffer with 0.45 U/µl DNase I enzyme. The slides were incubated for 1 min with CSK-DS before fixed using 10% formalin or Acetone: Methanol (50:50, v/v).

5.2.2 CSK extraction optimizing (Experimental development)

CSK extraction was applied to extract proteins localized at cytoplasm or nucleus to further identify the compartmentalization of proteins. To avoid any cells loss during the extraction process and evaluate the efficiency of the extraction, NHU cells and bladder cancer cell line

SCaBER go through each link of CSK extraction with the phenotype of the cells being captured by the microscope. The images clearly showed that cell membrane losses after wash with triton X-100 (Figure 5.2). After further washed with high salt buffer, the membrane of the nucleus has been removed. Followed by DNase I treated for 1 hour at 37 degree, the nucleus of the cells was vague in certain areas of the well. The results demonstrate that cell phenotype changes after each treatment and it is high possibility that the methods work properly. Then the CSK extraction model was tested on the NHU cell model. NHU cells were go through differentiation for 3 days and 7 days before the treatment. The phenotype of NHU cells shows slightly change after each treatment but not comparable to the change of SCaBER cells. The differentiated NHU cells forms a tight barrier, and it may affect the efficiency of each treatment. Further analysis such as western blot and immunofluorescence was applied to further test the efficiency of CSK extraction method in NHU cell model.

Figure 5. 1: Phenotype of cells go through CSK extraction.

SCaBER bladder cancer cell line
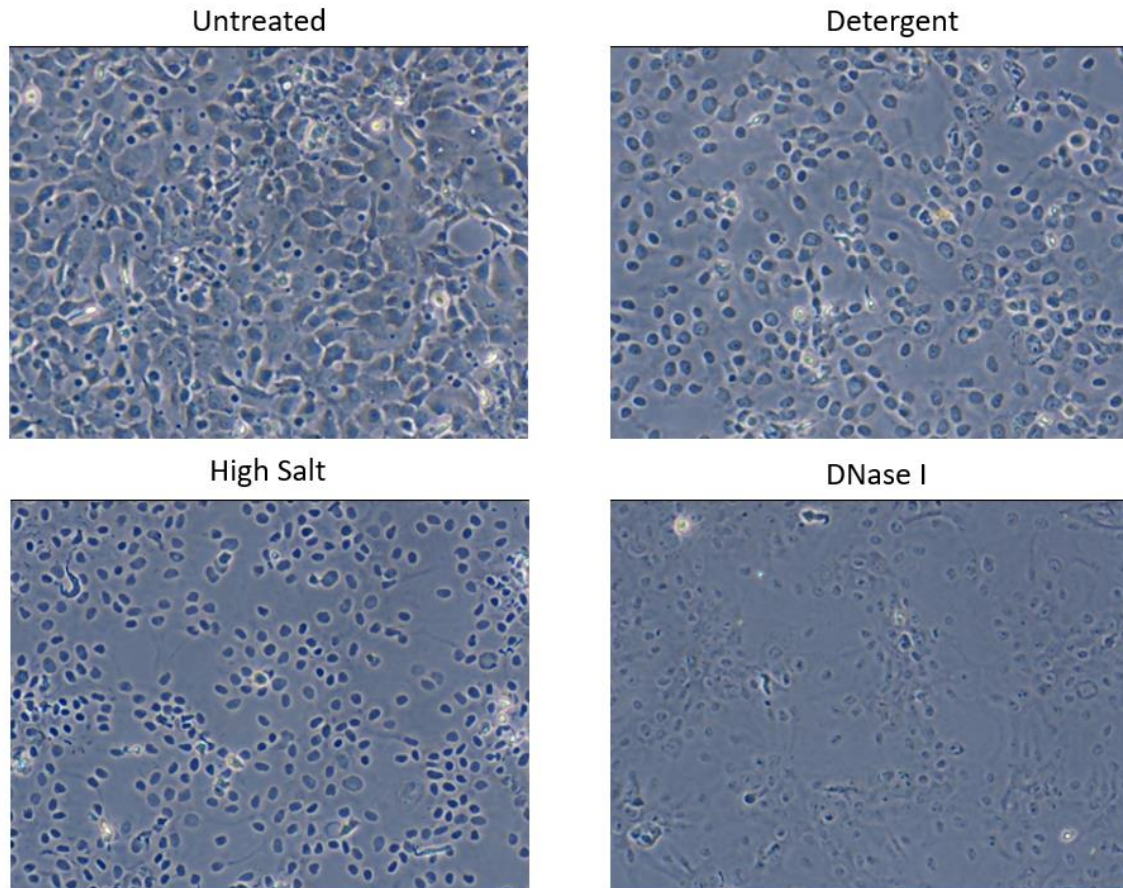
SCaBER cells were cultured to confluent. Then the cells were gone through detergent wash using Triton X-100 to remove the soluble protein in the cytoplasm. Next the cells further go through high salt wash with 5M NaCl to remove weakly bound protein in the nucleus. At last, the cells were gone through DNase I treatment at 37 degree for 1 hour to further remove DNA or chromatin bound proteins. Phenotype of the cells were captured using the microscope.

Y2607 differentiated 3 days

NHU cells were cultured to confluent and differentiated for 3 days before the extraction. Then the cells were gone through detergent wash using Triton X-100 to remove the soluble protein in the cytoplasm. Next the cells further go through high salt wash with 5M NaCl to remove weakly bound protein in the nucleus. At last, the cells were gone through DNase I treatment at 37 degree for 1 hour to further remove DNA or chromatin bound proteins. Phenotype of the cells were captured using the microscope.

Y2607 differentiated 7 days

Untreated

Detergent

High Salt

DNase I

NHU cells were cultured to confluent and differentiated for 3 days before the extraction. Then the cells were gone through detergent wash using Triton X-100 to remove the soluble protein in the cytoplasm. Next the cells further go through high salt wash with 5M NaCl to remove weakly bound protein in the nucleus. At last, 7the cells were gone through DNase I treatment at 37 degree for 1 hour to further remove DNA or chromatin bound proteins. Phenotype of the cells were captured using the microscope.
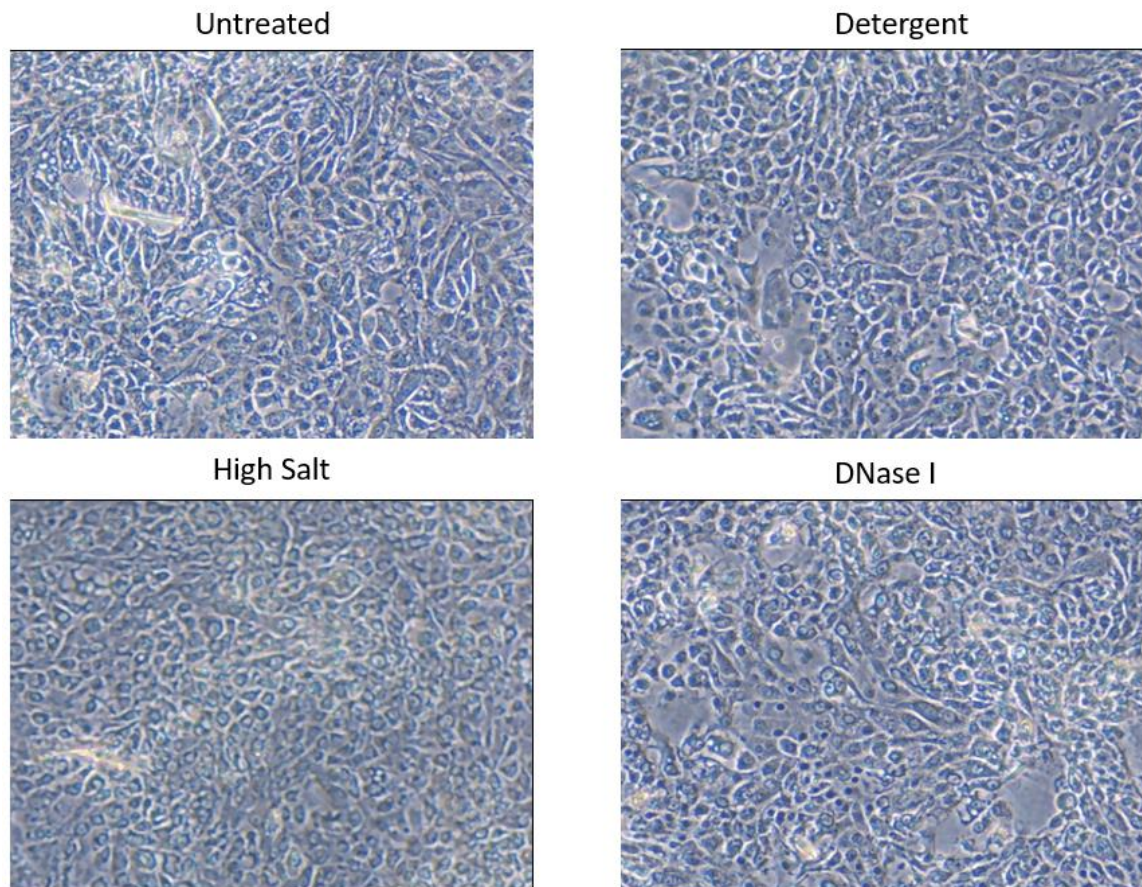
5.3 Results

5.3.1 Compartmentalization of PPARγ in NHU cells *in vitro*

5.3.1.1 PPARγ was not chromatin-bound in differentiated urothelial cells

As described in the method chapter, western blot can be applied after CSK extraction to analyze the compartmentalization of proteins. Urothelial cells were differentiated using TZPD differentiation method for 7 days. Both protein lysates of proliferating and differentiated urothelial cells were collected and then go through CSK extraction. As expected, proliferating urothelial cells show no expression of PPARγ protein. But the expression of histone 3 illustrated that the CSK extraction works in urothelial cells. Abundant expression of PPARγ was detected in urothelial cells differentiated for 7 days (Figure 5.2). Although the expression of histone3 suggested that the DNase I treatment was not fully works, it is clear that no PPARγ was suggested to be chromatin-bound in differentiated urothelial cells.

Figure 5. 2: Compartmentalization of PPARγ in undifferentiated and differentiated NHU cells.
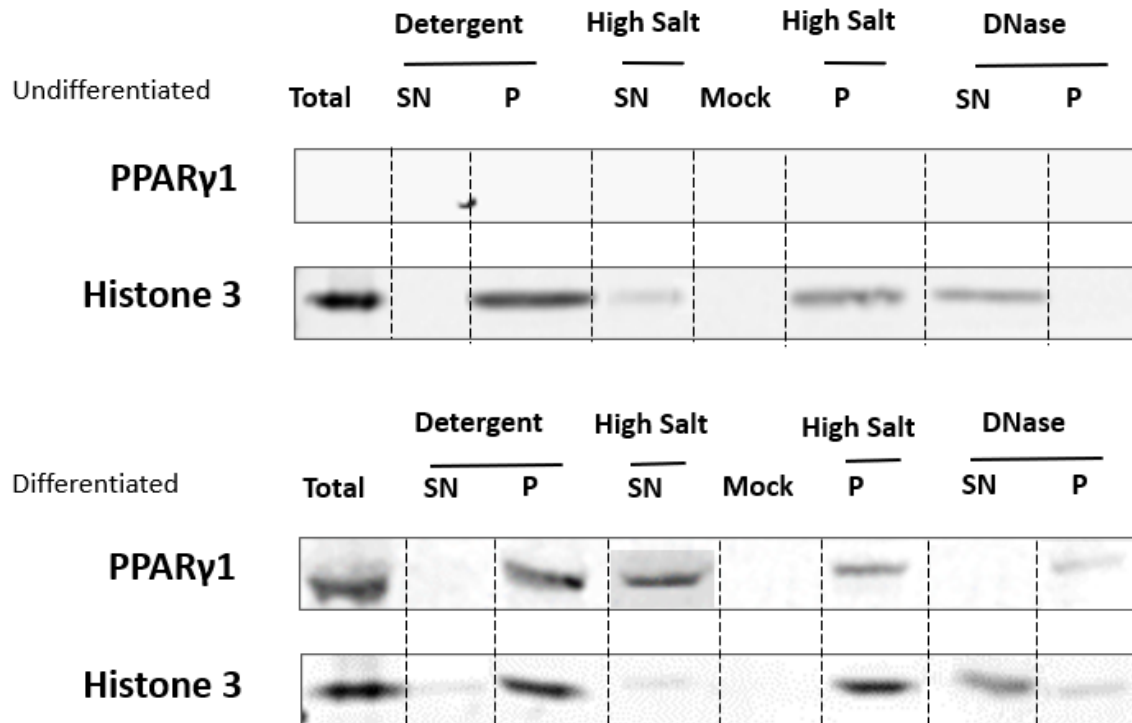
NHU cells were cultured to 50% confluent and harvest as proliferating NHU cells. NHU cells were cultured to 90% confluent and then TZPD differentiated for 7 days. The cells were harvest as differentiated NHU cells. Both proliferating and differentiated NHU cells were gone through CSK extraction followed by western blot analyze. PPARγ was labelled using antibodies D69 and 81B8. Histone3 was used to verify the DNase I treatment.

5.3.1.2 Compartmentalization of PPARγ in the nucleus changes during urothelial cells differentiation

Previous results found that PPARγ is not chromatin-bound in urothelial cells differentiated for 7 days. A time course experiment was set up to evaluate the compartmentalization of PPARγ during the urothelial cells

differentiation. The LDS14 is a nuclear matrix protein functions to verify the existing of cells after DNase I treatment (Figure 5.3). The urothelial cells were collected at specific day point and gone through CSK extraction followed by immunofluorescence analyze. The results demonstrated that nearly no PPARγ protein were resistant to high salt buffer wash (Nucleus tightly-bound) at early stage of differentiation (Figure 5.3). Expression of nucleus tightly-bound PPARγ protein was detected at day 3. No PPARγ protein was detected at day 6 after high salt buffer wash. Moreover, expression of PPARγ was lost after DNase I treatment at day 3 suggested PPARγ was bound to the chromatin at this specific time point in TZPD differentiation. These results suggested that PPARγ shows a compartmentalization change during TZPD differentiation and was chromatin-bound at day 3.

Figure 5. 3: Subcellular localization of PPARγ protein during urothelial cells differentiation.

TZPD day 6
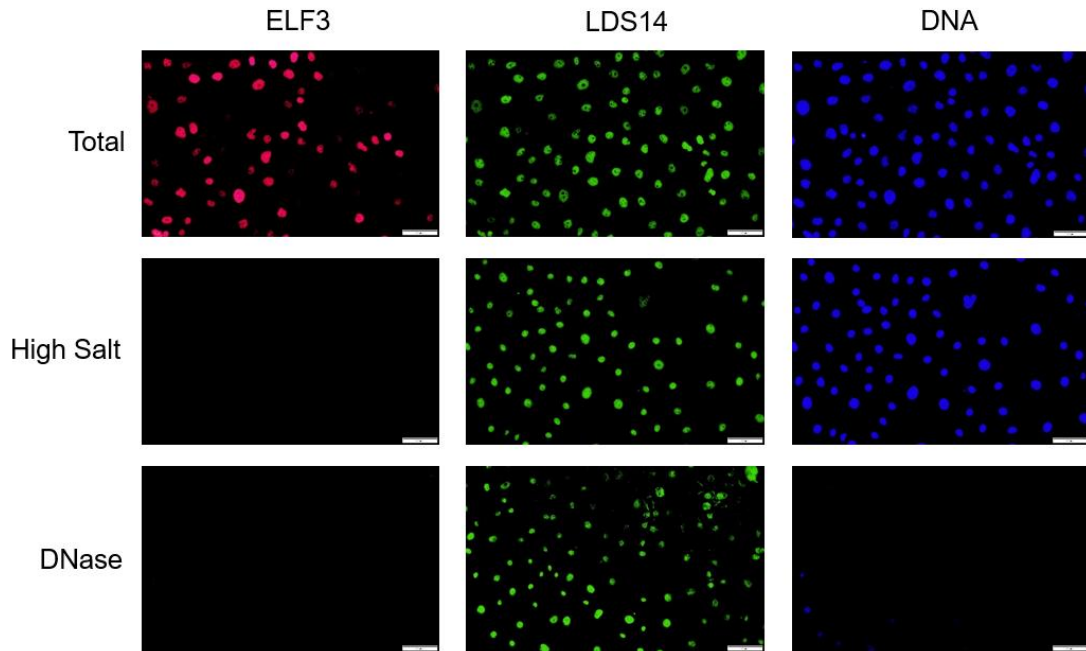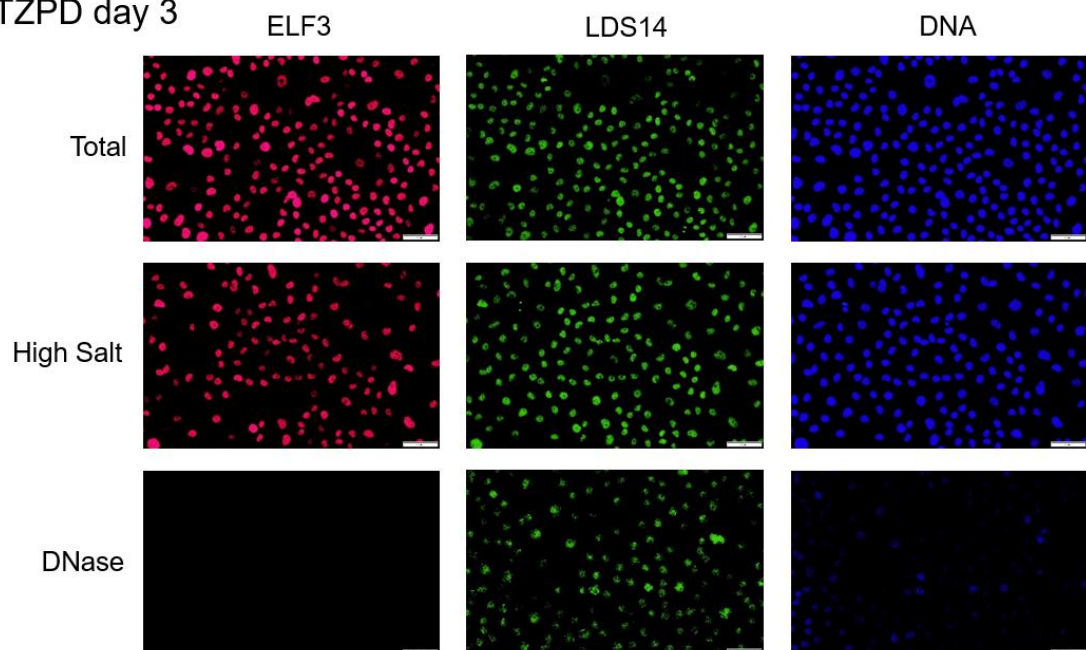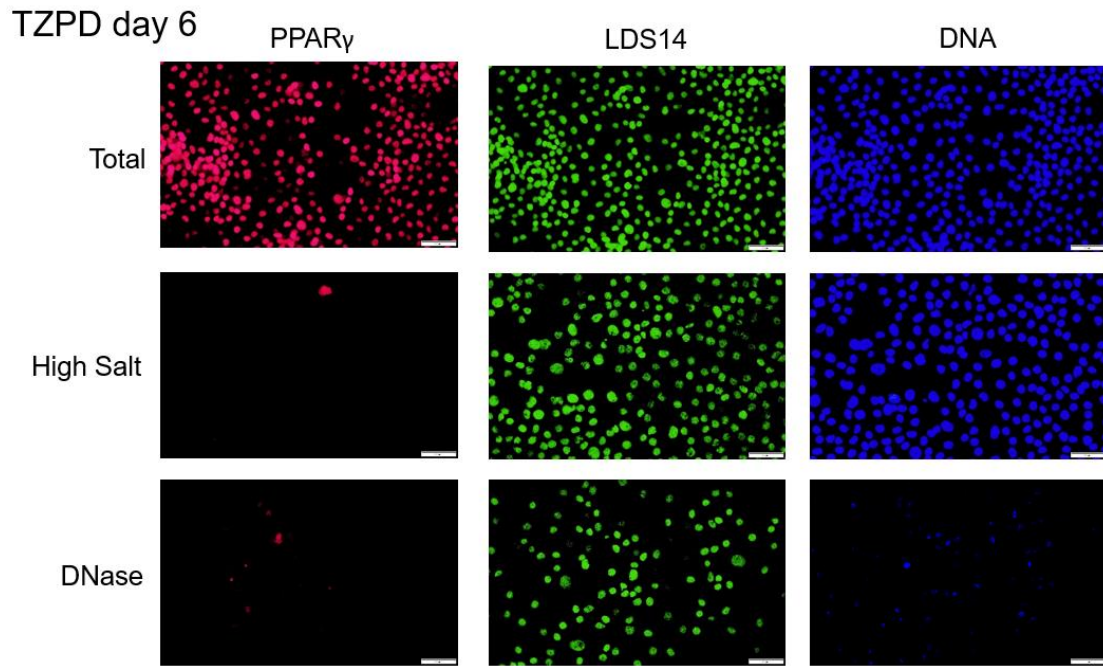
NHU cells were cultured to 90% confluent before initiating the differentiation process. Cells were fixed at different time points then go through different wash and treatment. Scale bar = 50 μM.

5.3.1.3 PPARγ is only chromatin-bound at early stage of urothelial cells differentiation

To further find whether PPARγ binds with chromatin during urothelial cells differentiation, protein lysate of urothelial cells was harvest at different time points during the differentiation process and then further go through CSK extraction followed by western blot analysis. The ki67 and claudin 4 was labelled to show the decrease of proliferation and the differentiation progression during the TZPD differentiation (Figure 8.10). The immunoluorescent results clearly showed that at day 1, PPARγ protein was detected and localized in the nucleus (Figure 5.4). However,

it was not tightly bound in the nucleus suggesting it was not functioning as nuclear receptor at this time point. This might be cause by the limited expression of PPARγ at the start of urothelial cells differentiation. At day 3, higher expression of PPARγ protein was detected and the expression of PPARγ after high salt wash verified it is tightly-bound in the nucleus at this time point. Obviously expression of PPARγ protein was detected in urothelial cells differentiated for 6 days as expected. However, the results showed that nearly no PPARγ protein is tightly-bound in the nucleus. These results support that there exist a compartmentalization change of PPARγ in the nucleus during urothelial cells differentiation but because the DNase I treatment was not conducted.

From western blot results at day 3, abundant expression of nucleus tightly-bound PPARγ protein was shown (Figure 5.5). It suggest that PPARγ signal on the blot was partially removed within the DNase I treatment. However, the histone 3 result showed that the DNase I treatment was not fully works on the protein lysates(Figure 5.5). Thus, it is hard to verify the chromatin binding of PPARγ. These evidence give some support to the previous research but needs to optimize the method to better verify these observations.

Figure 5. 4: PPARγ shows a compartmentalization change in the nucleus during NHU differentiation.
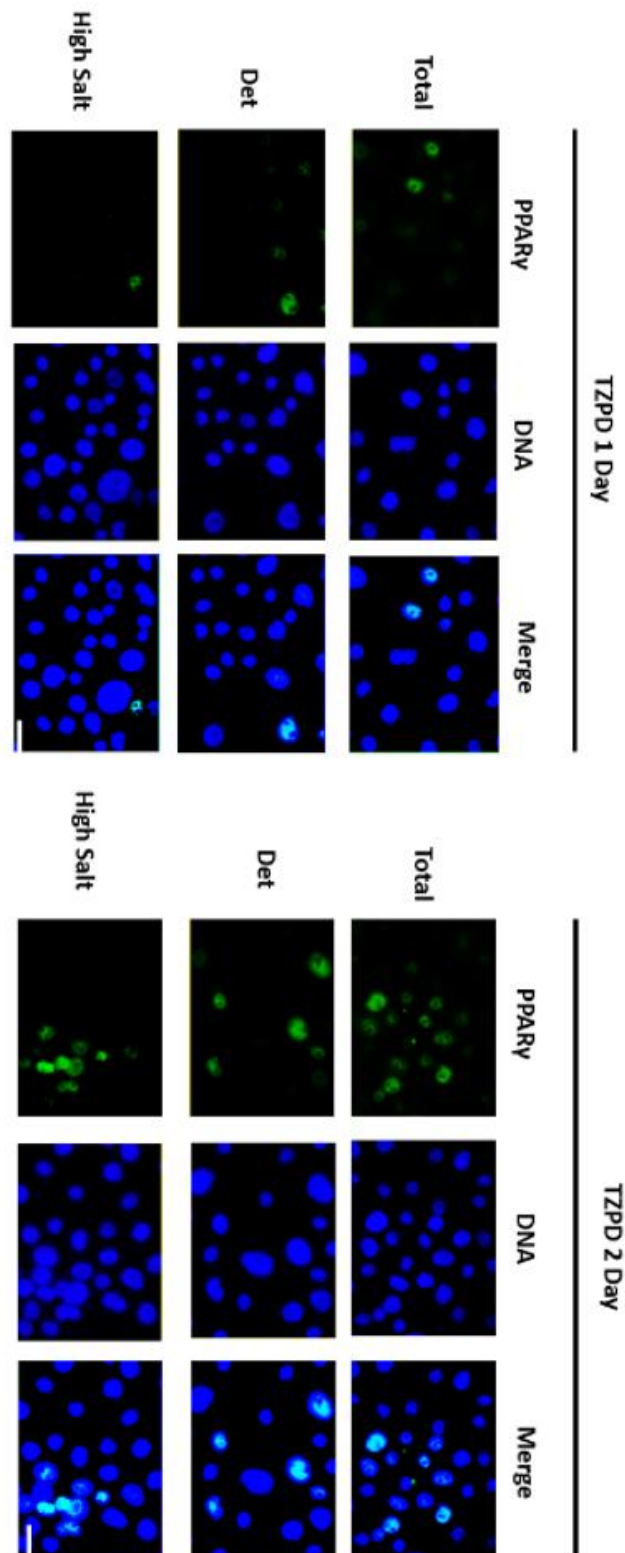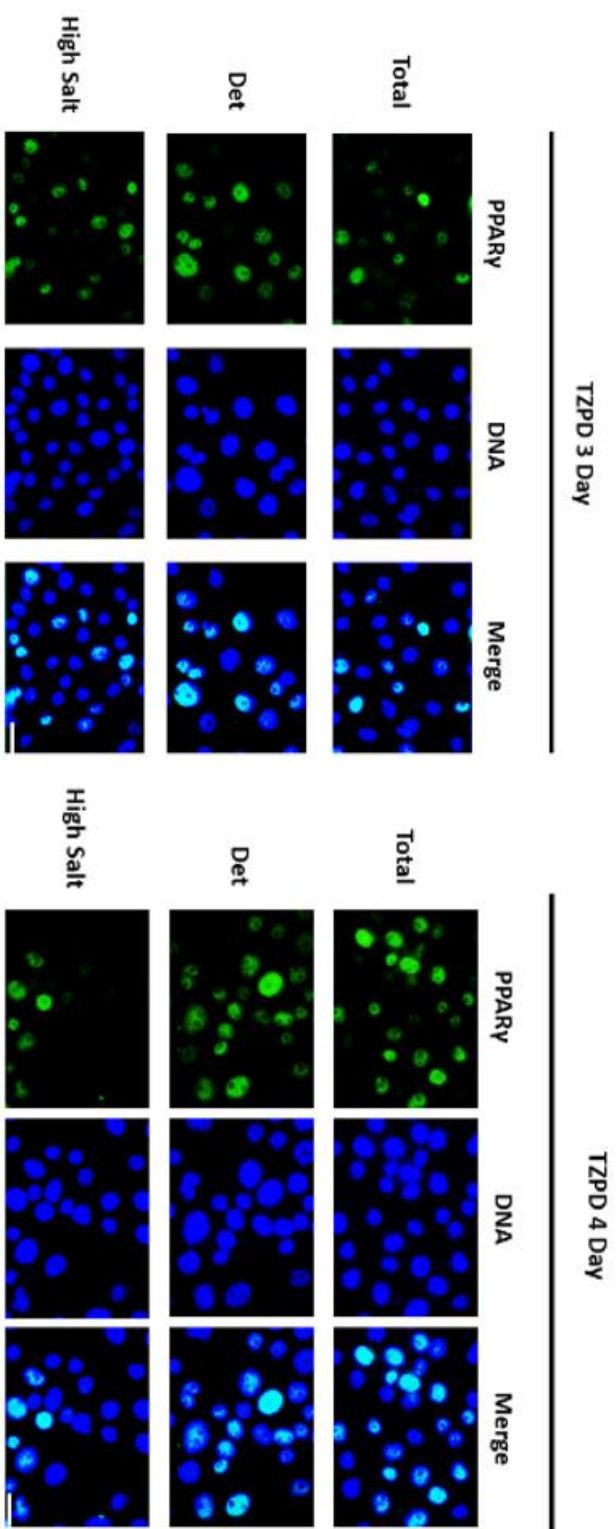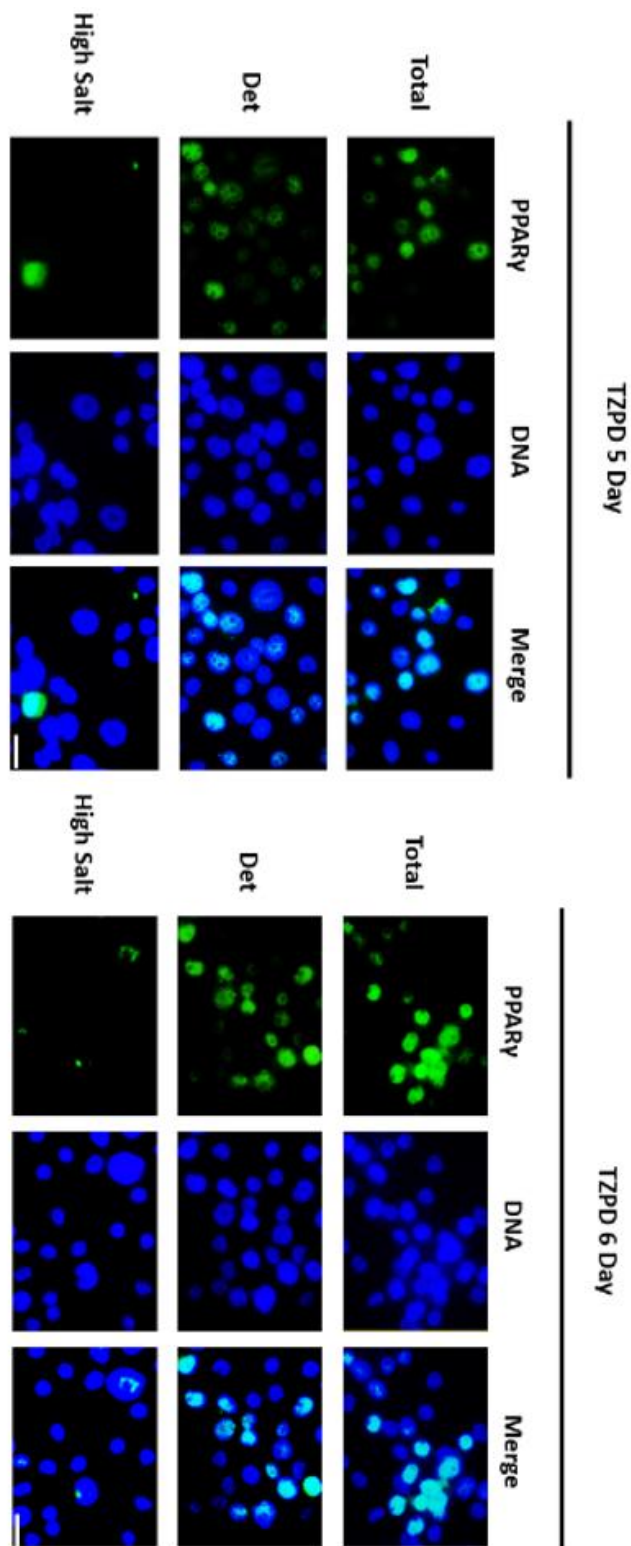
High Salt

Det

Total

PPARγ

DNA

Merge

TZPD 3 Day

High Salt

Det

Total

PPARγ

DNA

Merge

TZPD 4 Day

156

NHU cells were cultured to 90% confluent and then TZPD differentiated for 6 days. The differentiated NHU cells were gone through CSK extraction at everyday time point. Scale bar = 50 µM.

Figure 5. 5: PPARγ protein was not chromatin-bound at early and late stage of NHU cell differentiation.
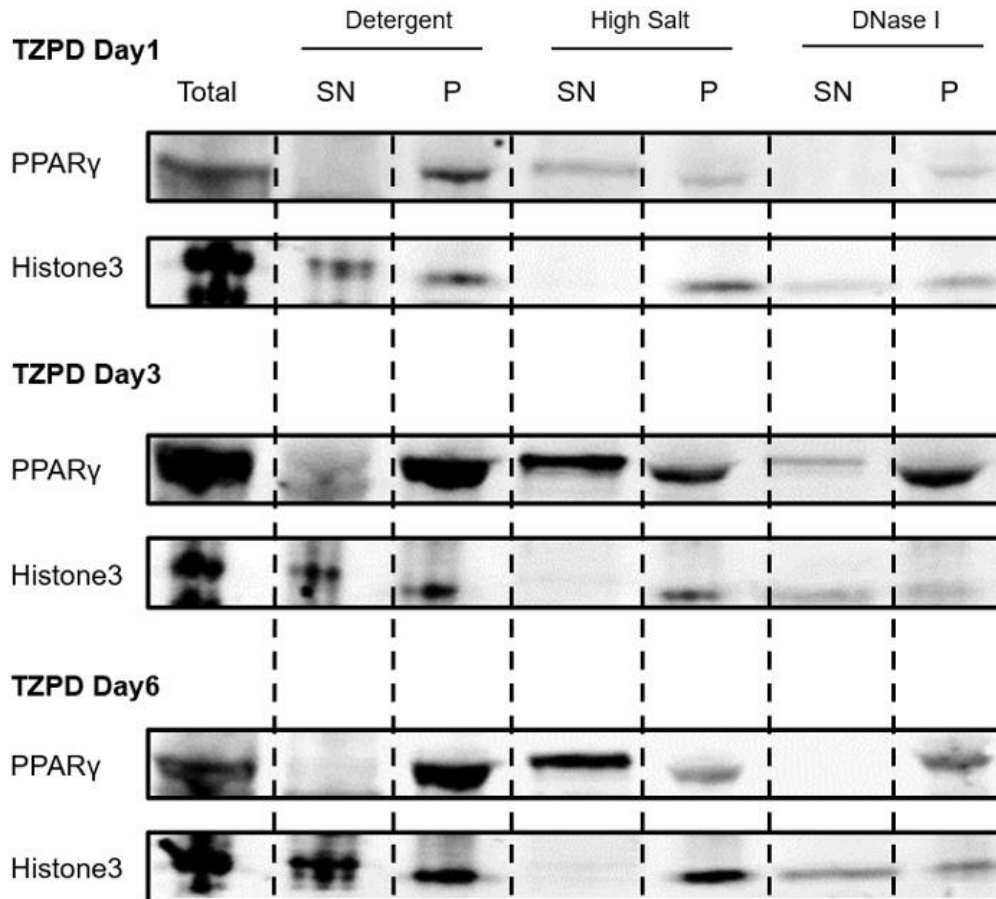
NHU cells were cultured to 90% confluent and then TZPD differentiated for 7 days. The cells were harvest as different time points during the differentiation process. The differentiated NHU cells were gone through CSK extraction and followed by analyze of western blot. PPARγ was label and histone3 was used to verify the DNase I treatment.

5.3.1.3 Quantification of tightly bound PPARγ protein in the nucleus during NHU cell differentiation

Known that PPARγ shows a compartmentalization change during urothelial cells differentiation, it is needed to quantify the expression of nuclear tightly-bound PPARγ protein during the differentiation process. The expression of PPARγ was analyzed using three independent NHU cell lines. Two different methods were applied to quantify the expression as described in the methods (Chapter 2, page). The results clearly showed that expression of PPARγ protein in the nucleus increase during differentiation (Figure 5.6). At the start of differentiation, PPARγ protein was tightly-bound in the nucleus of around 10% of cells. The proportion of nucleus tightly-bound PPARγ protein increase during differentiation but dramatically decreases start from day 5. The results verified previous findings that PPARγ protein shows the compartmentalization change during the differentiation. Moreover, it showed that heterogenetic expression of PPARγ protein in the nucleus during the urothelial cells differentiation.

Figure 5. 6: Expression of total PPARγ protein and nuclear tightly bound PPARγ protein during NHU cell differentiation.

Total

High salt wash
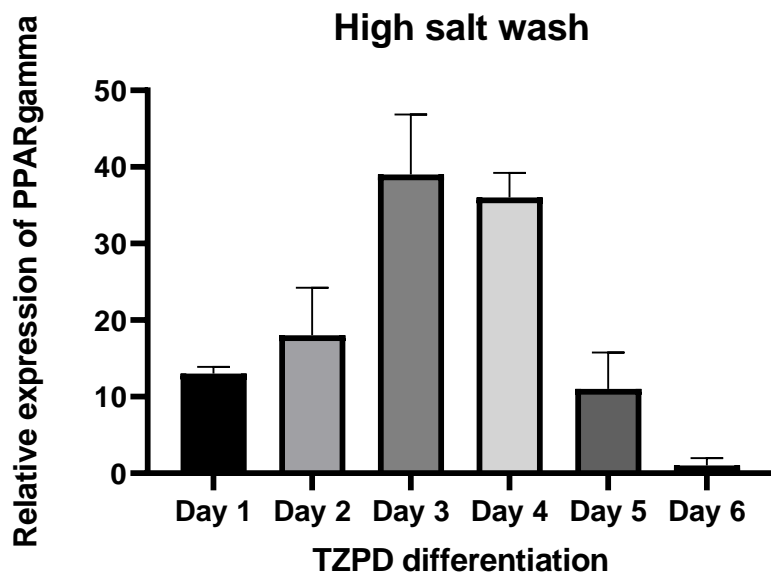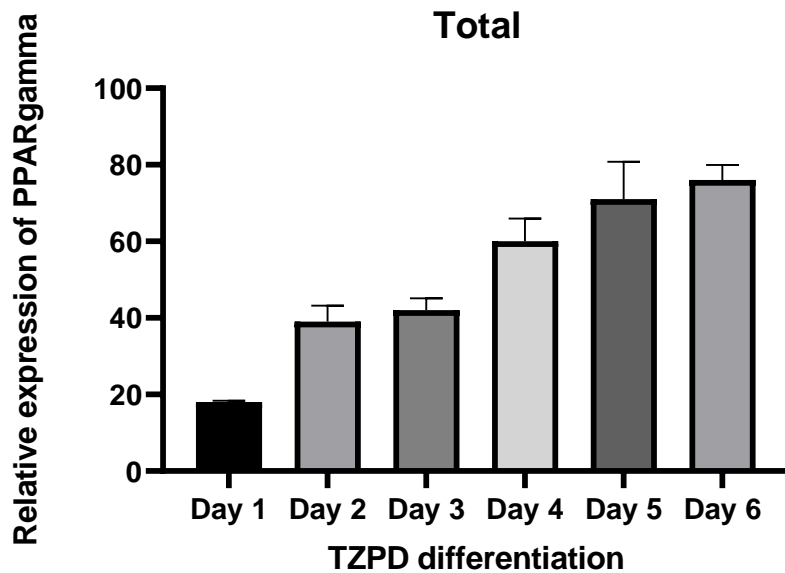
Y-axis represents the relative expression of PPARγ at everyday time point. X-axis represents the differentiation day time points. Three independent NHU cells were included and analyzed by either image J or tissue quest. Total represents NHU cells

without any treatment. High salt wash represents NHU cells go through Triton X-100 treatment and high salt buffer wash.

5.3.2 Compartmentalization of differentiation-associate transcription factors during NHU cell differentiation

ELF3 and FOXA1 was the transcription factors that demonstrate to be urothelial cells differentiation-associate. The expression of nucleus tightly bound ELF3 was much higher in day 1 and day 3 compared to day 6 (Figure 5.7). This suggested that ELF3 might functions at early stage of urothelial cells differentiation. However, results revealed that ELF3 was not chromatin-bound at day 1 suggesting it was not functioning at this time point. This might cause by the limited expression of ELF3 at early time point of urothelial cells differentiation. ELF3 protein was highly expressed after differentiated for 3 days or 6 days but also not chromatin bound. The results indicate that no ELF3 was chromatin-bound during the urothelial cells differentiation. It is because the DNase I treatment was not fully works according to the expression of histone 3.

Expression of FOXA1 was clearly shown in urothelial cells differentiated for 1 day, 3 day, and 6 days (Figure 5.8). They were mainly nucleus localized and resistant to the high salt buffer wash at day 1 and day 3. Small proportion of FOXA1 was resistant to high salt buffer wash at day 6 and suggested to be nucleus tightly-bound. However, no FOXA1 was

shown to be chromatin-bound during the urothelial cells differentiation. Further experiments were required to verify whether this finding was caused by unsuccessful DNase treatment.

Figure 5. 7: Differentiation-associate transcription factors ELF3 was not chromatin-bound during NHU cell differentiation.
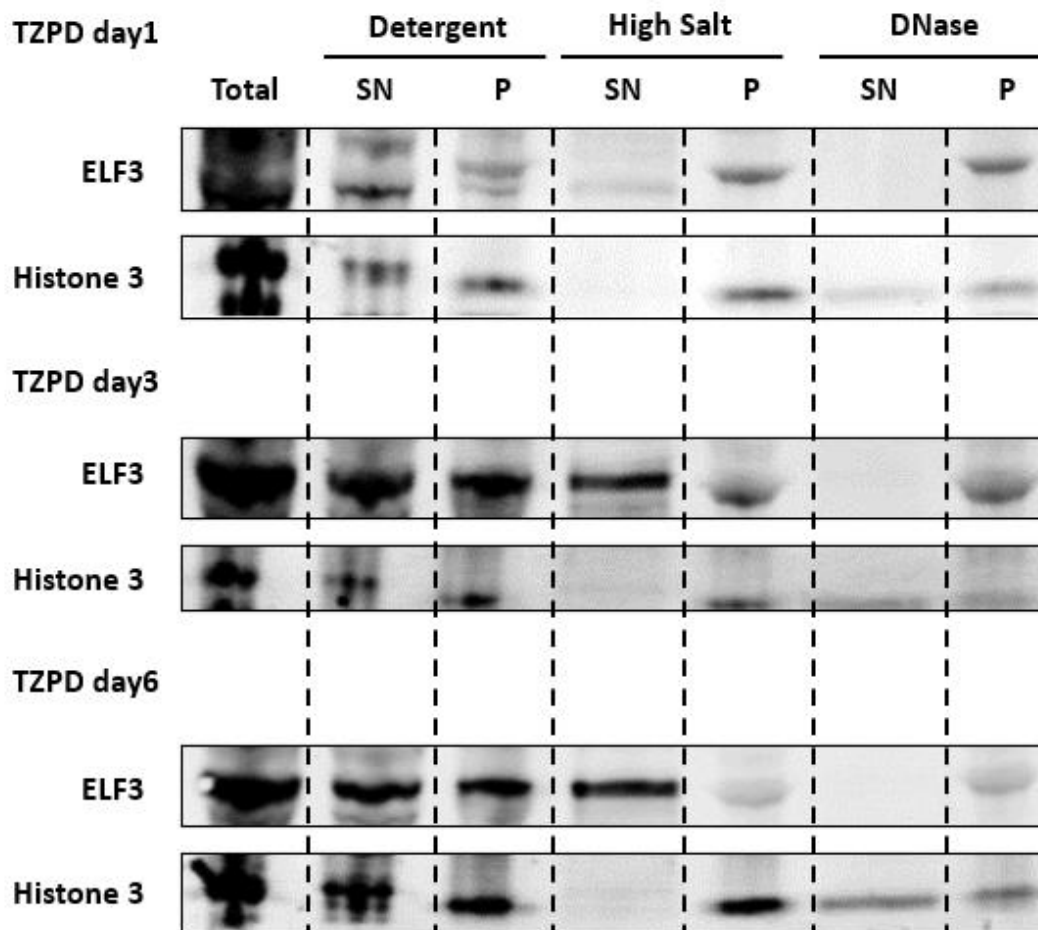

NHU cells were cultured to 90% confluent and then TZPD differentiated for 7 days. The cells were harvest as different time points during the differentiation process. The differentiated NHU cells were gone through CSK extraction and followed by

analyze of western blot. ELF3 was label and histone3 was used to verify the DNase I treatment.

Figure 5. 8: Differentiation-associate transcription factors FOXA1 was not chromatin-bound during NHU cell differentiation.
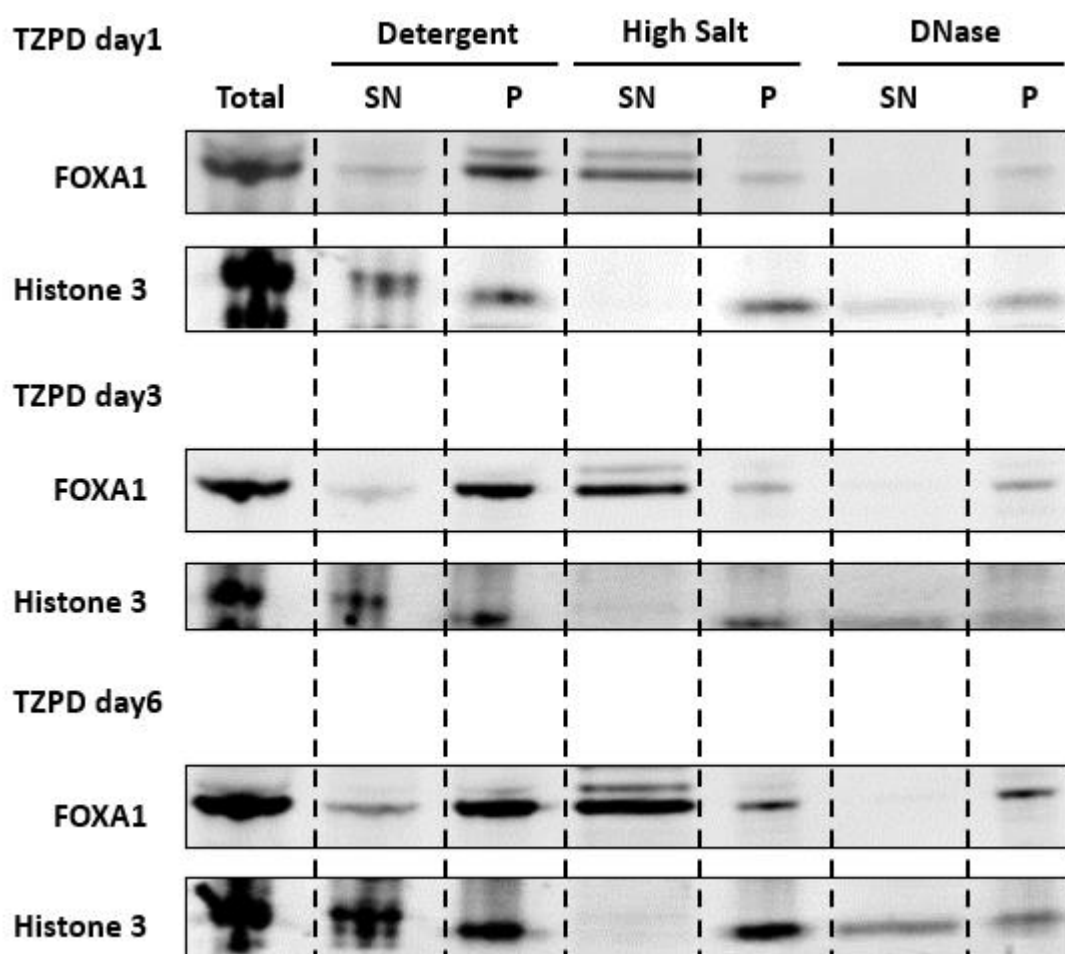
NHU cells were cultured to 90% confluent and then TZPD differentiated for 7 days. The cells were harvest as different time points during the differentiation process. The differentiated NHU cells were gone through CSK extraction and followed by analyze of western blot. ELF3 was label and histone3 was used to verify the DNase I treatment.

5.4 Discussion

5.4.1 PPARγ is chromatin-bound at specific window time during NHU cells differentiation

PPARγ is a nuclear receptor as described in the introduction chapter. PPARγ protein is demonstrated to initiate its regulation role on adipogenesis by forming a heterodimer with RXRα and binding to the specific PPRE region on the chromatin. PPARγ protein isoform 1 was shown to regulating the differentiation of urothelial cells but the underlying mechanism was not reported. To understand whether PPARγ regulates urothelial cell differentiation as a nuclear receptor, it is required to identify the localization of PPARγ during the differentiation progress. The results demonstrated that PPARγ was tightly-bouind in the nucleus in the urothelial cells within 24 hours of induction of differentiation following PPARγ activation (Section 5.3.2). However, it haven't included any earlier points than 24 hours so it stays unknown the time points PPARγ was nucleus localized. The localization of PPARγ in the nucleus was further revealed by subcellular extraction during NHU cells differentiation and the results found that PPARγ was chromatin-bound in the nucleus at day 3 of differentiation. ELF3, as a differentiation-associate transcription factor, its expression was directly regulated by PPARγ activity and was chromatin-bound at 72 hours. Thus,

PPARγ might still plays a role regulating NHU cells differentiation as a nuclear receptor to regulate the expression of transcription factor ELF3.

5.4.2 PPARγ does not function as a nuclear receptor at late stage of NHU cells differentiation

PPARγ has been shown to be nuclear localized in differentiated urothelial cells (Section 5.3.1). This research showed PPARγ protein was chromatin-bound in the early stage of urothelial differentiation and suggested to function as a nuclear receptor by regulating downstream transcription factors (Section 5.3.1.1). It is then identified that PPARγ protein start to detach from the chromatin at late stage of differentiation. Results demonstrated that nearly no PPARγ protein was chromatin-bound after TZPD differentiated for 6 days (Section 5.3.1.1). Thus, PPARγ might play a non-chromatin-bound role when differentiation process of NHU cells was finished. It is possible that PPARγ initiates the differentiation program of NHU cells but not needed when differentiation was finished. It might play a new role in differentiated NHU cells but its functions was not been identified.

5.5 Summary of findings

The research found PPARγ protein was always nucleus localized in NHU cells *in vitro*. Compartmentalization analyzed found it is not chromatin-bound in differentiated NHU cells *in vitro*. It is further verified that PPARγ proteins shows a compartmentalization change in the nucleus during NHU cells differentiation. It is chromatin-bound and functions at early stage of differentiation which suggested to regulates the differentiation process as a nuclear receptor. However, it detaches from the chromatin at late stage of differentiation but its non-chromatin bound role stays unknown. The differentiation-associate transcription factor ELF3 shows similar pattern with PPARγ and is chromatin-bound at early stage of differentiation. Next chapter will aiming to identify the non-chromatin bound role of PPARγ in differentiated NHU cells *in vitro*.

Chapter 6: Role of PPARγ in NHU cells regeneration and bladder cancer cell lines

6. Role of PPARγ in NHU cells regeneration and bladder cancer cell lines

6.1 Rationale and aim

In Chapter 3, it is showed that PPARγ regulates the differentiation of NHU cells. Moreover, the results also showed that activation of PPARγ was directly related with the expression ELF3 which is a NHU cells differentiation-associate transcription factor. However, in chapter 5 it illustrated that almost no PPARγ protein was not chromatin-bound in NHU cells differentiated more than 6 days even abundant PPARγ protein expression was detected. It is demonstrated in both TZPD and ABS/Ca^{2+} differentiation methods. This suggested that PPARγ might not functions as a nuclear receptor in the differentiated NHU cells. Differentiated NHU cells in situ is mitotic quiescent, it can regenerate quickly when damaged or wounded. The NHU cells will move to the wound area and can proliferate after wound healing. Thus, it is interesting to find out if PPARγ plays a role in the regeneration process of differentiated NHU cells. Because highly expression of PPARγ was detected in mitotically-quiescent differentiated NHU cells but PPARγ was not regulating the transcription as a nuclear receptor. The hypothesis is that PPARγ might activated during the regeneration process of NHU cells and is important

for barrier restitution during the regeneration process. In conclusion, this chapter aims to:

- Describe the localization of PPARγ during differentiated NHU cell regeneration process.

- Determine whether activation of PPARγ affects the regeneration of differentiated NHU cells.

- Study the downstream signaling of PPARγ and if it regulates the regeneration process of differentiated NHU cells.

6.2 Experimental approach

6.2.1 NHU cells wound healing cell model

NHU cells will be differentiated using ABS/Ca^{2+} differentiation method to form a tight barrier. The successfully forming of the barrier will be tested by TER mesurement (Methods section 2.5) as well as by the expression of tight junction proteins such as ZO1, ZO2, ZO3, and Claudin4. The differentiated NHU cells will be medium changed with drug or vehicle (0.1% v/v DMSO), 24 hours before wounding with a p20 pipette tip (Methods Section 2.3).

Figure 6. 1: NHU cells wound healing model.
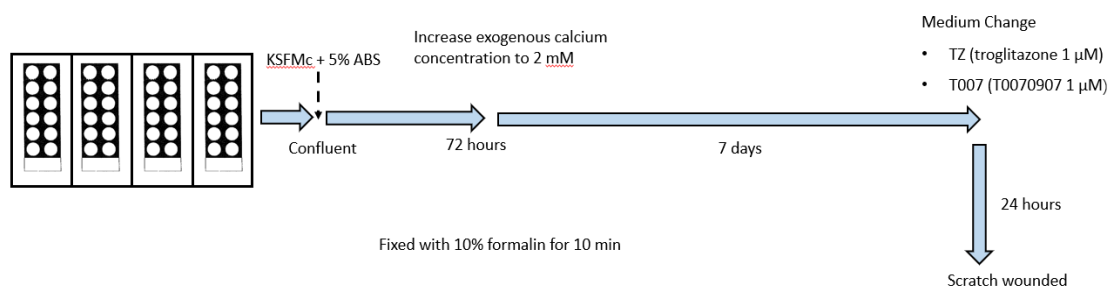
NHU cells were seeded on 12 well glass slides and differentiated using ABS/Ca^{2+} differentiation method. The medium was changed 24 hours before scratch wound. PPARγ agonist troglitazone or PPARγ inhibitor T0070907 were added 24 hours before scratch wound and remains in the medium during the regeneration processs. The regeneration process was monitored under the microscope and 12 well glass slides were fixed using 10% formalin.

6.2.2 Time lapse monitoring of NHU cells regeneration

To observe and quantify the regeneration process of differentiated NHU cells wounded healing assay will be recorded using the time lapse machine. The setting and use of the time lapse machine were illustrated in the method chapter. Here in this experiment, the camera was set to take the picture at the wound area every 10 minutes for 24 hours. The recorded pictures will be transformed into a movie. The wound area was calculated in the Image J software shown in Figure 6.2. It is done by manually drawing the line of the wound edge and then the software automatically calculated the circled area.

Figure 6. 2: Quantification of wound area.

The edge area was circle out using the ImageJ software. The area in the yellow line represented the unhealed wound area. The intensity and mean gray value of the unhealed wound area were calculated using the ImageJ software as shown below.

6.3 Results (Part A)

6.3.1 Expression of PPARγ and ELF3 during NHU cells regeneration

6.3.1.1 Expression of PPARγ during NHU cells regeneration

Expression of PPARγ was detected in the wound healing model of ABS/Ca^{2+} differentiated NHU cells. The NHU cells were ABS/Ca^{2+} differentiated for 7 days. The wound healing process was monitored under a microscope and cells were fixed at different time points during the whole NHU regeneration process.

As shown in Figure 6.2, the differentiated NHU cells were fully regenerated after 7 hours. The results clearly showed that PPARγ was highly expressed, and mainly nucleus localized during the regeneration process. But the expression of PPARγ at the wound area or behind the wound area shows no significant change during the regeneration process.

Figure 6. 3: Expression of PPARγ during the NHU cells regeneration.

0 hour   4 hour   8 hour

Start of regeneration

PPARγ at wound edge   DNA   Merge

PPARγ at region behind wound area   DNA   Merge
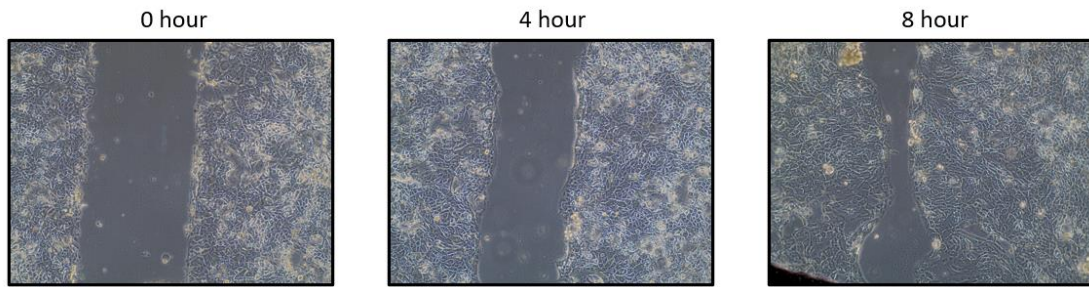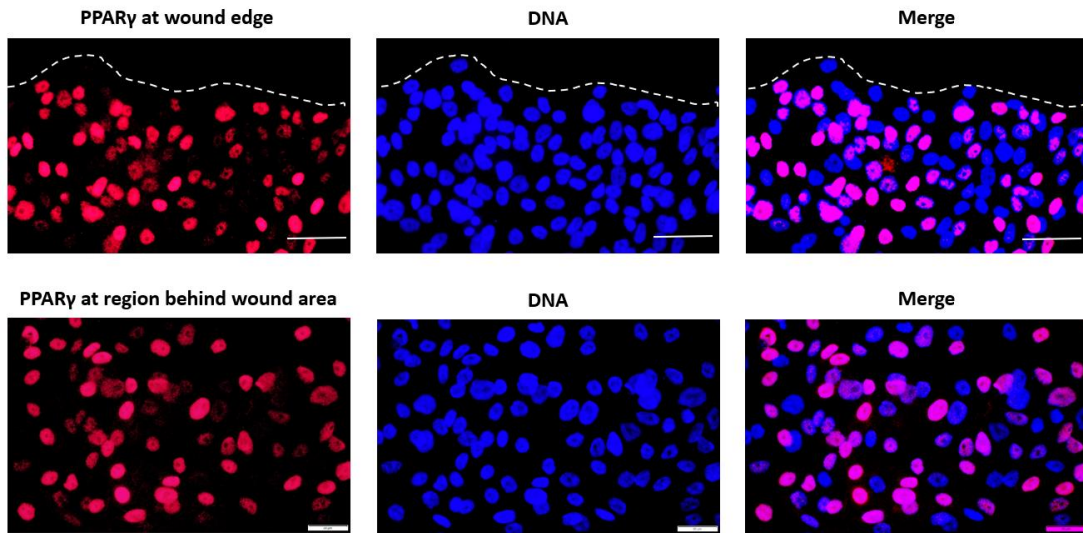
Scale bar=50 μM

4 hours after regeneration

Scale bar=50 μM
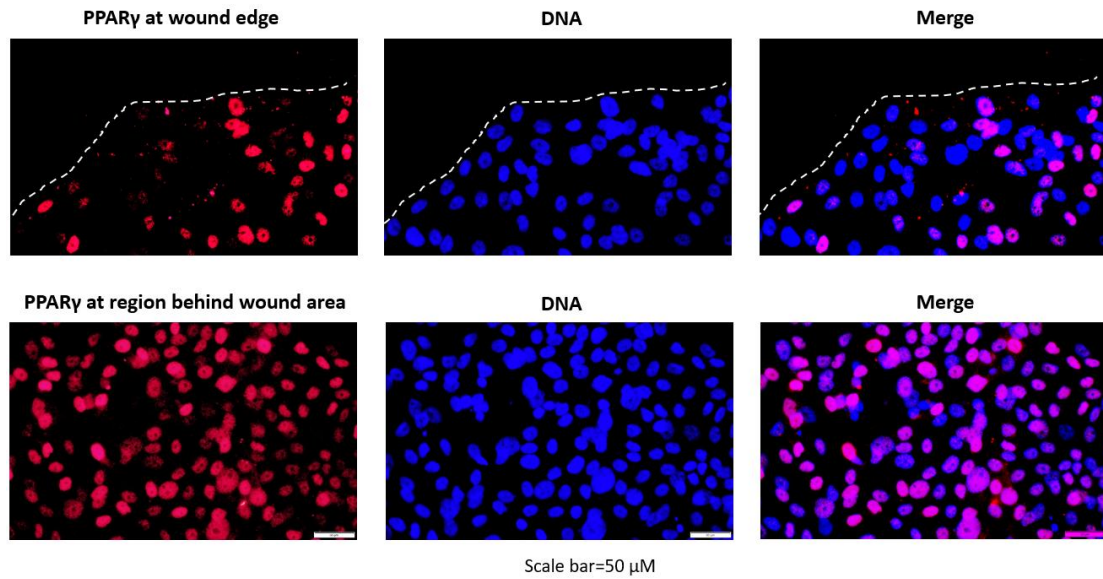
7 hours after regeneration

Scale bar=50 μM
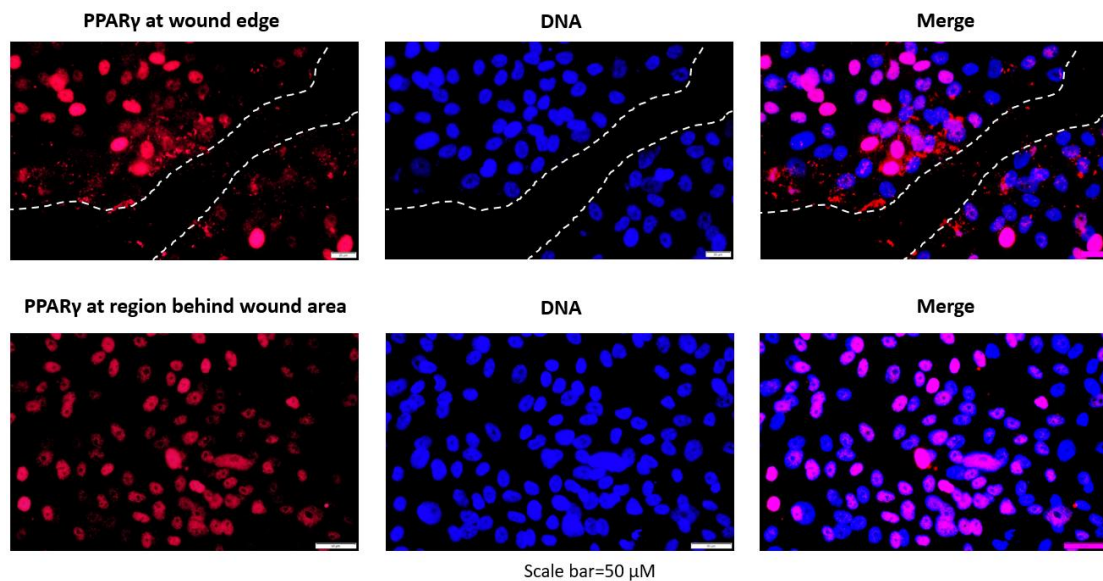
The regeneration process was monitored using time lapse machine. Pictures were taken to show the phenotype of NHU cells during the regeneration process. PPARγ protein was detected using 81B8 antibody and stained red. DNA was stained blue using Hochest33258. The picture was taken at both the wound edge area and the area behind the wound. Scale bar = 50 μm.

6.3.1.2 Expression of ELF3 during NHU regeneration

Being aware that expression of PPARγ was consistent during the NHU regeneration process, it is interesting to know whether the downstream target of PPARγ in the differentiation process changes during the regeneration process.

Results showed that high expression of ELF3 was observed during the whole regeneration process, but no obvious difference has been detected. It is suggested that either PPARγ was not function during the regeneration process or PPARγ was regulating other targets in the regeneration process. The next step will be aiming to identify whether the activation and inhibition of PPARγ affect the regeneration process.

Figure 6. 4: Expression of ELF3 durng NHU regeneration.

The slides were fixed using 10% formalin. ELF3 protein was detected using HPA003479 antibody and stained red. DNA was stained blue using Hoechst33258. Pictures were taken at the edge area during the whole regeneration process. Scale bar = 50 μM.

6.3.2 Role of PPARγ in NHU cells regeneration

6.3.2.1 Inhibition of PPARγ decrease the regeneration process of NHU cells

To verify whether the activation or inhibition of PPARγ will affect the regeneration process. PPARγ activator troglitazone and PPARγ inhibitor T0070907 were added 24 hours before scratch wounding. The cells were harvest and RNA was extracted to identify the differentiation state of the NHU cells. From Figure 6.4, the transcription of *PPARG* and differentiation-associated genes were comparable to differentiated NHU cells as well as in situ NHU cells. This suggested the NHU cells were successfully differentiated before scratch wounded.

To investigate the effect of PPARγ activation on NHU cell regeneration, differentiated NHU cells were cultured with PPARγ agonist and PPARγ inhibitor 24 hours before scratch wounded. The regeneration process was monitored under the time lapse machine. In three out of four independent experiments, it demonstrates that adding PPARγ inhibitor T0070907 significantly decreases the speed of NHU cell

migration**.** Further quantification on the slope of the regeneration speed also suggests that inhibition of PPARγ reduces the repairing speed of NHU cells.

Figure 6. 5: Transcription of PPARγ during NHU regeneration.
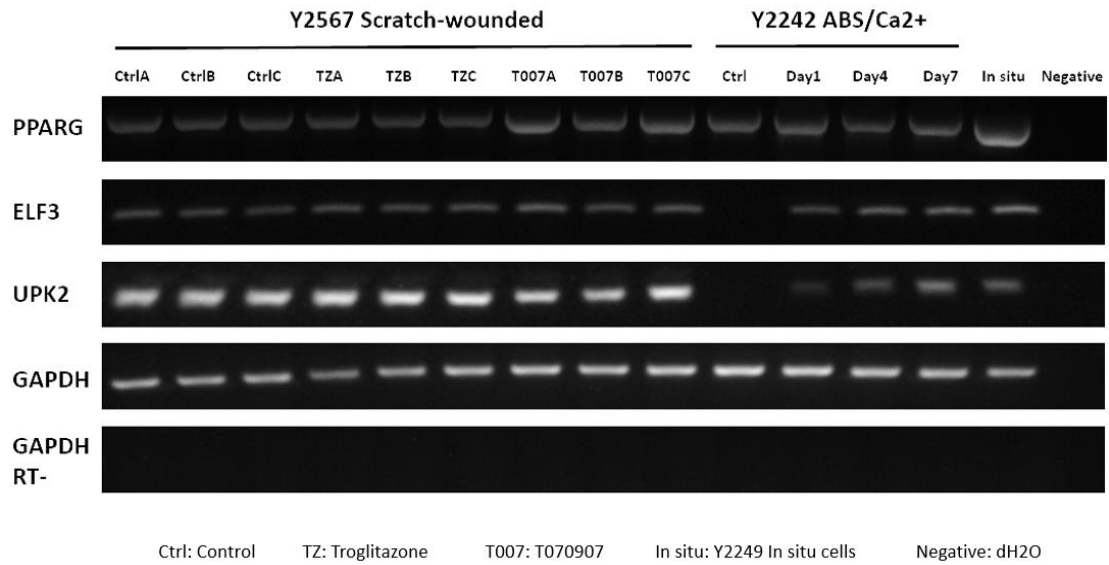
Transcription of *PPARG*, *ELF3*, *UPK2*, and *GAPDH* was detected using RT-PCR. Transcription of genes was detected in three independent replicates of Y2567 NHU cells. Y2242 ABS/Ca^{2+} differentiated NHU cells and in situ NHU cells were used as the positive control.

Figure 6. 6: Inhibition of PPARγ decrease the migration of NHU cells during wound healing process.
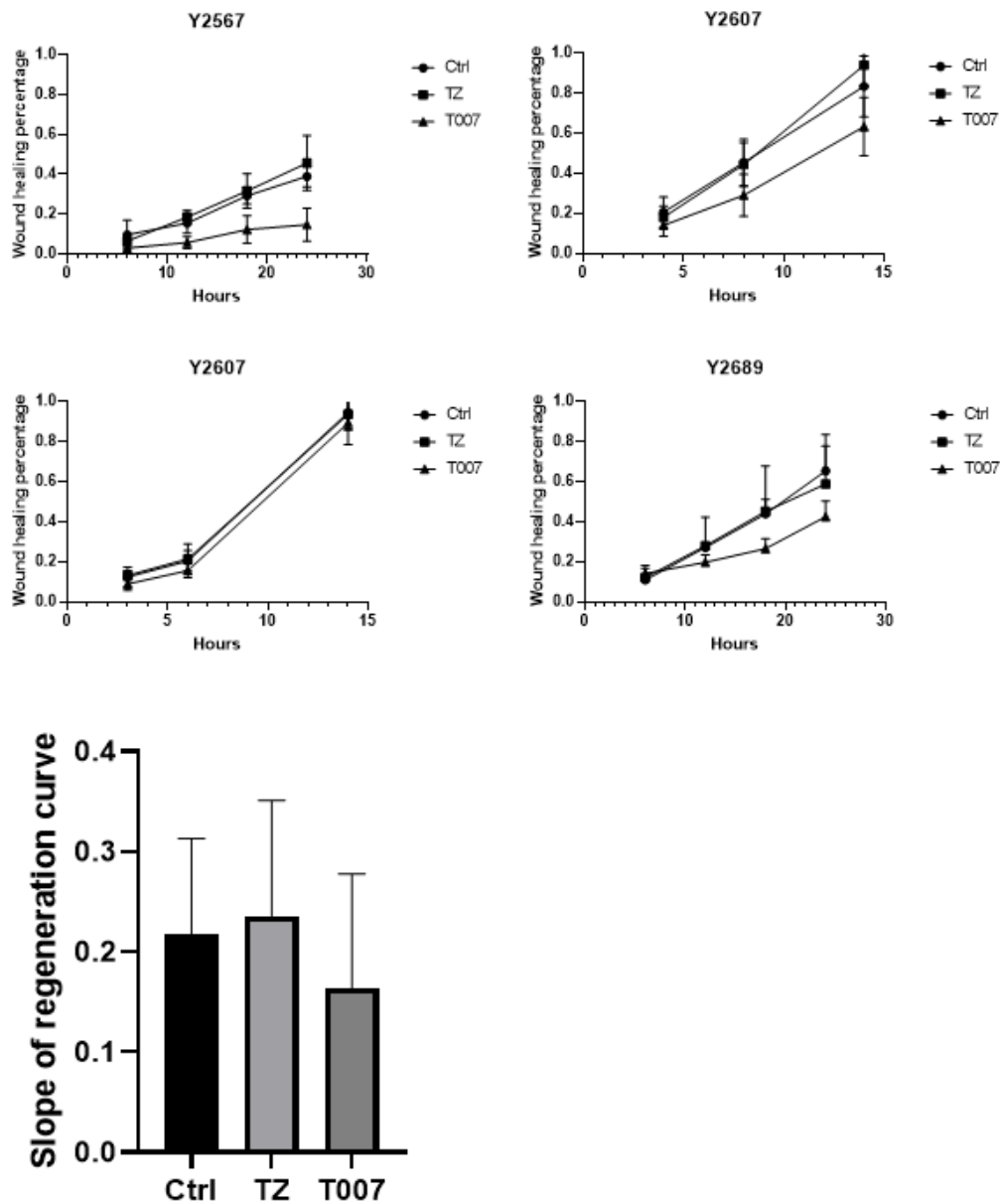
The regeneration process was quantified based on the unhealed wound area and the time. The scratch wound assay was conducted in four independent NHU cell lines. In 3 out of 4 NHU cell lines, inhibition of PPARγ significantly decreases the regeneration speed. The slope of the regeneration curve of each NHU cell was calculated. One way Anova analysis suggests there was no significant difference between Ctrl, TZ, and T007 groups.

6.3.2.2 Expression of PPARγ and ELF3 in PPARγ activated or inhibited NHU cells during regeneration.

Inhibition of PPARγ was affecting the regeneration speed of NHU cells but the expression of PPARγ shows no change. Here the immunofluorescent results illustrated that the localization of PPARγ during NHU regeneration was not changed with the adding of PPARγ agonist or PPARγ inhibitor. It is suggesting that the activation or inhibition of PPARγ did not change the subcellular localization of PPARγ protein during the regeneration process. ELF3 was the downstream target of PPARγ in NHU differentiation, it is interesting to know whether the expression of ELF3 changes during NHU regeneration with the adding of PPARγ agonist and PPARγ inhibitor. In Figure 6.7, it is showed that expression of ELF3 shows no significant change during the regeneration process. Thus, ELF3 might not the downstream target of PPARγ regulating the regeneration process of NHU cells. EGFR signaling was known to be involved in the proliferation and migration process in several cells. Here, the expression of EGFR was detected in PPARγ activated and PPARγ inhibited NHU cells during NHU regeneration. Expression of EGFR was enriched in the wound edge especially at the end of regeneration but no difference being observed between PPARγ activated and PPARγ inhibited NHU cells. This suggests PPARγ was not regulating NHU cell regeneration through EGFR signaling.

Figure 6. 7: Expression of PPARγ, ELF3 and EGFR in PPARγ activated or inhibited NHU cells during regeneration.

EGFR

| 0 hours | 4 hours | 8 hours |

TZ

T007
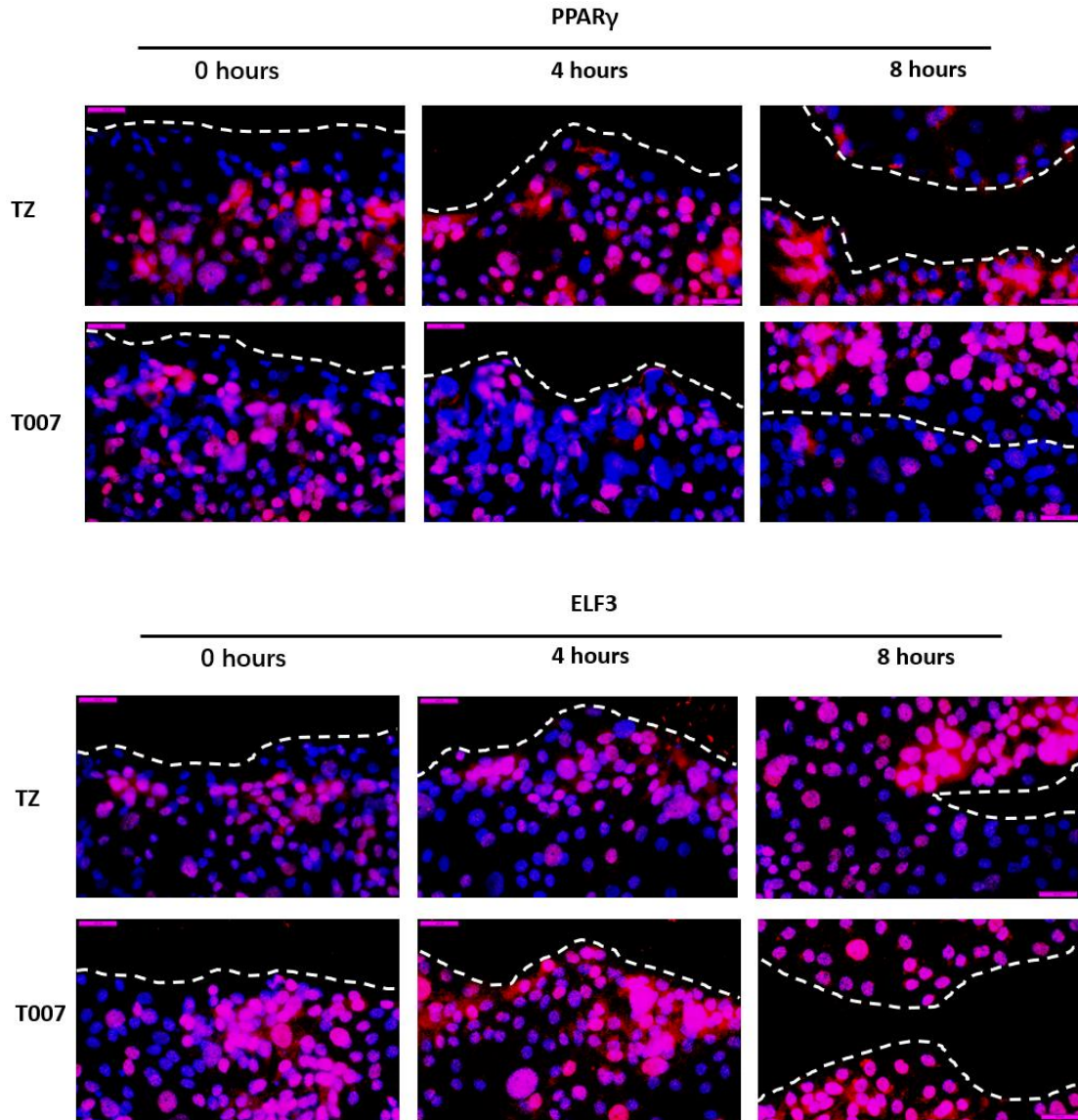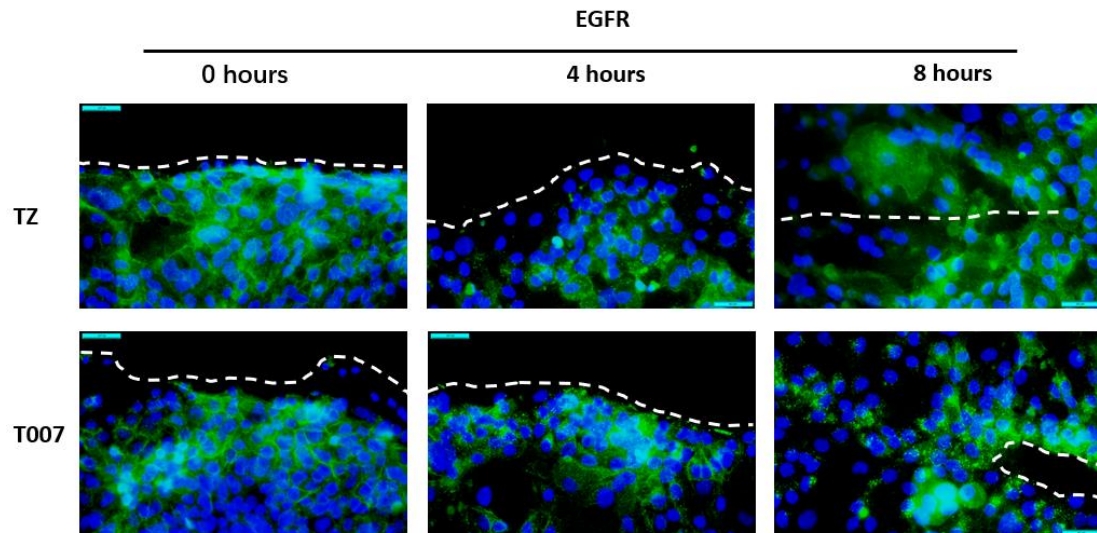
NHU cell DNA was stained blue using Hoechst33258. PPARγ and ELF3 were stained blue and merged with the DNA picture. EGFR was stained green and merged with the DNA picture. Images were taken at different time points during the NHU regeneration process. Cells were fixed using 10% formalin. Scale bar = 50 μM.

6.3.2.3 Expression of tight junction proteins in PPARγ activated or inhibited NHU cells during regeneration.

Previous in the lab we have identified that ABS/Ca^{2+} differentiated NHU cells highly express tight junction proteins. These proteins help forms a barrier against toxic particles in situ. The tight junction proteins may resist the NHU cells to migrate after being wounded. ZO1 and ZO3 were typical tight junction proteins. Their expression during the regeneration process was detected in PPARγ activated and PPARγ inhibited NHU cells.

Figure 6. 8: Expression of tight junction proteins in PPARγ activated or inhibited NHU cells during regeneration.

ZO1
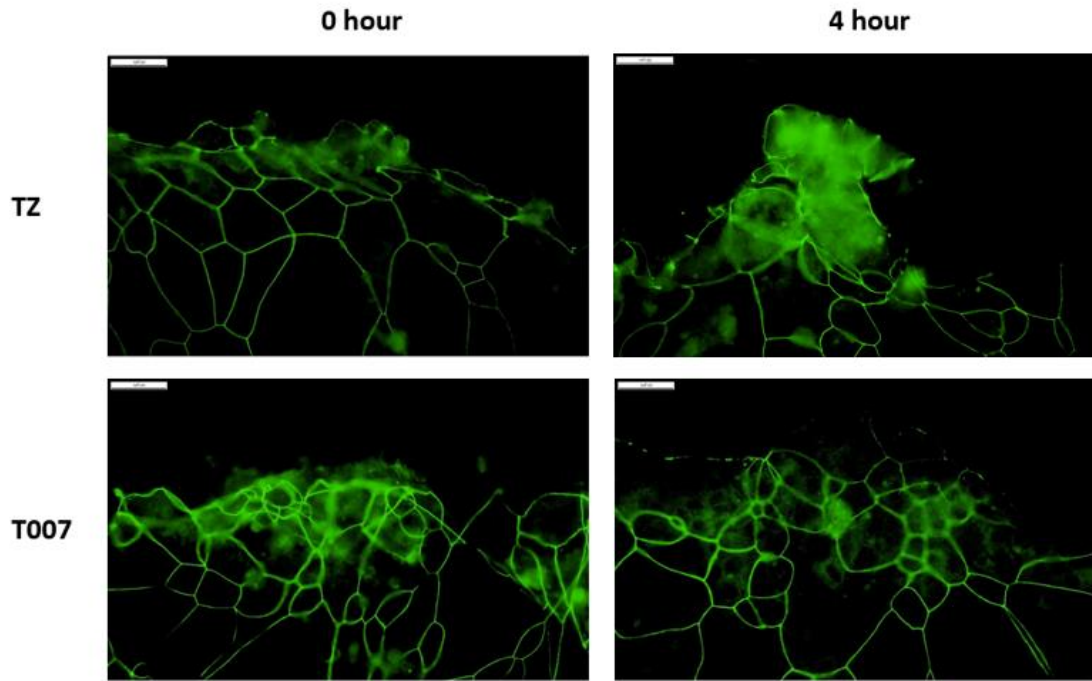
ZO3
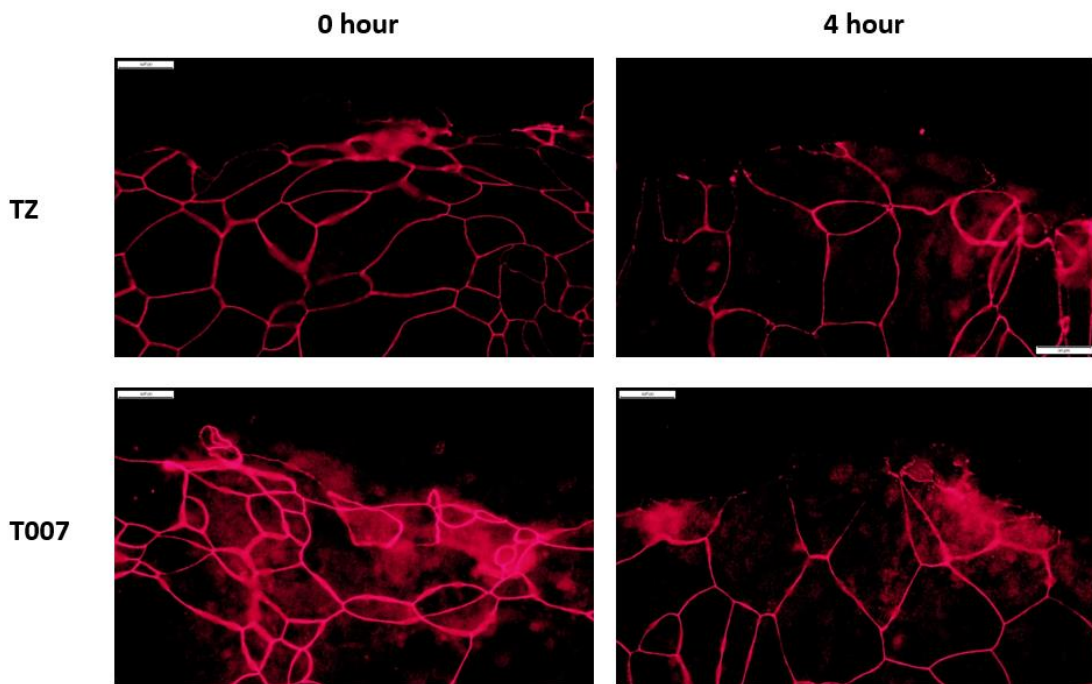
NHU cell DNA was stained blue using Hoechst33258. ZO3was stained blue and merged with the DNA picture. ZO1 was stained green and merged with the DNA picture. Images were taken at different time points during the NHU regeneration process. Cells were fixed using 10% formalin. Scale bar = 50 µM.

6.3.3 Activation of PPARγ regulate the NHU regeneration through TGF-β signalling

Literature in our lab has proved that TGF-β signaling was regulating the regeneration process of NHU cells (Fleming et al., 2012). Activation of TGF-β promotes the regeneration of NHU cells. Phosphorylation of Smad3 represents the activation of TGF-β signaling. P-Smad3 was mainly nucleus localized in PPARγ activated NHU cells at the beginning of regeneration while it is more cytoplasmic localized in PPARγ inhibited NHU cells. During the regeneration process, P-Smad3 was nucleus localized in both PPARγ activated and PPARγ inhibited NHU cells. The results suggest that inhibition of PPARγ prevents P-Smad3 from entering the nucleus at the beginning of regeneration. In another word, inhibition of PPARγ inhibit the activation of TGF-β signaling and in turn, decrease the regeneration process of NHU cells.

Figure 6. 9: Expression of P-Smad3 in PPARγ activated or inhibited NHU cells during regeneration.
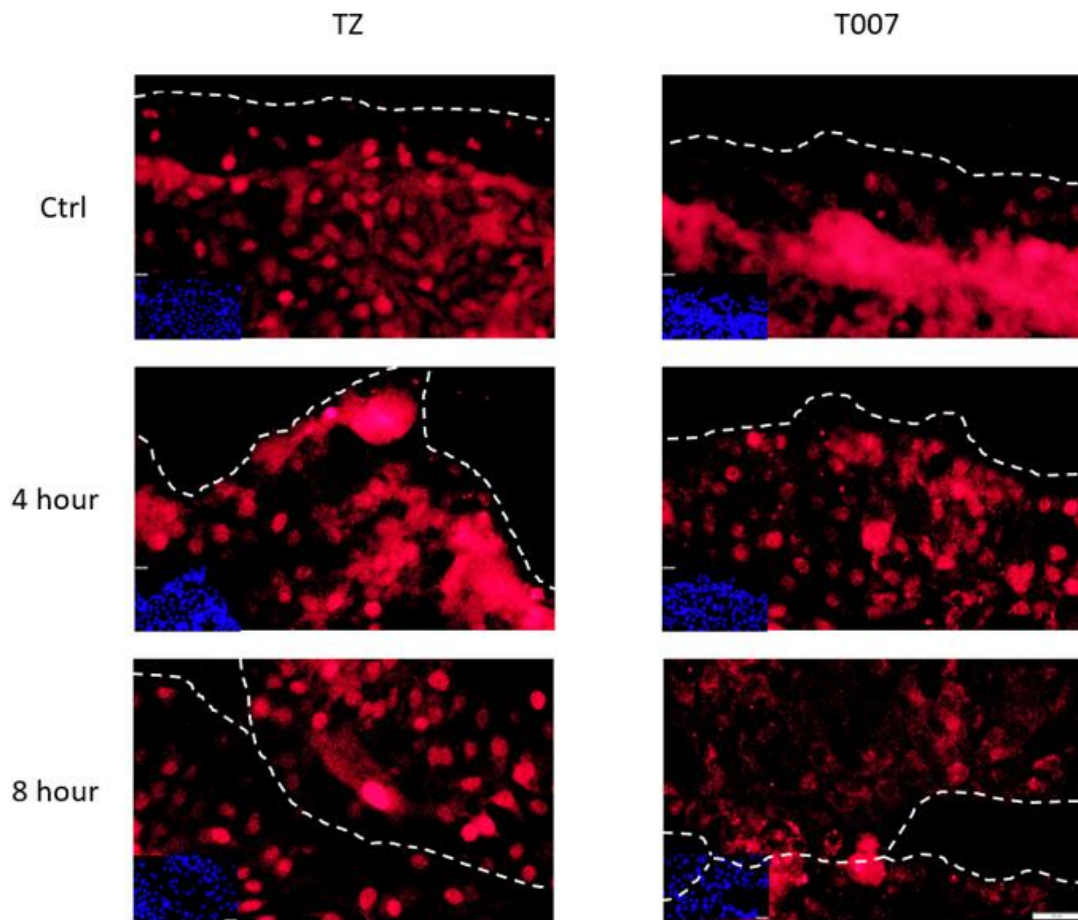
NHU cell DNA was stained blue using Hoechst33258. P-Smad3 was stained red and merged with the DNA picture. Images were taken at different time points during the NHU regeneration process. Cells were fixed using methanol Acetone. Scale bar = 50 μM.

6.4 Dissussion (Part A): Involvement of PPARγ in regulating the regeneration process of differentiated NHU cells

Urothelial cells are mitotically-quiescent in the urothelium but can proliferate when damaged or injured (Section 1.5). *In vitro*, ABS/Ca^{2+} differentiated urothelial cells form a tight barrier and can regenerate when scratch wounded. The observations showed that PPARγ protein was mainly nuclear localized during the regeneration process. The expression intensity of PPARγ shows no difference at or behind the wound edge during the regeneration process (Section 6.3.1.1). To assess whether PPARγ functions in regulating the regeneration of urothelial cells, it showed that treating differentiated NHU cells with PPARγ inhibitor prior to the scratch wounding significantly reduced the migration of NHU cells towards the wound edge in differentiated urothelial cells, without affecting the protein expression (Section 6.3.2.1). In the literature, it has been demonstrated that TGF-β signaling positively regulates wound repair of differentiated urothelial cells and the intensity of nuclear localized pSMAD3 increased with addition of exogenous TGF-β1 (Fleming et al., 2012). The results found pSMAD3 was more cytoplasmic localized in PPARγ inhibited urothelial cells (Section 6.3.3), suggesting that PPARγ might regulate the migratory speed of differentiated urothelial cells through TGF-β signaling. Thus,

PPARγ might play a new role regulating the regeneration of differentiated urothelial cells.

6.5 Summary of findings (Part A)

The results indicate that expression of PPARγ protein shows no difference during the regeneration process as well as its reporter ELF3. Further experiment identified that inhibition of PPARγ using T0070907 attenuate the wound healing speed of NHU cells. However, the expression of PPARγ and ELF3 was not affected by the treatment of PPARγ agonist troglitazone and PPARγ inhibitor T0070907. The tight junction proteins were also not affected by the activation and inhibition of PPARγ during the regeneration process. P-Smad3 as the downstream of TGFβ was more nucleus localized in troglitazone treated NHU cells. The PPARγ protein might regulate the regeneration process of NHU cells through promoting the nucleus transport of p-Smad3 but still needs further verification.

6.6 Rationale and aims (Part B)

Bladder cancer cells were suggested to involved from normal urothelial cells in situ. Previously studies had identified *PPARG* highly transcribed in luminal subtype bladder cancer and inhibition of PPARγ was suggested to be a potential therapy. However, the role of PPARγ in luminal bladder

cancer is not well understood. The results identified PPARγ promote the wound healing process in NHU cells, and it is possible that bladder cancer cells hijack the role of PPARγ in normal urothelial cells to overcome its cell cycle arrest. The hypothesis is PPARγ plays a role in luminal bladder cancer cells to promote its proliferation. In conclusion, the chapter aims to:

- Expression of PPARγ in bladder cancer cell lines.

- Compartmentalization of PPARγ in luminal bladder cancer cell lines.

- Role of PPARγ in luminal bladder cancer cell's proliferation.

6.7 Results (Part B)

6.7.1 PPARγ protein express in both basal-like and luminal bladder cancer cell lines

Bladder cancer cell lines SCaBER, 5637, RT4, RT112, and UMUC9 were brough up and cultured to 50% confluence. SCaBER and 5637 were suggested to be basal-like bladder cancer cell lines while RT4, RT112, and UMUC9 were luminal bladder cancer cell lines. The results showed that PPARγ protein was expressed in both basal-like and luminal bladder cancer cell lines (Figure 6.10). The expression intensity of PPARγ protein

is higher in luminal bladder cancer cell lines and UMUC9 showed the most abundant expression of PPARγ protein.

Figure 6. 10: Expression of PPARγ protein in bladder cancer cell lines.
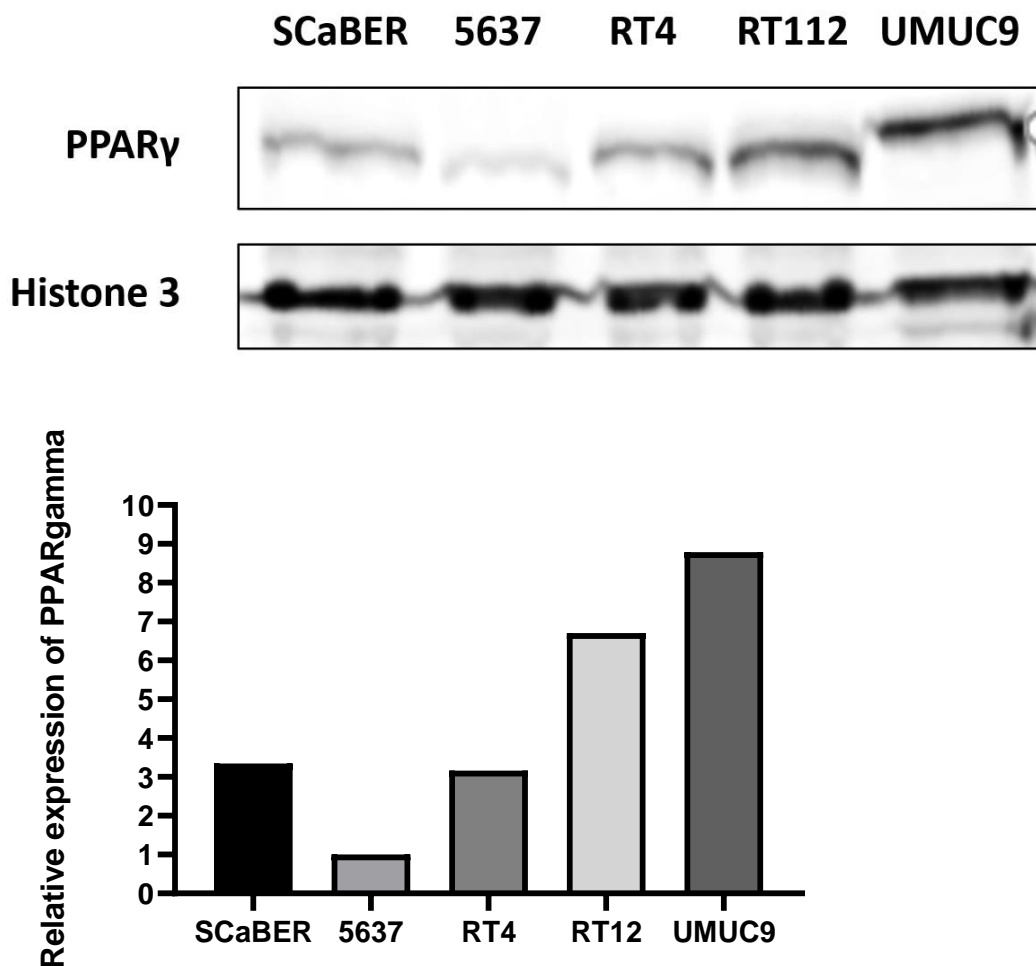
The picture on the top illustrates the expression of PPARγ in bladder cancer cell lines. Bladder cancer cell lines were cultured to 50% confluence and protein lysates was harvested. PPARγ was detected using antibody 81B8 while histone 3 is used as housekeeping antibody. The graph below represents the relative expression of PPARγ in different bladder cancer cell lines. The quantification of the PPARγ expression was calculated using image J software.

6.7.2 PPARγ is not chromatin-bound in luminal bladder cancer cell lines

The expression of PPARγ was detected in luminal bladder cancer cell lines previously (Section 6.7). Luminal bladder cancer cells were characterized by high transcription of PPARγ downstream genes and suggested that PPARγ should be activated in luminal bladder cancer cells. The results revealed the compartmentalization of PPARγ in luminal bladder cancer cell lines UMUC9 and RT112. PPARγ was mainly nucleus localized in both UMUC9 and RT112 bladder cancer cells but cytoplasmic PPARγ has also been detected (Figure 6.11). However, the immunofluorescence results found no PPARγ was detected after high salt buffer wash indicate PPARγ was not tightly bound in the nucleus. Western blot results verified the finding. The results demonstrate PPARγ protein was nucleus localized but not chromatin-bound in both UMUC9 and RT4 luminal bladder cancer cell lines. The compartmentalization of PPARγ in basal-like bladder cancer lines stays unknown.

Figure 6. 11: Immunofluorescent results of PPARγ localization in the nucleus of luminal bladder cancer cell lines.
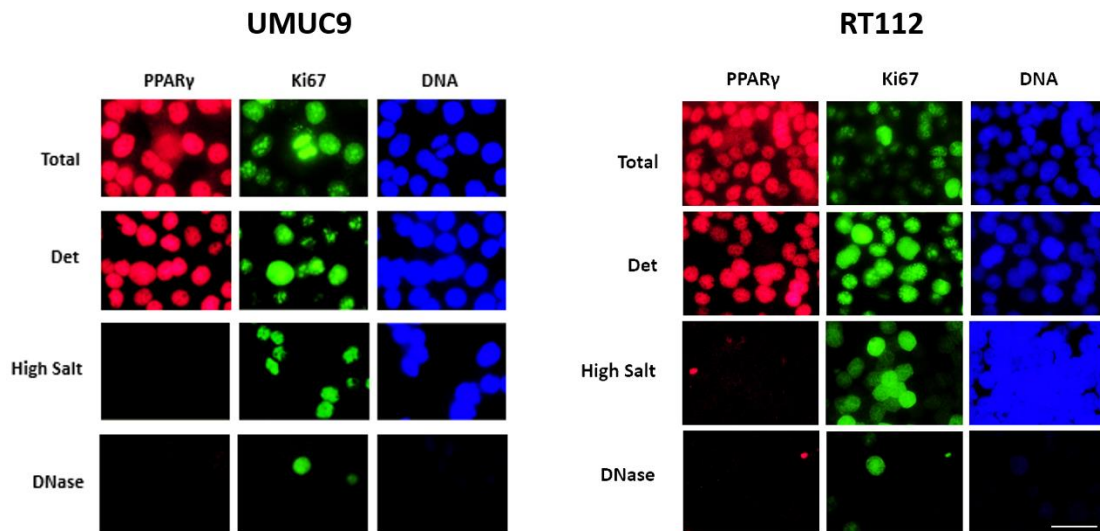
UMUC9 and RT 112 were fixed using 10% formalin. Picture shows the expression of PPARγ after each wash and treatment. PPARγ was labeled using antibody 81B8. Ki67 is a proliferating marker. Scale bar = 50 μM.

Figure 6. 12: Western blot results of PPARγ compartmentalization in luminal bladder cancer lines.
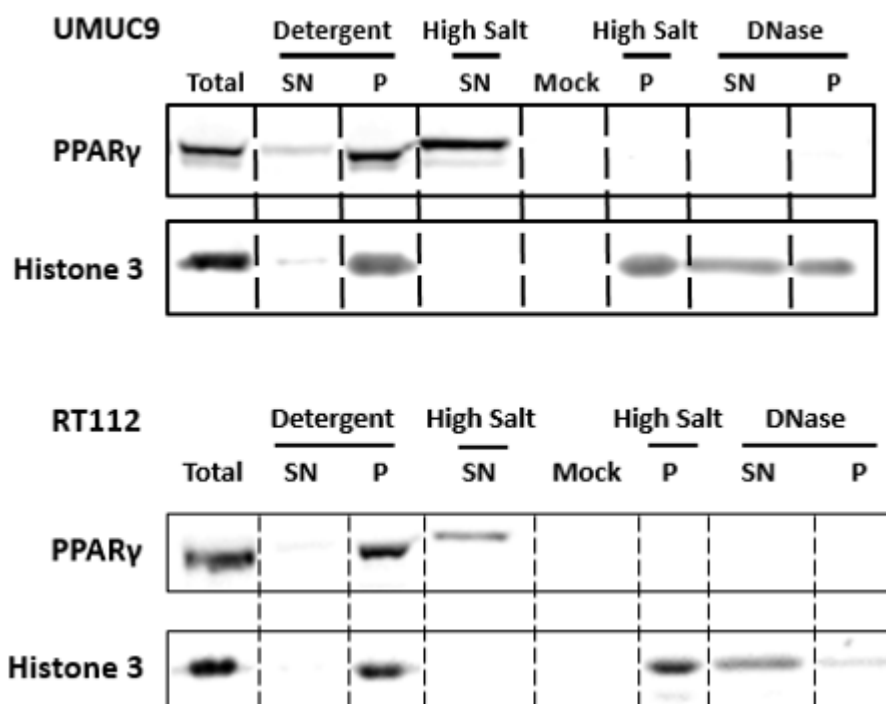
Bladder cancer cells were cultured to 50% confluent. The bladder cancer cells were then gone through CSK extraction and followed by analyze of western blot. PPARγ was label and histone3 was used to verify the DNase I treatment.

6.7.3 Inhibition of PPARγ doesn't globally attenuate the cell viability of luminal bladder cancer cell lines

PPARγ was identified to be non-chromatin bound in luminal bladder cancer cells, but previous literature reported inhibition of PPARγ affects the proliferation of bladder cancer cells (Section 1.6). In order to identify the function of PPARγ in luminal bladder cancer cell lines, inhibition and activation of PPARγ was included with further analysis of Alamar Blue

assay. The results found inhibition of PPARγ using T0070907 does not affect the cell viability of RT4 and RT112 cells. But the cell viability of UMUC9 cells was significantly downregulates when PPARγ was inhibited (Figure 6.13). Activation of PPARγ shows no effect on cell viability of all luminal bladder cancer cell lines. To access whether PPARγ directly regulates the proliferation of UMUC9 cells, UMUC9 cells were treated with PPARγ agonist troglitazone (TZ) or its inhibitor T0070907 (T007) for up to 7 days. The result illustrated that the cell number of UMUC9 cells did not affect by either activation or inhibition of PPARγ. The cell metabolism of TZ or T007 treated luminal bladder cancer cell lines was not measured.

Figure 6. 13: Inhibition of PPARγ only affect the cell viability of luminal bladder cancer cell line UMUC9.
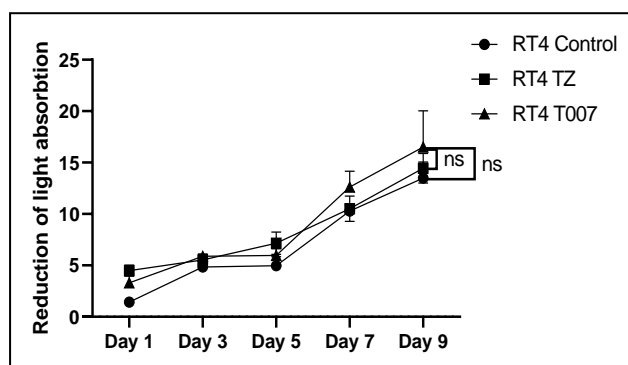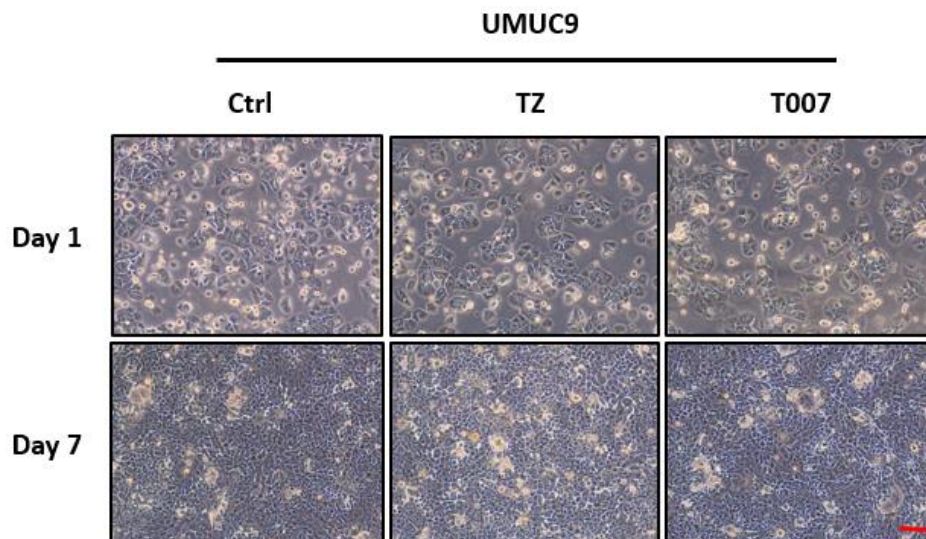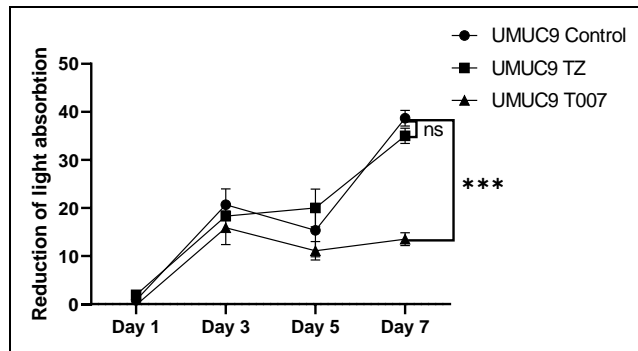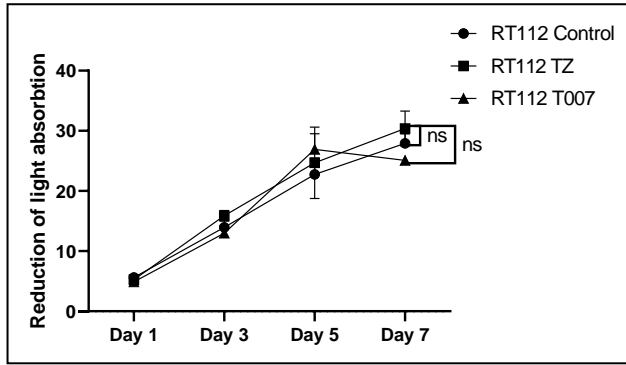
Three graphs on the top represent the results of Alamar Blue assay of three luminal bladder cancer cell lines RT4, RT112, and UMUC9. Y-axis showed the reduction of light absorption which represents the cell viability. X-axis represents the measuring day time points. The picture below showed the cell density and morphology of UMUC9 cells at day 1 and day 7 treatment. Scale Bar=100 μm.

6.8 Discussion (Part B): Role of PPARγ in bladder cancer cells

The transcription of *PPARG* was identified in bladder cancer and suggested to control the expression of biomarkers of luminal bladder cancer (Choi et al., 2014). The RNAseq results found transcription of *PPARG* was significantly lower in basal like bladder cancer cell lines compared to luminal bladder cancer cell lines (Section 6.6.1). The research further identify the expression intensity of PPARγ protein was higher in luminal bladder cancer cell lines but also obviously expressed in some basal bladder cancer cell lines (Section 6.6.1). This suggest PPARγ might also functions in basal like bladder cancer cells despite of its low gene transcription. It is the genes controlled by PPARγ that separates basal and luminal bladder cancer cell lines. Literature has reported the cell viability and proliferation of bladder cancer cell line T24 was affected by inhibition of PPARγ activity (Cheng et al., 2019). The results found the cell viability of luminal bladder cancer cell line UMUC9 was downregulated by the inhibition of PPARγ but other bladder cancer cell lines shows no difference (Section 6.6.3). UMUC9 has aberrantly high transcription of *PPARG* and mutation of *PPARG* was reported so

194

that it might be the mutated PPARγ controlling the cell viability of UMUC9 bladder cancer cell lines. Moreover, the investigation further identify the localization of PPARγ in luminal bladder cancer cell lines and found PPARγ was mainly nucleus localized. However, it is further found PPARγ was not tightly bound in the nucleus in luminal bladder cancer cell lines. It suggests PPARγ is not chromatin-bound and doesn't function as nuclear receptor in luminal bladder cancer cell lines. PPARγ was also reported to express in bladder cancer cells and involved in migration and invasion of bladder cancer cells (Yang et al., 2013). The previous results showed that PPARγ was not tightly bound in the nucleus of differentiated urothelial cells and inhibition of PPARγ reduce the migration of urothelial cells during wound healing. Thus, PPARγ might also functions to regulate the migration and invasion of bladder cancer cells but needs further experiments to discover the mechanism underlying it.

6.9 Summary of findings (Part B)

Transcription of *PPARG* was significantly higher in luminal bladder cancer cells but the expression of PPARγ protein was detected in both basal-like and luminal bladder cancer cells. PPARγ protein was obviously expressed in luminal bladder cancer cell lines but identified to be non-chromatin

bound. A small proportion of cytoplasmic PPARγ protein was also observed in luminal bladder cancer cell lines. The activation and inhibition of PPARγ protein did not affect the cell viability of RT4 and RT112 cells. However, inhibition of PPARγ attenuate the cell viability rather than the proliferation of UMUC9 cells.

Chapter 7: Discussion

7. Conclusions

7.1 Overview

Urothelium serves as the tight barrier epithelium in the human body while the balance between the differentiation and proliferation of urothelial cells is import to maintain its function. Prior to this thesis, PPARγ is a nuclear receptor that functions to regulate adipogenesis but its activation was identified to triggle the differentiation of NHU cells *in vitro* (Liu et al., 2019; Varley et al., 2006; Varley et al., 2004). Transcription variants of *PPARG* encodes three identical protein isoforms of PPARγ protein but their expression in NHU cells was not been reported. Moreover, studies investigated the downstream transcription factor genes upregulated by PPARγ activation in urothelial cells, little was done to investigate the expression and subcellular localization of PPARγ protein during differentiation (Varley et al., 2009; Varley et al., 2006). The *in vitro* NHU cell model used in this thesis provides an ideal cell model to better characterize the role of PPARγ in human urothelial cells.

The present study firstly discovered the *PPARG* transcription variants and PPARγ protein isoforms in the NHU cells. Results found *PPARG* encoding PPARγ1 was dominantly expressed in human urothelial cells. The results further reveals the subcellular localization of PPARγ and

suggesting it shows a compartmentalization change in the nucleus during the differentiation process. PPARγ was also identified to participate in the regeneration of NHU cells and promote the migration of NHU cells towards the wound. The compartmentalization of PPARγ in luminal bladder cancer cell lines was demonstrated to share similarity with post-differentiated NHU cells. These results provide the first evidence that PPARγ obtains distinct mechanism *in vitro* to regulate the differentiation and regeneration process of NHU cells while bladder cancer cell lines might hijack the function of PPARγ in NHU cell regeneration.

7.2 Transcription of *PPARG* and Expression of PPARγ protein in human urothelial cells

Previous studies have illustrated the existence of *PPARG* transcription variants in the human body (Aprile et al., 2014; Omi et al., 2005). In this study, 12 transcription variants of *PPARG* have been identified. The results showed that *PPARG* encoding PPARγ1 was dominantly transcribed in situ while further investigation demonstrate PPARγ1 was dominantly expressed in NHU cells *in vitro*. In adipogenesis, PPARγ2 was suggested to play the regulatory role rather than PPARγ1 but the underlying mechanism stays unknown (Saladin et al., 1999). Morevoer,

another paper using PPARγ knock out mice with the restoration of either PPARγ1 or PPARγ 2 and demonstrated that PPARγ2 isoform functions to accelerate mouse prostatic carcinogenesis (Strand et al., 2012). The absence of the transcription and expression of PPARγ2 suggests it is not required in NHU cells. This suggested PPARγ might adopt a different mechanism controlling the differentiation of urothelial cells compared to other cells types.

Transcription of *PPARG* was continuously detected but expression of PPARγ protein was only obviously observed within the differentiation. The results suggested that EGFR signaling was responsible for the translation of PPARγ protein but the mechanism remains unknown (Section 4.3.1). The adding of PPARγ inhibitor T0070907 could rescue the cell death from the overexpression of PPARγ1. This indicates it is the activation not the expression of PPARγ that was lethal to NHU cells. Thus, NHU cell proliferation and activation of PPARγ were in turn inhibit each other in undifferentiated NHU cells. There might exist a upstream regulator of PPARγ controlling the switch of proliferation to differentiation in NHU cells. However, it is the first evidence illustrating the translation of PPARγ in human urothelial cells and may provide a promising direction to illustrate the regulatory mechanism of PPARγ expression *in vivo*.

7.3 PPARγ in urothelial cell differentiation

Expression of PPARγ protein was detected after the initiation of both the NHU cell TZPD differentiation or ABS/Ca^{2+} differentiation. The abundance of protein expression slowly increase in the first few days but showed no significant difference later (Section 3.3.5). This supports previous findings in the literature that PPARγ might function as a regulator to initiate NHU cell differentiation (Varley et al., 2004). It is important to identify the activation of PPARγ during NHU cell differentiation to verify its regulatory role. PPARγ is well known to function as a nuclear receptor in adipogenesis, where FABP4 has been shown to be a downstream reporter of PPARγ activation (Lamas Bervejillo et al., 2020). ELF3 is a transcription factor reported to be associated with NHU cell differentiation (Bock et al., 2014). The results using TZPD differentiation found expression of FABP4 and ELF3 protein to be consistent with the expression of PPARγ, whilst inhibition of PPARγ activity using T0070907 attenuated expression of both (Section 4.3.2); this suggests they were regulated by PPARγ activation. By contrast, in ABS/Ca^{2+} differentiation, the expression of PPARγ and ELF3 was clearly detected but no expression of FABP4 was found during the whole progress. Moreover, treatment with T0070907 (Section 3.4.2) did not attenuate expression of ELF3 protein abundance. This suggests that if expression of FABP4 is a direct marker of PPARγ activation then PPARγ is

expressed but not activated in ABS/Ca^{2+} differentiation. It is possible that PPARγ was the side product of the activation of NHU cell ABS/Ca2+ differentiation upstream regulator. It also raises the possibility that other pathways may regulate expression of ELF3.

If PPARγ functions as a nuclear receptor in NHU cell differentiation, the chromatin-binding of PPARγ is likely to reflect its activation state. PPARγ protein was bound to the chromatin at early (1 to 5 days) post-initiation of differentiation but became less tightly bound in the nucleus in TZ/PD differentiated NHU cells. Notably, the PPARγ ligand troglitazone was removed after 24 hours in the TZPD differentiation protocol. Troglitazone was known also known to binds with farnesoid X receptor (FXR) while FXR was activated by PPARγ to promote lipogenesis in adipocytes (Kaimal et al., 2009; Shinohara and Fujimori, 2020).Thus, removal of PPARγ might affect the activation status and hence chromatin binding of PPARγ in the later stages of differentiation. In the ABS/Ca^{2+} differentiation process, where no exogenous PPARγ ligand was added, PPARγ protein was also suggested to be tightly bound in the nucleus at day 3, becoming less tightly bound in late (day 6) differentiated NHU cells. This suggests a parallel process, however, the DNase treatment could not be made to work in differentiated ABS/Ca^{2+} cells, preventing solid evidence about its binding target in the nucleus. In

conclusion, the results indicate a role for PPARγ as a nuclear receptor in initiation of NHU cell differentiation but raises questions still to be resolved about the regulation and role of ELF3 and the role of PPARγ in the post-differentiated urothelial cell.

7.4 PPARγ in urothelial cell regeneration

PPARγ protein was abundantly expressed in ABS/Ca^{2+} post-differentiated NHU cells but its function was not being investigated before. Regeneration is an important biological progress of NHU cells to reform the barrier after being damaged or wounded. The results firstly identified that inhibition of PPARγ significantly decrease the wound repairing speed of post-differentiated NHU cells *in vitro*. However, the activation of PPARγ using its agonist troglitazone did not accelerate the repairing speed compared to the control group. It suggest there might existing endogenous ligand in the culturing medium. Previous report in the lab showed that TGF-β signaling was function to promote the wound repairing of differentiated NHU cells (Fleming et al., 2012). Smad3 was the downstream of TGF-β and its phosphorylation indicate the activation of the signaling. The observation found few p-Smad3 was transport into the nucleus under the inhibition of PPARγ. PPARγ might functions in post-differentiated NHU cells to regulate its wound repairing process

through TGF-β signaling. However, literatures generally reported that PPARγ were negatively regulating TGF-β signaling (Nemeth et al., 2019; Sun et al., 2006; Tan et al., 2010). Thus, the experiments needs to be repeated to verify the observation about the positive regulatory role of PPARγ on TGF-β signaling in NHU cell regeneration.

7.5 PPARγ in bladder cancer cell lines

Transcriptome analysis of *PPARG* in bladder cancer cell lines suggested it is highly associated with luminal subtype bladder cancer(Choi et al., 2014). Its activation also reports to influence the proliferation of bladder cancer cell line UMUC9 which suggested to be a therapeutic target of luminal subtype bladder tumor(Biton et al., 2014). Its mutation was also reported in the literature and the mutation sites might contributes to its function in the bladder cancer cell lines(Rochel et al., 2019). The results reveal an obvious expression of PPARγ protein in both basal and luminal subtypes of bladder cancer cell lines. The activation or inhibtion of PPARγ only affects the proliferation of bladder cancer cell line UMUC9. UMUC9 contains large scale of mutated PPARγ and the mutated PPARγ might plays an essential role contributes to its proliferation. Further evidence illustrated that PPARγ was mainly soluble localized in the luminal bladder cancer cell lines which was similar to post-differentiated

NHU cells. The activation of PPARγ was suggest to be toxic to NHU cell proliferation so it might be true that PPARγ was not promoting the proliferation of luminal bladder cancer cell lines. PPARγ was involved in the migration of post-differentiated NHU cell in the regeneration progress. The localization of PPARγ in bladder cancer cell lines was similar to its localization in post-differentiated NHU cells. Thus, luminal bladder cancer cells might hijact the function of PPARγ to promot its metastasis.

7.6 Future work

Although the transcription of *PPARG* and expression of its protein isoforms in NHU cells were well investigated, the mechanism underlying its regulatory role in NHU cell differentiation was only partially revealed. PPARγ activation reporters has been reported and study in the lab suggests differentiation-associate genes were upregulated by the activation of PPARγ (Varley et al., 2009). However, the results found expression of the adipogenesis-associated PPARγ reporter FABP4 and ELF3 as another potential downstream target were attenuated by PPARγ inhibition during TZPD differentiation. The absence of FABP4 despite detection of PPARγ protein expression in ABS/Ca^{2+} differentiation question whether activation of PPARγ happens. It is essential to

construct a PPARγ activation reporter system to verify its activation in ABS/Ca2+ differentiation process. Moreover, it is also important to study the expression of FABP4 in ABS/Ca^{2+} differentiation under the treatment of PPARγ agonist troglitazone to verify if it could also be the reporter of PPARγ activation in ABS/Ca^{2+} differentiation. The chromatin-binding of PPARγ could identify its activation as nuclear receptor in NHU cells but its chromatin binding was not illustrated in ABS/Ca^{2+} differentiation. The DNAse treatment on ABS/Ca^{2+} differentiated NHU cells should be repeated to illustrated the activation of PPARγ in ABS/Ca^{2+} differentiation. The results can also helps to verify whether thenuclear compartmentalization change of PPARγ was artificially affects by the adding and removing of its ligand troglitazone in TZPD differentiation.

The Scratch-wound experiment of NHU cells generate interesting and novel observation that inhibition of PPARγ attenuate the migration of NHU cells. Further experiments should be focused on the relationship between PPARγ activation and TGF-β signalling during regeneration to illustrated its molecular mechanisms. An inhibitor of TGF-β signalling could be compared against inhibition of PPARγ. The results could helps to verify whether activation of PPARγ was essential for the activation of TGF-βR signaling in NHU cell regeneration. Future research would also reveal the localization of PPARγ in the nucleus during wound healing to

identify whether it regulates the regeneration process as a nuclear receptor. The alongside observation suggested the compartmentalization of PPARγ in luminal bladder cancer cell lines was similar to its localization in post-differentiated NHU cells. The role of PPARγ in bladder cancer cell metastasis should be analyzed to determine whether the luminal bladder cancer cell lines hijack the function of PPARγ in normal NHU cells. This could provide a direction to discover a promising therapeutic target for luminal subtype bladder cancer.

Chapter 8 : Appendix

8. Appendix

8.1 Suppliers

Company Name	Web Address
Abcam Ltd	www.abcam.com
Agar Scientific	www.agarscientific.com
Agilent	www.genomics.agilent.com
Ambion	www.lifetechnologies.com
Applied Biosystems	www.appliedbiosystems.com
BD Biosciences	www.bdbiosciences.com
Bioline	www.bioline.com
Bio-Rad	www.bio-rad.com
CellPath	www.cellpath.co.uk
Cell Signaling	www.cellsignal.com
Clontech	www.clontech.com
Corning	www.corning.com
Civco Medical Solutions	www.civco.com
DAKO UK Ltd	www.dako.com
Eurofins Genomics	www.eurofinsgenomics.eu
FEI	www.fei.com
Fisher Scientific	www.fisher.co.uk
GraphPad	www.graphpad.com
Greiner	www.greinerbioone.com
Harlan Sera-labs	www.seralab.co.uk
Hycult Biotechnology	www.hycultbiotech.com
Leica Biosystems	www.leicabiosystems.com
Li-Cor	www.licor.com
Jencons	www.jenconsusa.com
Life Technologies Ltd	www.lifetechnologies.com
Merck-Millipore	www.merckmillipore.com

Company Name	Web Address
Nalgene	www.thermoscientific.com
New England Biolabs	www.neb.com
Olink Bioscience	www.olink.com
Olympus	www.olympus.co.uk
Pierce	www.piercenet.com
Promega	www.promega.co.uk
Qiagen	www.qiagen.com
Raymond A Lamb	www.fisher.co.uk
Roche	www.roche.co.uk
R&D Systems	www.rndsystems.com
Sarstedt	www.sarstedt.com
Scientific Laboratory Supplies Ltd (SLS)	Swww.scientificlabs.co.uk
Sigma-Aldrich Ltd	www.sigmaaldrich.com
SLS	www.scientificlabs.co.uk
Solent Scientific	www.solentsci.com
Starlab (UK) Ltd	www.starlab.co.uk
Syngene	www.syngene.co.uk
Tebu Bio Ltd	www.tebu-bio.com
Thermo Scientific	www.thermoscientific.com
Vector labs	www.vectorlabs.com
VWR	www.uk.vwr.com

8.2 Recipes for stock solutions

8.2.1 General solutions

Tris Buffered Saline (TBS)

50 mM Tris-HCl (pH 7.6) and 150 mM NaCl in dH2O.

Tris Buffered Saline Tween-20 (TBST)

50 mM Tris-HCl (pH 7.6) 150 mM NaCl and 1% Tween-20 in dH2O.

Phosphate Buffered Saline (PBS)

137 mM NaCl, 2.7 mM KCl, 3.2 mM Na2HPO4, pH 7.2 in ddH2O. PBS was prepared from tablets (Sigma) and autoclaved.

8.2.2 Cell culture solutions

Cholera Toxin

Cholera toxin (Sigma) prepared to 30 ng/ml (sterile) in KSFM (without supplements). Aliquots of 5 ml stored at 4o C and diluted 1:1000 in KSFMc for use.

Collagenase IV

Collagenase (Sigma) diluted to a final concentration of 100 U/ml in Hank's Balanced Salt Solution (Invitrogen; containing Ca2+ and Mg2+) and 10mM HEPES (pH 7.6). Filter sterilised 5 ml aliquots stored at -20°C.

EDTA

0.1% or 1% (w/v) EDTA (Fisher Scientific) stock solutions made in PBS and autoclaved.

L-Glutamine

5 ml aliquots of L-glutamine (Sigma) stored at -20o C.

Transport Medium

500 ml Hank's Balanced Salt Solution (Invitrogen; containing Ca2+ and Mg2+), 10 mM HEPES and 500,000 kallikrein inactivating units (KIU) Aprotinin (Nordic Group).

Stripper Medium

500 ml Hank's balanced salt solution (without Ca2+ and Mg2+), 10 mM HEPES, 500,000 KIU Aprotinin (Nordic Group) and 0.1% (w/v) EDTA.

Trypsin in Versene (TV)

20 ml Trypsin (Sigma), 4 ml 1% EDTA, 176 ml Hank's balanced salt solution (without Ca2+ and Mg2+). 5 ml aliquots stored at -20o C. Appendices 261

Trypsin Inhibitor (TI)

100mg Trypsin Inhibitor (from Soybean; Sigma) dissolved in 5 ml PBS and filter sterilised. 100 µl aliquots stored at -20o C (note: one aliquot of TI inhibits the activity of 1ml TV).

8.2.3 Immunoblotting solutions

SDS Electrophoresis Sample Buffer (2x)

125 mM Tris-HCl (pH6.8), 20% glycerol (w/v), 200 mM sodium fluoride, 2 mM sodium orthovanadate, 40 mM tetra-sodium pyrophosphate, dH2O to 50 ml. Aliquot (1 ml) and store at -20o C.

Ponceau (10x)

5 g Ponceau, 10 ml glacial acetic acid, dH2O to 100 ml

Western Blot Transfer Buffer

20 mM Tris, 150 mM glycine, 20% methanol (v/v), dH2O to 1 Liter

8.2.4 Molecular biology solutions

DEPC (nuclease-free) water

0.1% Diethylpyrocarbonate (Sigma) in 1 L dH2O. Autoclavedmto inactivate.

10 x TBE

108 g Tris, 55 g Boric acid, 20 ml 1M EDTA, to 1 L in dH2O

8.3 Abbreviations list

ABS : Adult bovine serum

AUM: Asymmetric unit membrane

CK: Cytokeratin

dsDNA: (double-stranded deoxyribonucleic acid)

FBS:Fetal bovine serum

IC : Interstitial cystitis

KSFM : Keratinocyte Serum Free Medium

NHU : Normal Human Urothelial

PPAR : Peroxisome Proliferator-activated receptor

PPRE : Peroxisome proliferator response elements

RXR: Retinoid x receptor

TJ : Tight junction

TER : Transepithelial Electrical Resistance UTI – urinary tract infection

TZ: Troglitazone

8.4 Transcription of *PPARG* and expression of PPAR γ during NHU cells differentiation

8.4.1 Transcription of *PPARG2* transcription variants in NHU cells

Figure 8. 1: Transcription of *PPARG*2 in NHU cells.
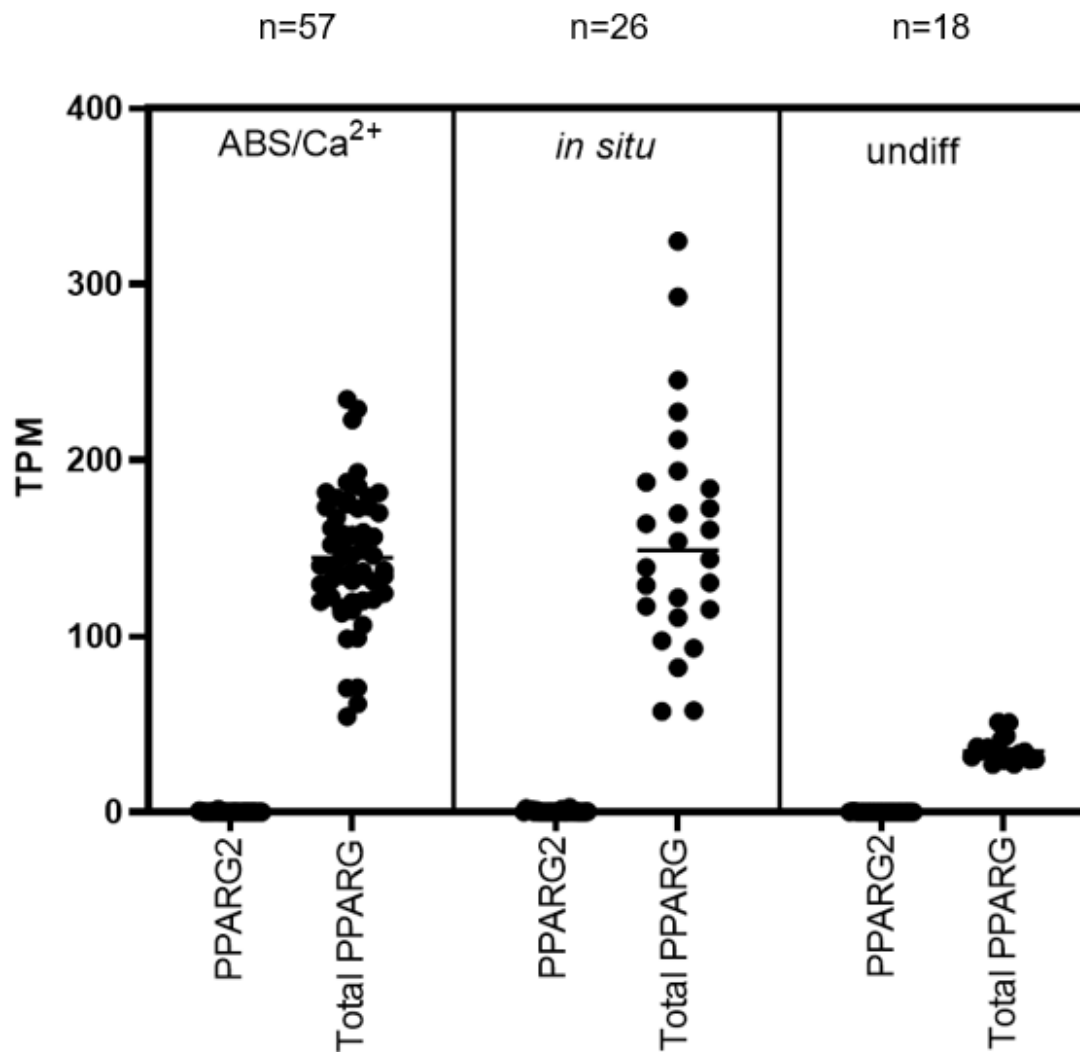
RNAseq data about the transcription of *PPARG*2 and total *PPARG* was illustrated above and TPM was show in different NHU cells. ABS/Ca2+ represents NHU cells differentiated using ABS/Ca2+ differentiation for 7 days. In situ represents *in vivo* NHU cells. Undiff represents undifferentiated NHU cells.

8.4.2 Transcription of differentiation-associate genes during NHU differentiation

Figure 8. 2: qRT-PCR result of transcription of GATA3 during NHU cells TZPD differentiation.
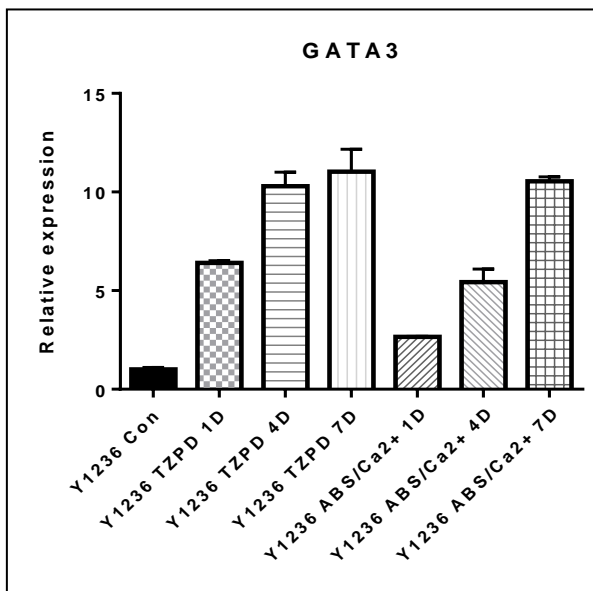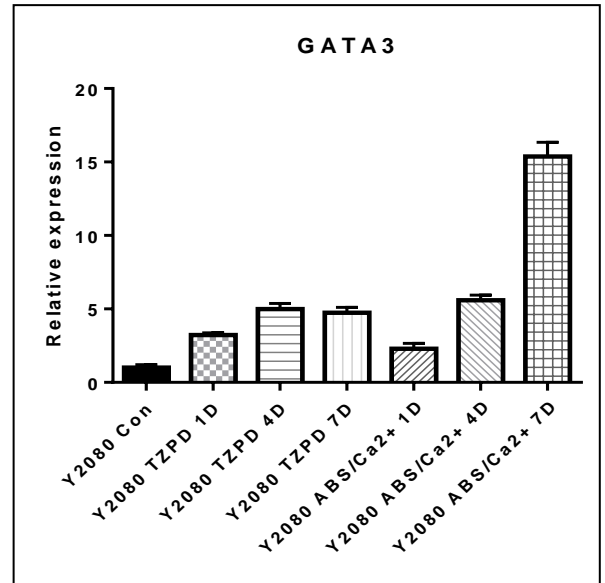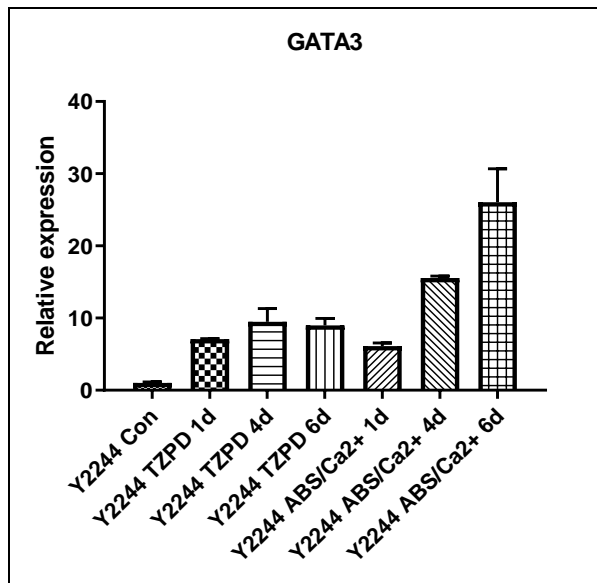
Three independent NHU cell lines Y2244, Y2080, and Y1236 were included. Undifferentiated NHU cells were harvest as control. NHU cells were either TZPD or ABS/Ca2+ differentiated for 7 days and harvest at day 4 and day 7. Relative expression represents the transcription of GATA3 in differentiated NHU cells compared to the control which normalized to 1.

Figure 8. 3: qRT-PCR result of transcription of UPK2 during NHU cells TZPD differentiation.
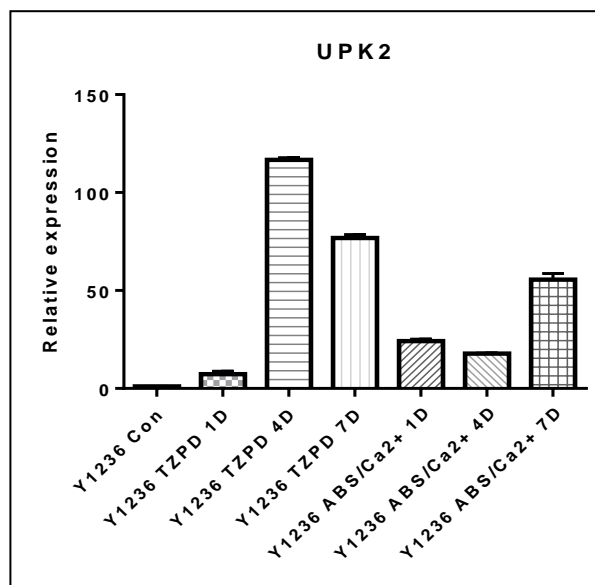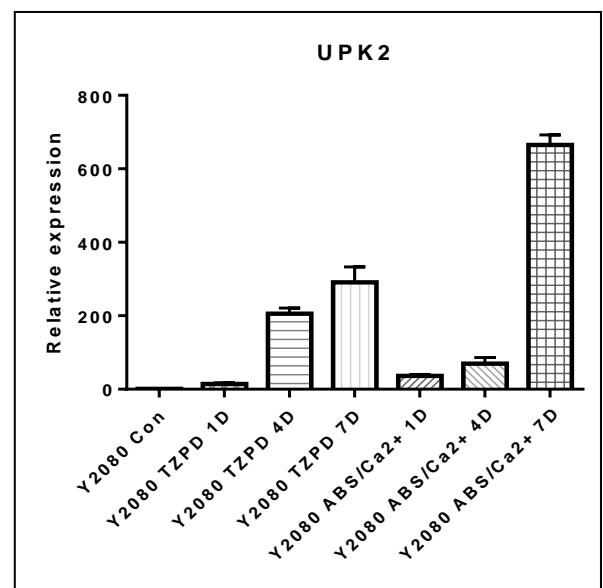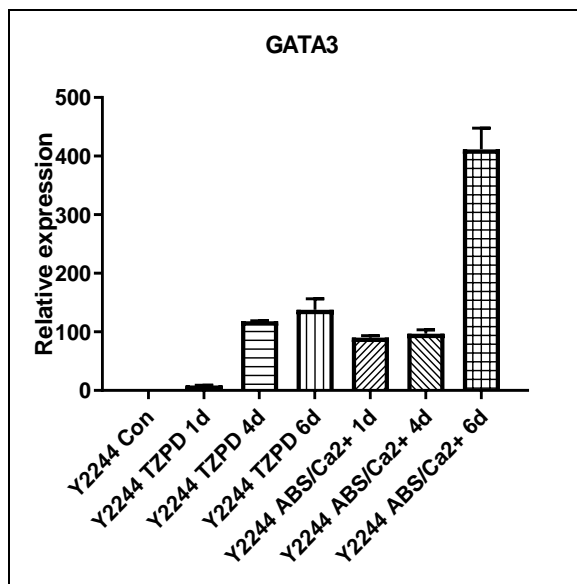
Three independent NHU cell lines Y2244, Y2080, and Y1236 were included. Undifferentiated NHU cells were harvest as control. NHU cells were either TZPD or ABS/Ca^{2+} differentiated for 7 days and harvest at day 4 and day 7. Relative expression represents the transcription of UPK2 in differentiated NHU cells compared to the control which normalized to 1.

8.4.3 Additional results of expression of PPARγ in NHU cells

Figure 8. 4: Expression of PPARγ in NHU cells .
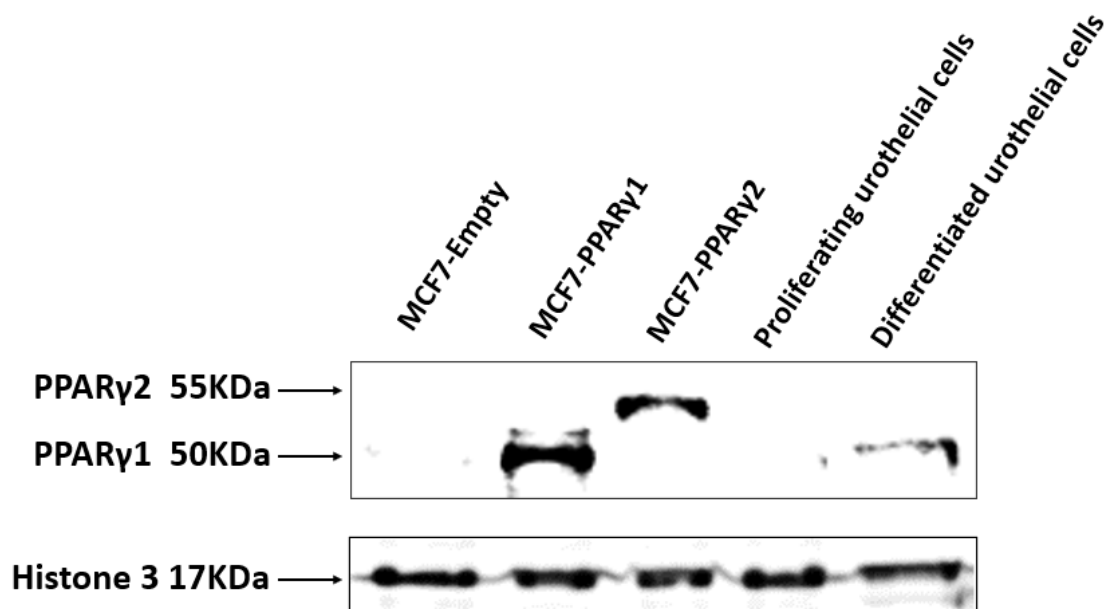
Western blot was applied to detect the expression of PPARγ protein in NHU cells. 20 μg of total protein was loaded. Histone 3 was used as housekeeping protein. MCF-7 breast cancer cells transduced with empty vector, PPARγ protein isoform 1, and PPARγ protein isoform2 were used as negative and positive control. Antibody 81B8 was applied to detect the PPAR protein isoform1 (PPARγ1) and PPARγ protein isoform 2 (PPARγ2) at 50 and 55 kDa.

Figure 8. 5：Quantification of PPARγ protein expression during NHU cells differentiation using Image J.
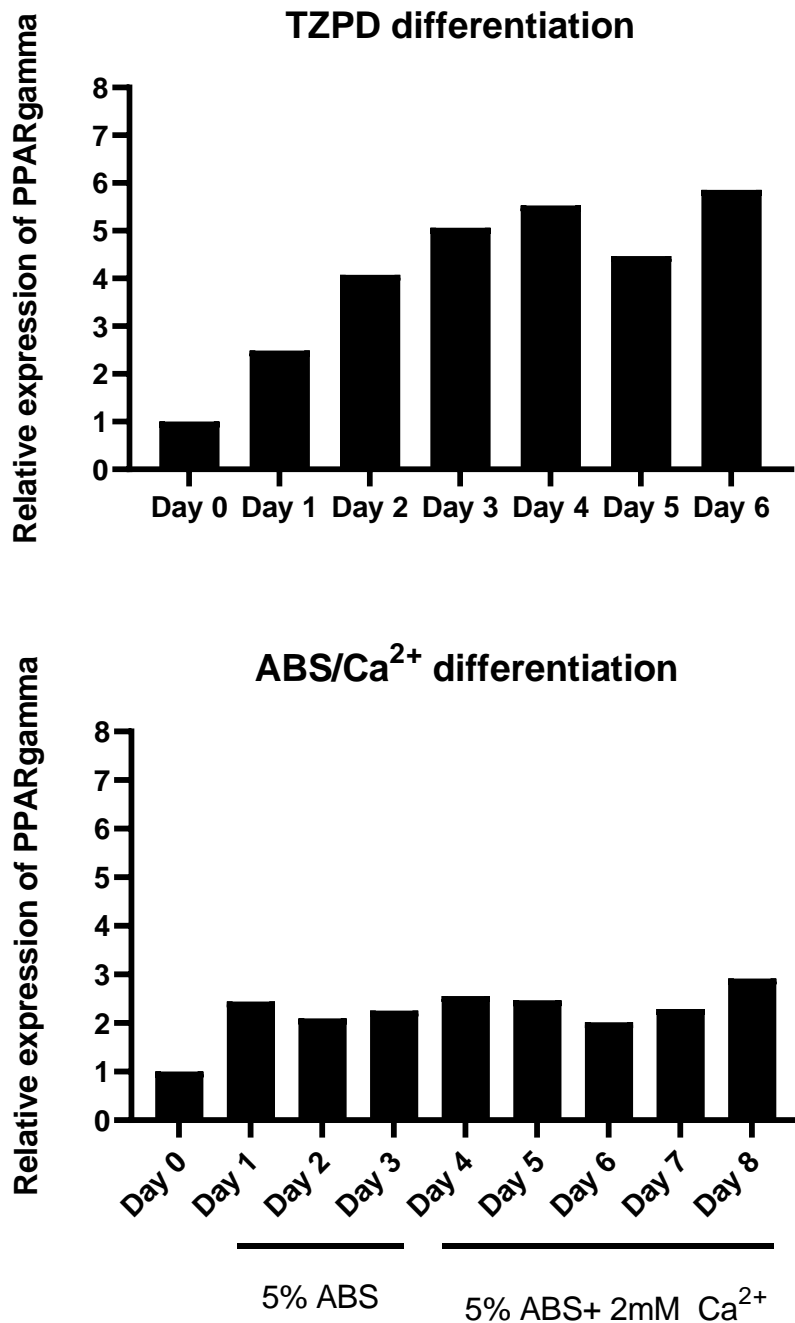
The expression of PPARγ protein was quantified in Image J software. Y axis represents the relative expression of PPARγ compared to day 0. X axis of the above graph

represent the day-time points of TZPD differentiation process. X axis of the second graph represent the day-time points of the two stages of ABS/Ca^{2+} differentiation.

8.5 Translation of PPARγ protein and its downstream target in Normal Human Urothelial (NHU) cells

8.5.1 Additional results of expression of PPARγ in troglitazone and PD153035 treated urothelial cells

Figure 8. 6: Expression of PPARγ in troglitazone and PD153035 treated urothelial cells.
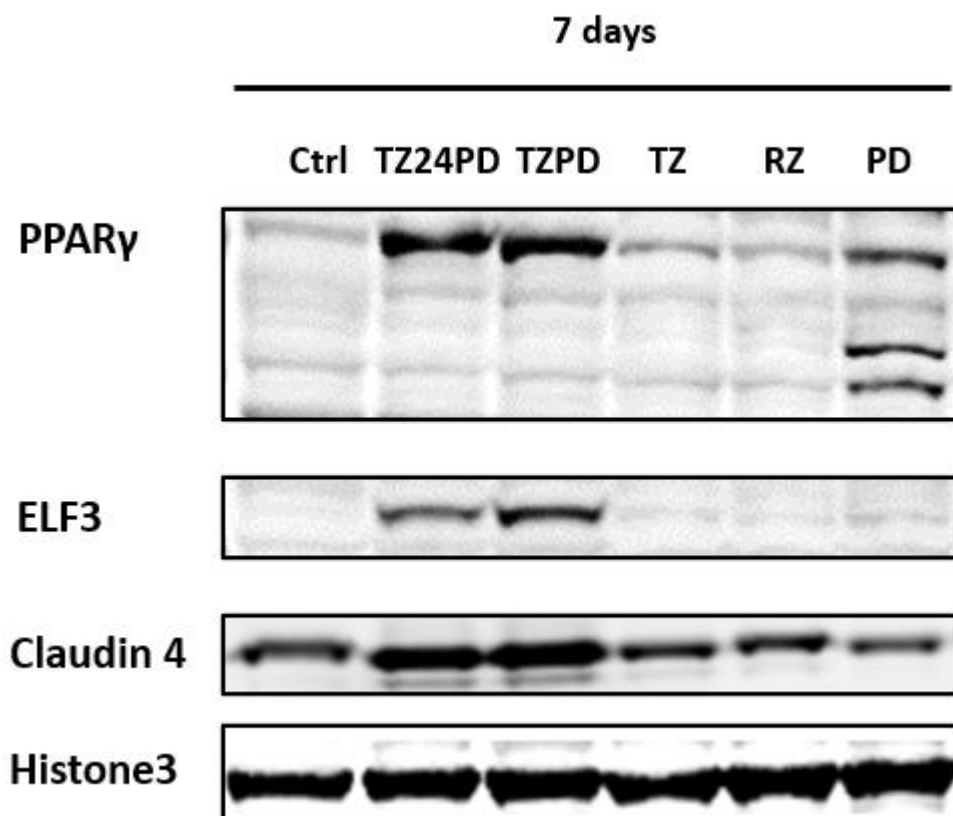
A)

7 days

Ctrl TZ24PD TZPD TZ RZ PD

PPARγ

ELF3

Claudin 4

Histone3

NHU cells were treated with 0.1% DMSO (Control), 1µM troglitazone and PD153035 with TZ removed after 24 hours (TZ24PD), 1µM troglitazone and PD153035 (TZPD), 1 µM troglitzone (TZ), 1µM Rosiglitazone (RZ), and 1µM PD153035 (PD) for 7 days. NHU cells were cultured to 90% confluence and started the treatment. Protein lysates were harvest at day 7. Expression of PPARγ and ELF3 was detected using western blot shown in the left graph. β-actin was used as housekeeping protein.

B)
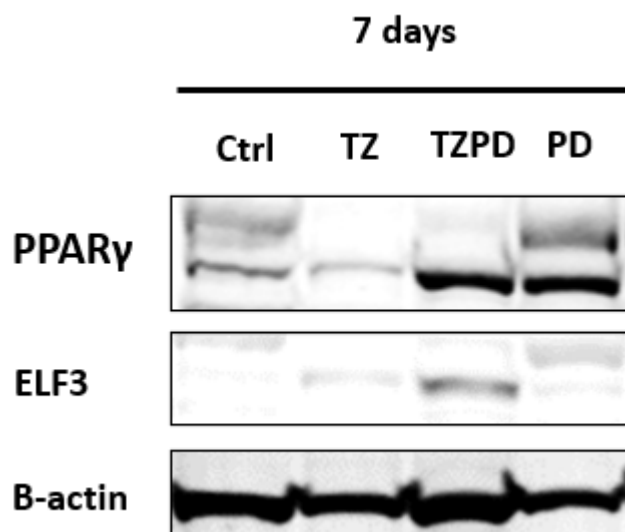
NHU cells were treated with 0.1% DMSO (Control), 1µM troglitazone and PD153035 (TZPD), 1 µM troglitzone (TZ) or 1µM PD153035 (PD) for 7 days. NHU cells were cultured to 90% confluence and started the treatment. Troglitazone was removed after 24 hours in the TZPD differentiation group. Protein lysates were harvest at day 7. Expression of PPARγ and ELF3 was detected using western blot shown in the left graph (One of the three results). β-actin was used as housekeeping protein.

8.5.2 Morphology of NHU cells treated with different inhibitor and agonist

Figure 8. 7: Morphology of NHU cells treated with different inhibitor and agonist.
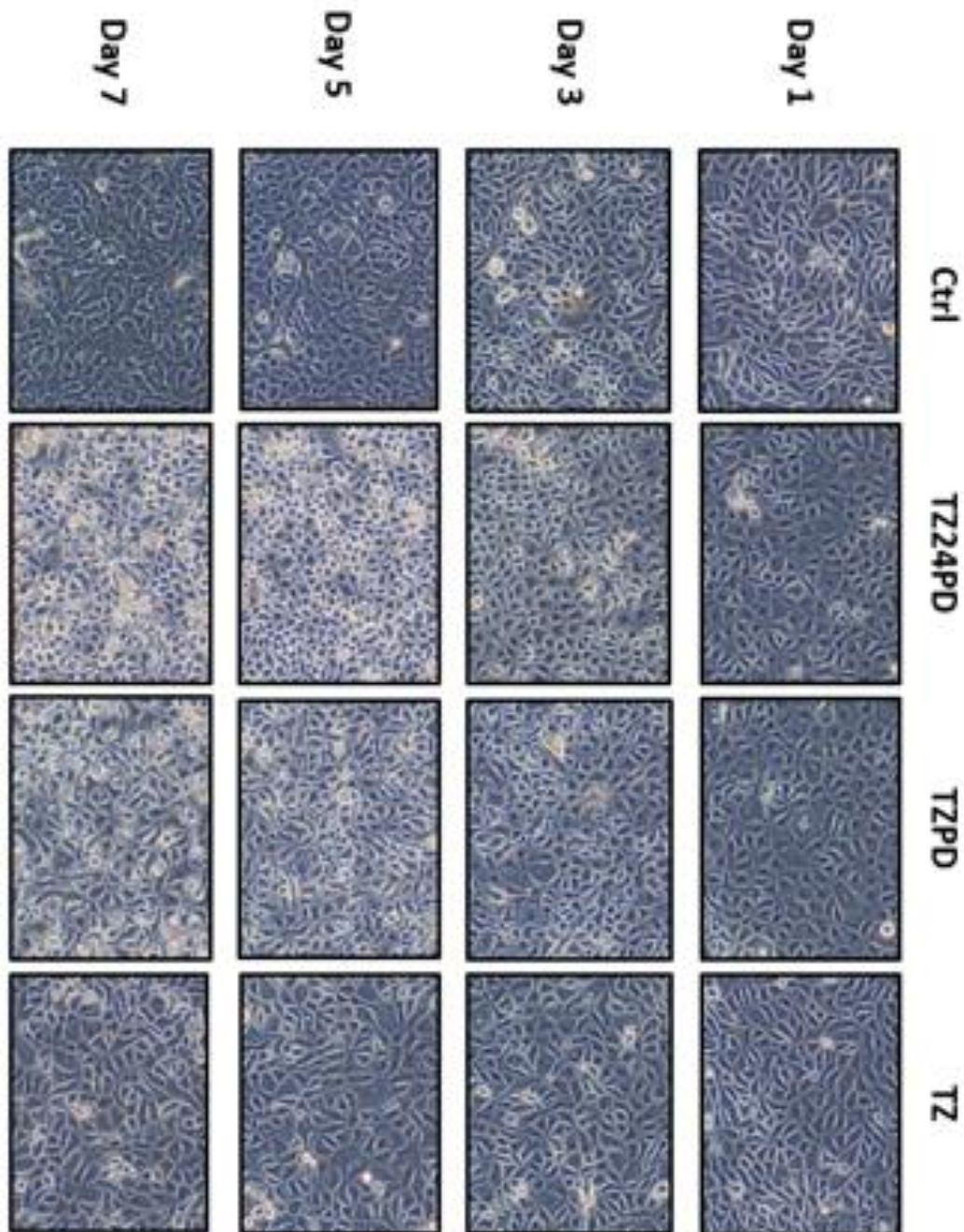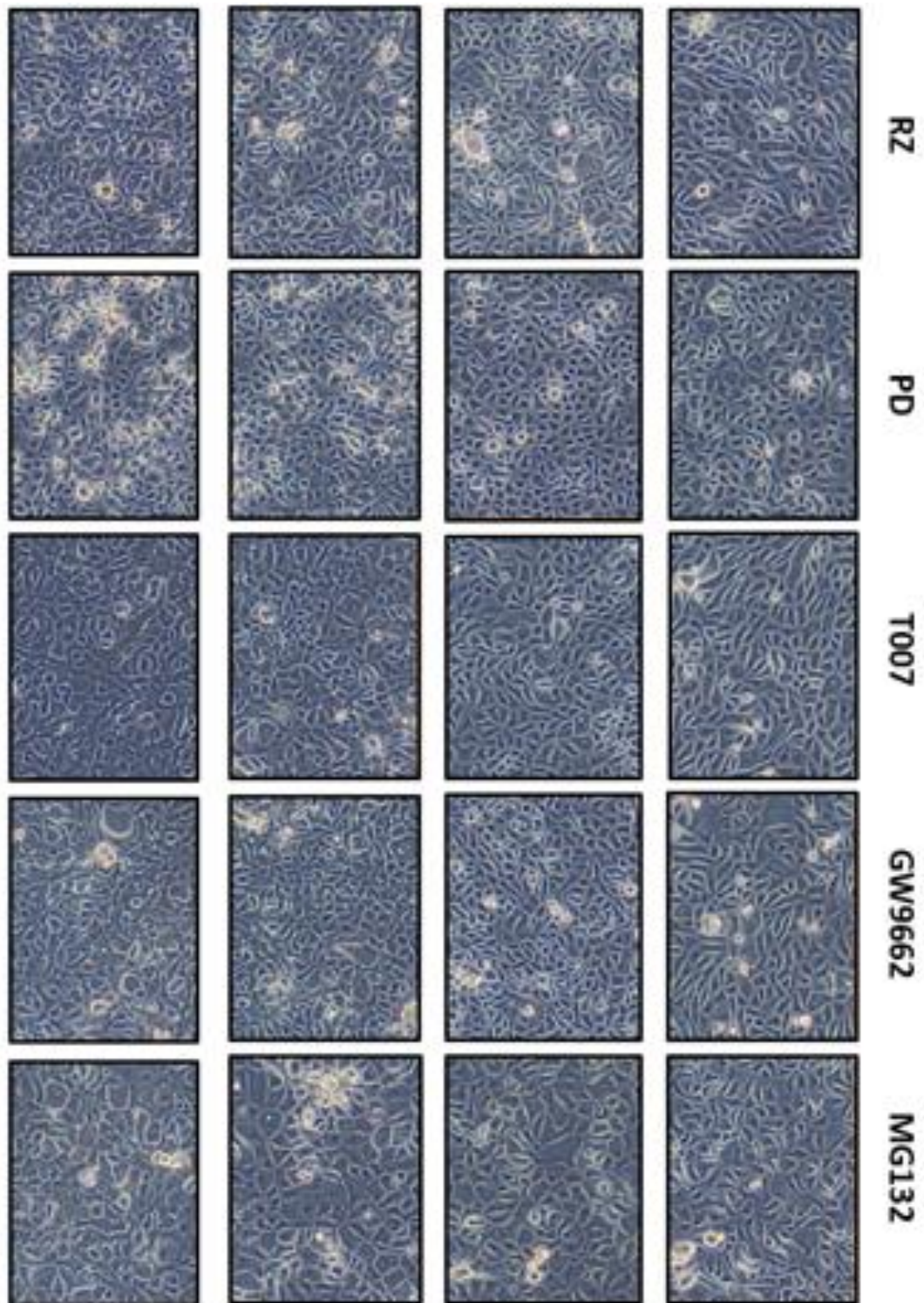
NHU cells were treated with 0.1% DMSO (Control), 1µM troglitazone and PD153035 with TZ removed after 24 hours (TZ24PD), 1 µM troglitazone and PD153035 (TZPD), 1 µM troglitzone (TZ), 1µM Rosiglitazone (RZ), 1 µM PD153035 (PD), 1 µM T0070907 (T007), 1 µM GW9662, and 5 µM MG132 for 7 days. NHU cells were cultured to 90%

confluence and started the treatment. Morphology of cells were captured every two days start from day 1.

8.5.3 Inhibition of proteasome did not stable the expression of PPARγ protein

Figure 8. 8: Expression of PPARγ in MG132 treated NHU cells.
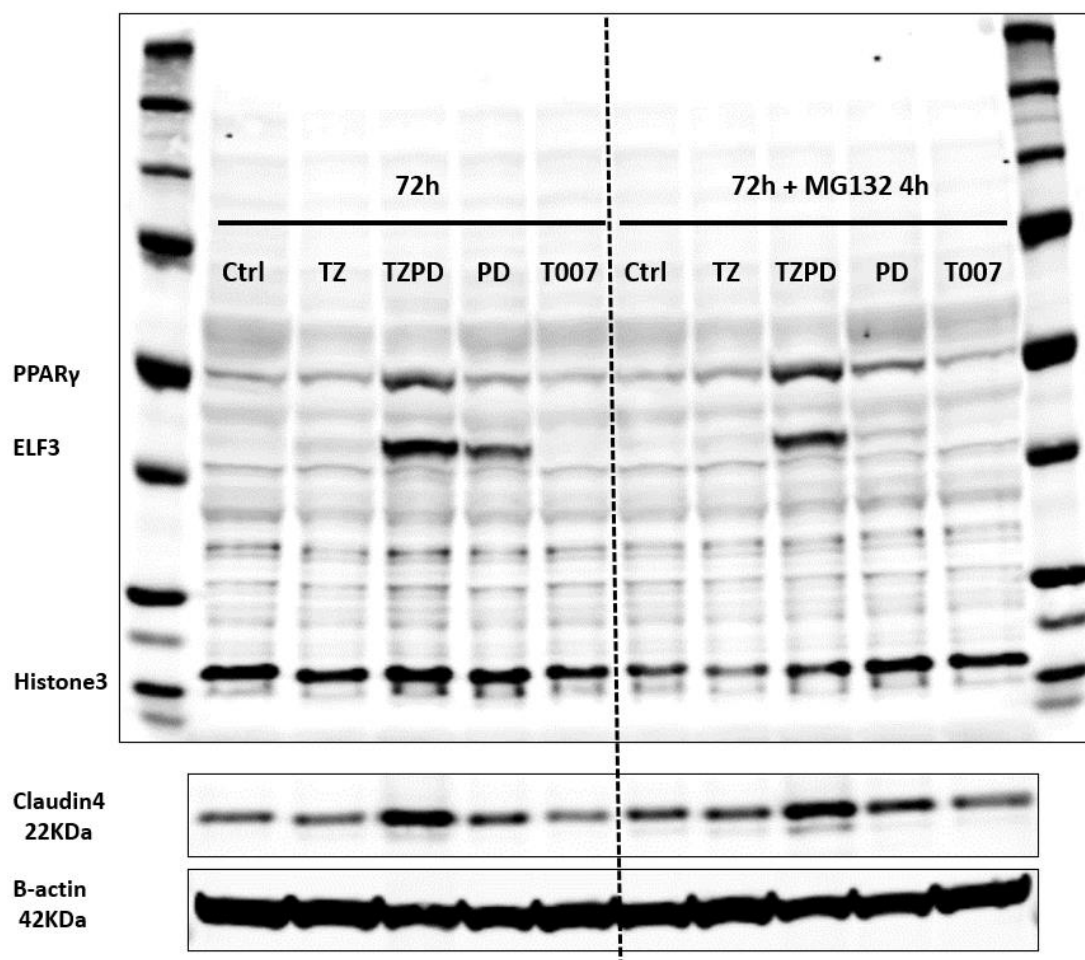
NHU cells were treated with 0.1% DMSO (Control), 1 μM troglitzone (TZ), 1 μM troglitazone and PD153035 (TZPD), 1 μM PD153035 (PD), and 1 μM T0070907 (T007) for 72 hours. NHU cells were cultured to 90% confluence and started the treatment. Right represent NHU cells treated with proteasome inhibitor MG132 at concentration 5 μM for another 4 hours. Protein lysates were harvest at day 3.

Expression of PPARγ and ELF3 was detected using western blot shown in the left graph. β-actin was used as housekeeping protein.

8.6 Compartmentalization of PPARγ changes during NHU cell differentiation

8.6.1 Compartmentalization of PPARγ during ABS/Ca^{2+} differentiation

Figure 8. 9: Compartmentalization of PPARγ during ABS/Ca2+ differentiation.
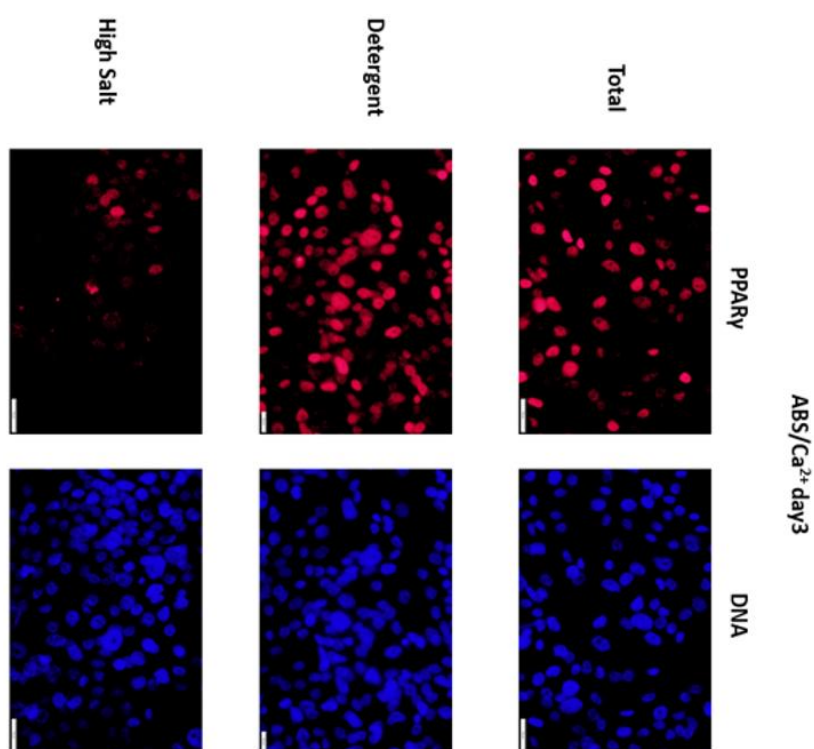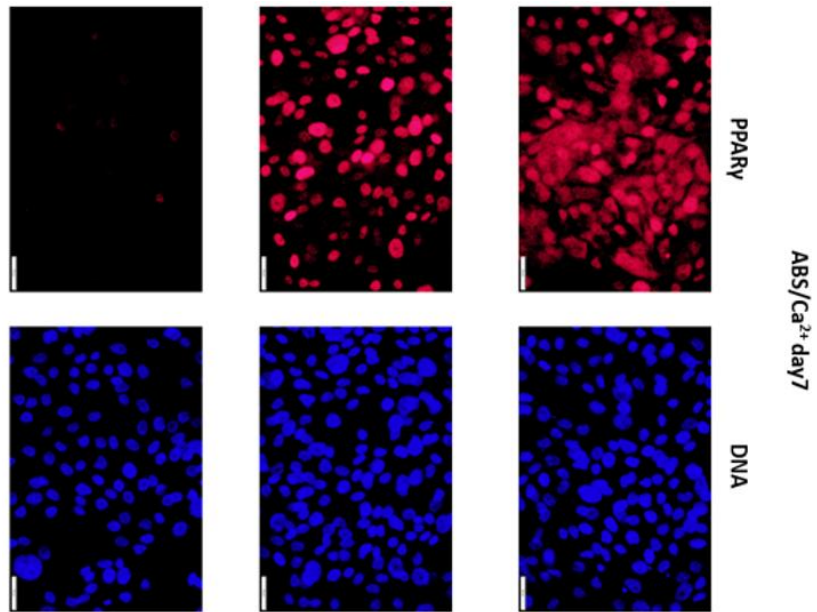
NHU cells were cultured to 90% confluent before initiating the differentiation process. Cells were fixed at day3 and day 7 then go through different wash and treatment. Scale bar = 50 μM.

8.6.2 Compartmentalization of ELF3 during ABS/Ca^{2+} differentiation

Figure 8. 10: Expression of Ki67 and claudin4 during NHU cell differentiation.
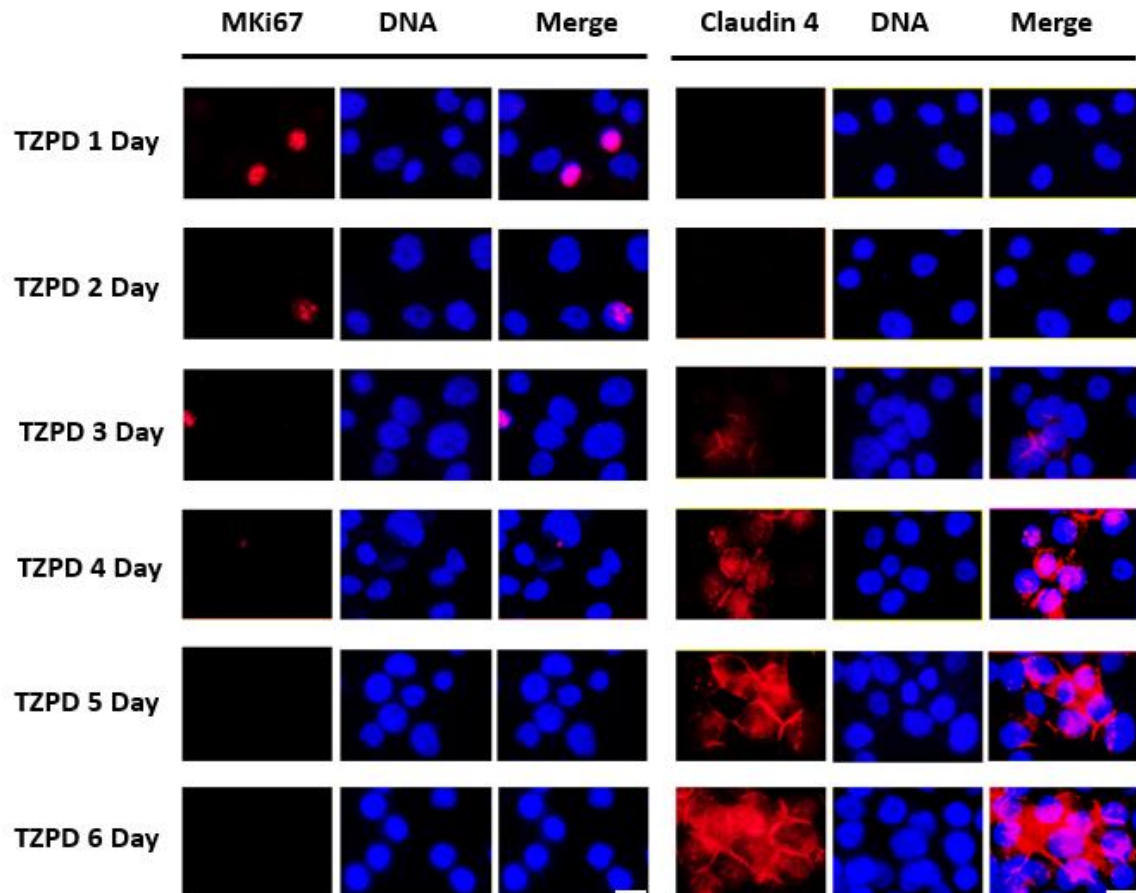
NHU cells were cultured to 90% confluent and then TZPD differentiated for 6 days. The differentiated NHU cells were fixed in the 12 well slides using 10% formalin at each day. The slides then further label with ki67 (left) and claudin4 (right) to verify the proliferation and differentiation state of NHU cells. Scale bar = 50 μM.

Figure 8.11: Compartmentalization of ELF3 during ABS/Ca2+ differentiation.
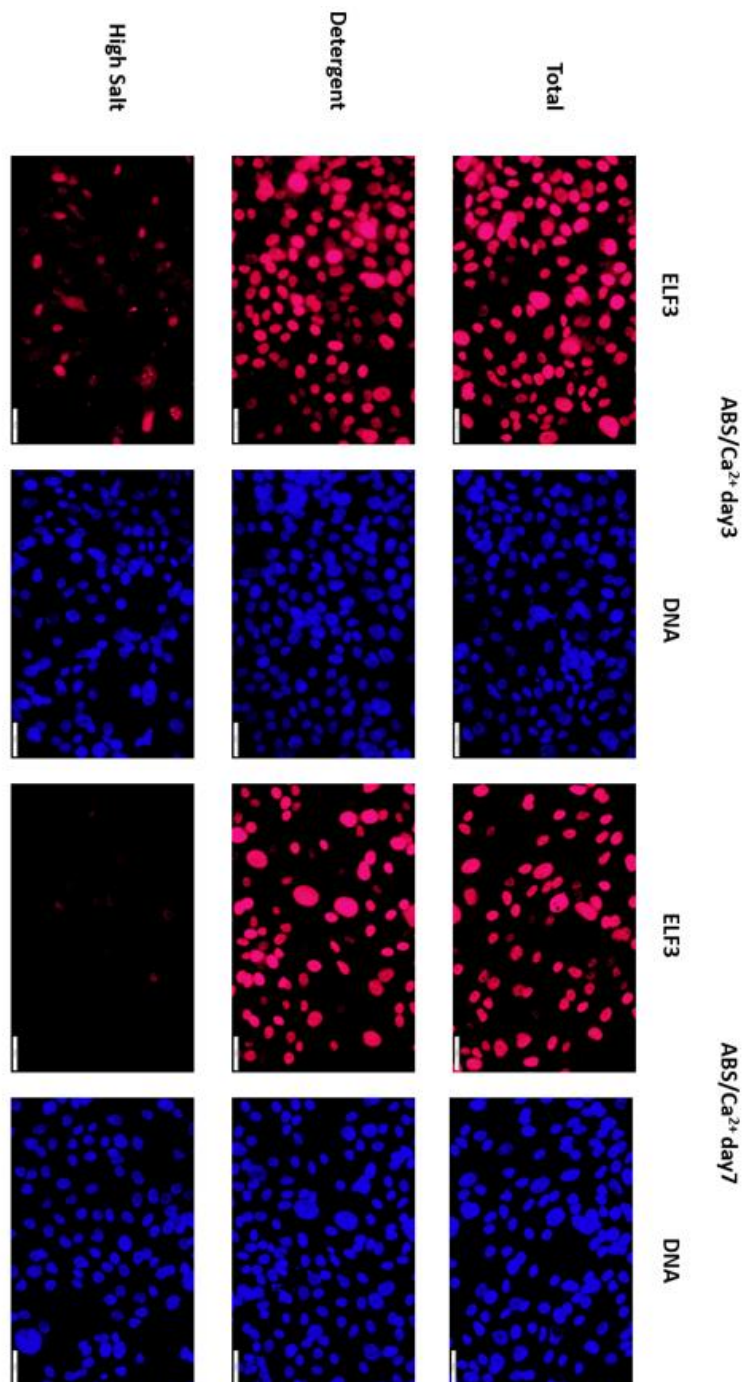
NHU cells were cultured to 90% confluent before initiating the differentiation process. Cells were fixed at day3 and day 7 then go through different wash and treatment. Scale bar = 50 μM.

8.7 Role of PPARγ in NHU cells regeneration and bladder cancer cell lines

8.7.1 Inhibition of TGF-β has no effect on expression of PPARγ in NHU cells

Figure 8. 12: Inhibition of TGF-β has no effect on expression of PPARγ in NHU cells.
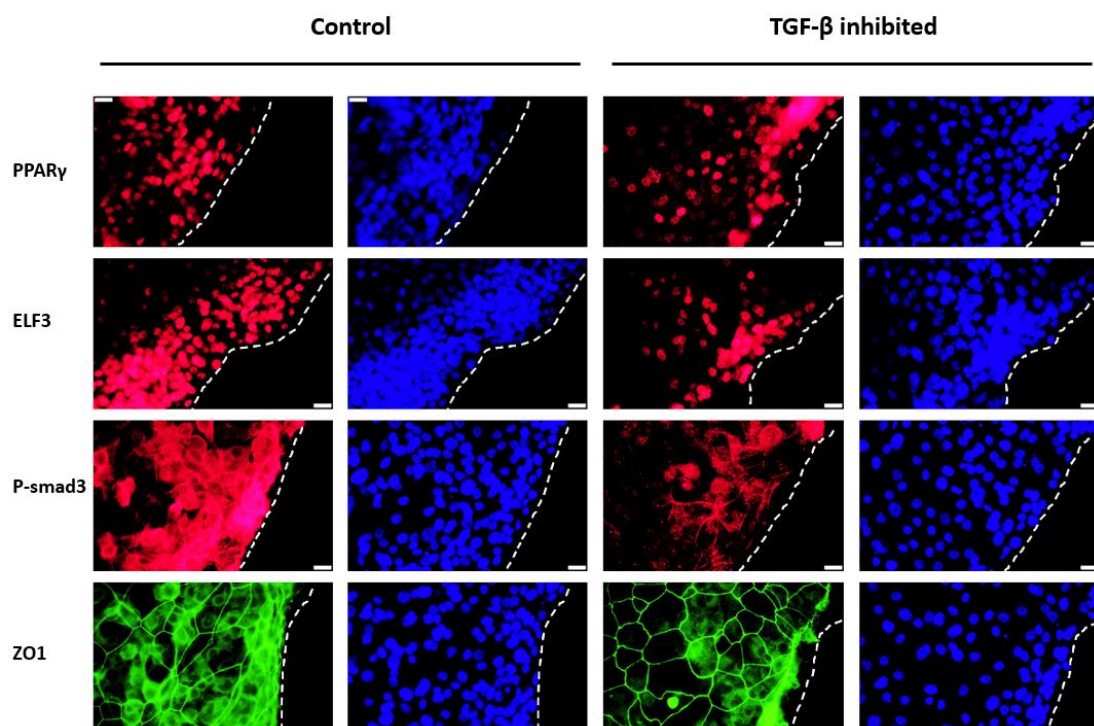
NHU cells were ABS/Ca^{2+} differentiated and treated with/without TGF-β inhibitor 24 hours before scratch wounded. PPARγ protein was detected using 81B8 antibody and stained red. ELF3, P-smad3 were stained red. ZO1 was stained green. DNA was stained blue using Hochest33258. The picture was taken at the wound edge area. Scale bar = 50 μM.

8.7.2 Inhibition of PPARγ attenuate the migration of NHU cells towards the wound edge

Figure 8. 13: Inhibition of PPARγ attenuate the migration of NHU cells towards the wound edge.
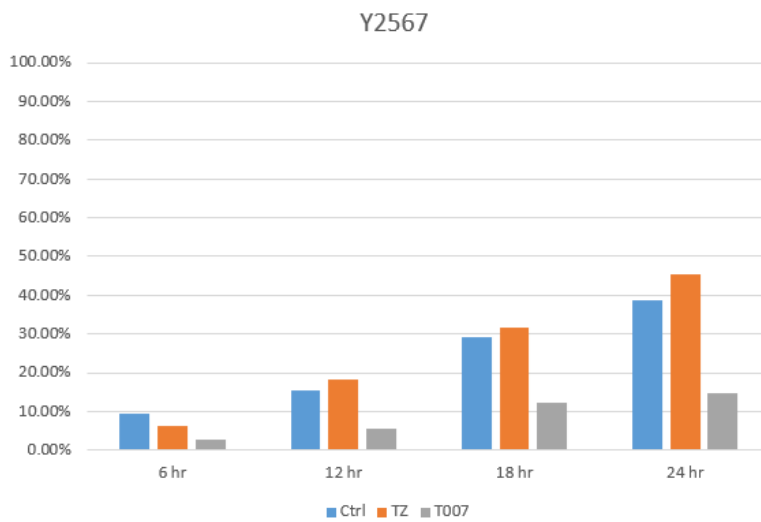
One way Anova	6 hr	12 hr	18 hr	24 hr
P-value	0.369546	0.030351	0.025821	0.018712

Y2607
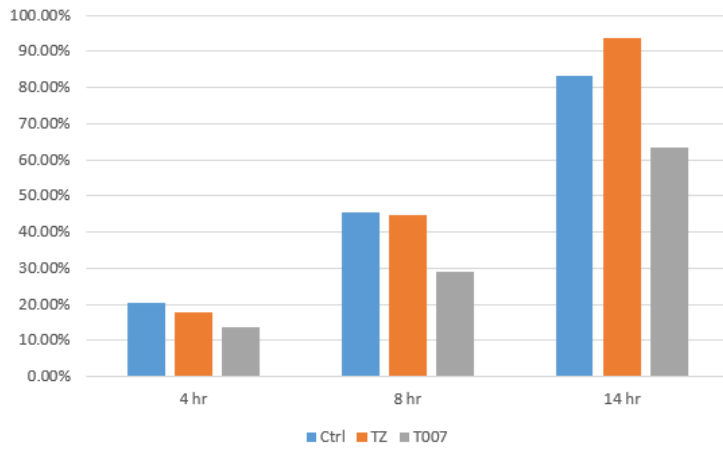
One way Anova	4 hr	8 hr	14 hr
P-value	0.472361	0.08329	0.04008

Y2471
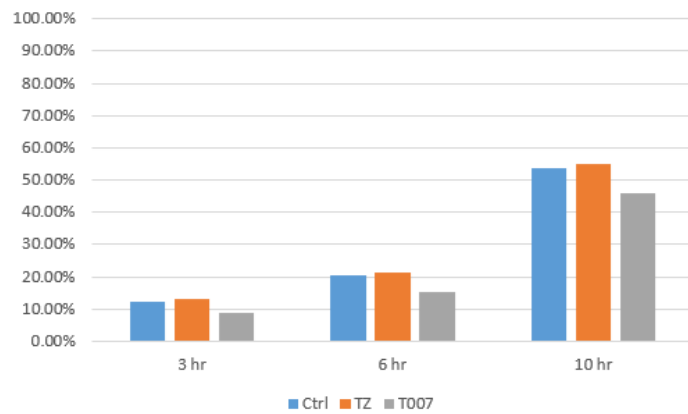
One way Anova	3 hr	6 hr	10 hr
P-value	0.255076	0.21836	0.265703

Y2607
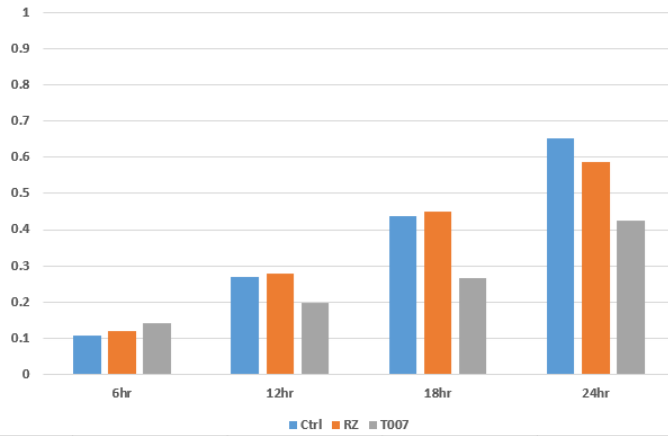
One way Anova	6 hr	12 hr	18 hr	24 hr
P-value	0.610352	0.444444	0.207554	0.18185

Ctrl stands for control. TZ stands for troglitazone. T007 stands for T0070907. ABS/Ca2+ differentiated NHU cells were untreated or treated with either 1 µM troglitazone or 1 µM T0070907 for 24 hours prior to scratch wounded. Y-axis represents the healing percentage of the wound area. X-axis represents the time points.

Chapter 9: Reference

9. Reference:

A, I.J., Jeannin, E., Wahli, W., and Desvergne, B. (1997). Polarity and specific sequence requirements of peroxisome proliferator-activated receptor (PPAR)/retinoid X receptor heterodimer binding to DNA. A functional analysis of the malic enzyme gene PPAR response element. The Journal of biological chemistry *272*, 20108-20117.

Aboushwareb, T., Zhou, G., Deng, F.M., Turner, C., Andersson, K.E., Tar, M., Zhao, W., Melman, A., D'Agostino, R., Jr., Sun, T.T.*, et al.* (2009). Alterations in bladder function associated with urothelial defects in uroplakin II and IIIa knockout mice. Neurourology and urodynamics *28*, 1028-1033.

Acharya, P., Beckel, J., Ruiz, W.G., Wang, E., Rojas, R., Birder, L., and Apodaca, G. (2004). Distribution of the tight junction proteins ZO-1, occludin, and claudin-4, -8, and -12 in bladder epithelium. American journal of physiology Renal physiology *287*, F305-318.

Adams, M., Reginato, M.J., Shao, D., Lazar, M.A., and Chatterjee, V.K. (1997). Transcriptional activation by peroxisome proliferator-activated receptor gamma is inhibited by phosphorylation at a consensus mitogen-activated protein kinase site. The Journal of biological chemistry *272*, 5128-5132.

Alroy, J., and Gould, V.E. (1980). Epithelial-stromal interface in normal and neoplastic human bladder epithelium. Ultrastructural pathology *1*, 201-210.

Aprile, M., Ambrosio, M.R., D'Esposito, V., Beguinot, F., Formisano, P., Costa, V., and Ciccodicola, A. (2014). PPARG in Human Adipogenesis: Differential Contribution of Canonical Transcripts and Dominant Negative Isoforms. PPAR research *2014*, 537865.

Barak, Y., Nelson, M.C., Ong, E.S., Jones, Y.Z., Ruiz-Lozano, P., Chien, K.R., Koder, A., and Evans, R.M. (1999). PPAR gamma is required for placental, cardiac, and adipose tissue development. Molecular cell *4*, 585-595.

Barbatelli, G., Murano, I., Madsen, L., Hao, Q., Jimenez, M., Kristiansen, K., Giacobino, J.P., De Matteis, R., and Cinti, S. (2010). The emergence of cold-induced brown adipocytes in mouse white fat depots is determined predominantly by white to brown adipocyte transdifferentiation. American journal of physiology Endocrinology and metabolism *298*, E1244-1253.

Baser, A., Skabkin, M., Kleber, S., Dang, Y., Gulculer Balta, G.S., Kalamakis, G., Gopferich, M., Ibanez, D.C., Schefzik, R., Lopez, A.S.*, et al.* (2019). Onset of differentiation is post-transcriptionally controlled in adult neural stem cells. Nature *566*, 100-104.

Bernardo, G.M., and Keri, R.A. (2012). FOXA1: a transcription factor with parallel functions in development and cancer. Bioscience reports *32*, 113-130.

Berry, D.C., Jiang, Y., and Graff, J.M. (2016). Emerging Roles of Adipose Progenitor Cells in Tissue Development, Homeostasis, Expansion and Thermogenesis. Trends in endocrinology and metabolism: TEM *27*, 574-585.

Biton, A., Bernard-Pierrot, I., Lou, Y., Krucker, C., Chapeaublanc, E., Rubio-Perez, C., Lopez-Bigas, N., Kamoun, A., Neuzillet, Y., Gestraud, P.*, et al.* (2014). Independent component analysis uncovers the landscape of the bladder tumor transcriptome and reveals insights into luminal and basal subtypes. Cell reports *9*, 1235-1245.

Blasig, I.E., Winkler, L., Lassowski, B., Mueller, S.L., Zuleger, N., Krause, E., Krause, G., Gast, K., Kolbe, M., and Piontek, J. (2006). On the self-association potential of transmembrane tight junction proteins. Cellular and molecular life sciences : CMLS *63*, 505-514.

Bock, M., Hinley, J., Schmitt, C., Wahlicht, T., Kramer, S., and Southgate, J. (2014). Identification of ELF3 as an early transcriptional regulator of human urothelium. Developmental biology *386*, 321-330.

Brembeck, F.H., Opitz, O.G., Libermann, T.A., and Rustgi, A.K. (2000). Dual function of the epithelial specific ets transcription factor, ELF3, in modulating differentiation. Oncogene *19*, 1941-1949.

Burgermeister, E., and Seger, R. (2007). MAPK kinases as nucleo-cytoplasmic shuttles for PPARgamma. Cell cycle *6*, 1539-1548.

Camp, H.S., Tafuri, S.R., and Leff, T. (1999). c-Jun N-terminal kinase phosphorylates peroxisome proliferator-activated receptor-gamma1 and negatively regulates its transcriptional activity. Endocrinology *140*, 392-397.

Carpenter, A.R., Becknell, M.B., Ching, C.B., Cuaresma, E.J., Chen, X., Hains, D.S., and McHugh, K.M. (2016). Uroplakin 1b is critical in urinary tract development and urothelial differentiation and homeostasis. Kidney international *89*, 612-624.

Chandra, V., Huang, P., Hamuro, Y., Raghuram, S., Wang, Y., Burris, T.P., and Rastinejad, F. (2008). Structure of the intact PPAR-gamma-RXR-nuclear receptor complex on DNA. Nature *456*, 350-356.

Chawla, A., Schwarz, E.J., Dimaculangan, D.D., and Lazar, M.A. (1994). Peroxisome proliferator-activated receptor (PPAR) gamma: adipose-predominant expression and induction early in adipocyte differentiation. Endocrinology *135*, 798-800.

Cheng, J., Huang, H., Zhang, Z.T., Shapiro, E., Pellicer, A., Sun, T.T., and Wu, X.R. (2002). Overexpression of epidermal growth factor receptor in urothelium elicits urothelial hyperplasia and promotes bladder tumor growth. Cancer research *62*, 4157-4163.

Cheng, S., Qian, K., Wang, Y., Wang, G., Liu, X., Xiao, Y., and Wang, X. (2019). PPARgamma inhibition regulates the cell cycle, proliferation and motility of bladder cancer cells. Journal of cellular and molecular medicine *23*, 3724-3736.

Choi, W., Porten, S., Kim, S., Willis, D., Plimack, E.R., Hoffman-Censits, J., Roth, B., Cheng, T., Tran, M., Lee, I.L*., et al.* (2014). Identification of distinct basal and luminal subtypes of muscle-invasive bladder cancer with different sensitivities to frontline chemotherapy. Cancer cell *25*, 152-165.

Chung, S.S., Ahn, B.Y., Kim, M., Choi, H.H., Park, H.S., Kang, S., Park, S.G., Kim, Y.B., Cho, Y.M., Lee, H.K*., et al.* (2010). Control of adipogenesis by the SUMO-specific protease SENP2. Molecular and cellular biology *30*, 2135-2146.

Colopy, S.A., Bjorling, D.E., Mulligan, W.A., and Bushman, W. (2014). A population of progenitor cells in the basal and intermediate layers of the murine bladder urothelium contributes to urothelial development and regeneration. Developmental dynamics : an official publication of the American Association of Anatomists *243*, 988-998.

Cross, W.R., Eardley, I., Leese, H.J., and Southgate, J. (2005). A biomimetic tissue from cultured normal human urothelial cells: analysis of physiological function. American journal of physiology Renal physiology *289*, F459-468.

Das, S., Chattopadhyay, D., Chatterjee, S.K., Mondal, S.A., Majumdar, S.S., Mukhopadhyay, S., Saha, N., Velayutham, R., Bhattacharya, S., and Mukherjee, S. (2021). Increase in PPARgamma inhibitory phosphorylation by Fetuin-A through the activation of Ras-MEK-ERK pathway causes insulin resistance. Biochimica et biophysica acta Molecular basis of disease *1867*, 166050.

Dean, J.M., He, A., Tan, M., Wang, J., Lu, D., Razani, B., and Lodhi, I.J. (2020). MED19 Regulates Adipogenesis and Maintenance of White Adipose Tissue Mass by Mediating PPARgamma-Dependent Gene Expression. Cell reports *33*, 108228.

Deng, F.M., Liang, F.X., Tu, L., Resing, K.A., Hu, P., Supino, M., Hu, C.C., Zhou, G., Ding, M., Kreibich, G.*, et al.* (2002). Uroplakin IIIb, a urothelial differentiation marker, dimerizes with uroplakin Ib as an early step of urothelial plaque assembly. The Journal of cell biology *159*, 685-694.

Diezko, R., and Suske, G. (2013). Ligand binding reduces SUMOylation of the peroxisome proliferator-activated receptor gamma (PPARgamma) activation function 1 (AF1) domain. PloS one *8*, e66947.

Dreyer, C., Krey, G., Keller, H., Givel, F., Helftenbein, G., and Wahli, W. (1992). Control of the peroxisomal beta-oxidation pathway by a novel family of nuclear hormone receptors. Cell *68*, 879-887.

Dussault, I., and Forman, B.M. (2000). Prostaglandins and fatty acids regulate transcriptional signaling via the peroxisome proliferator

activated receptor nuclear receptors. Prostaglandins & other lipid mediators *62*, 1-13.

Evans, R.M., Barish, G.D., and Wang, Y.X. (2004). PPARs and the complex journey to obesity. Nature medicine *10*, 355-361.

Fajas, L., Auboeuf, D., Raspe, E., Schoonjans, K., Lefebvre, A.M., Saladin, R., Najib, J., Laville, M., Fruchart, J.C., Deeb, S*., et al.* (1997). The organization, promoter analysis, and expression of the human PPARgamma gene. The Journal of biological chemistry *272*, 18779-18789.

Fajas, L., Fruchart, J.C., and Auwerx, J. (1998). PPARgamma3 mRNA: a distinct PPARgamma mRNA subtype transcribed from an independent promoter. FEBS letters *438*, 55-60.

Farmer, S.R. (2008). Molecular determinants of brown adipocyte formation and function. Genes & development *22*, 1269-1275.

Fishwick, C., Higgins, J., Percival-Alwyn, L., Hustler, A., Pearson, J., Bastkowski, S., Moxon, S., Swarbreck, D., Greenman, C.D., and Southgate, J. (2017). Heterarchy of transcription factors driving basal and luminal cell phenotypes in human urothelium. Cell death and differentiation *24*, 809-818.

Fleming, J.M., Shabir, S., Varley, C.L., Kirkwood, L.A., White, A., Holder, J., Trejdosiewicz, L.K., and Southgate, J. (2012). Differentiation-associated reprogramming of the transforming growth factor beta receptor

pathway establishes the circuitry for epithelial autocrine/paracrine repair. PloS one *7*, e51404.

Floyd, Z.E., and Stephens, J.M. (2002). Interferon-gamma-mediated activation and ubiquitin-proteasome-dependent degradation of PPARgamma in adipocytes. The Journal of biological chemistry *277*, 4062-4068.

Forman, B.M., Chen, J., and Evans, R.M. (1997). Hypolipidemic drugs, polyunsaturated fatty acids, and eicosanoids are ligands for peroxisome proliferator-activated receptors alpha and delta. Proceedings of the National Academy of Sciences of the United States of America *94*, 4312-4317.

Fruchart, J.C. (2009). Peroxisome proliferator-activated receptor-alpha (PPARalpha): at the crossroads of obesity, diabetes and cardiovascular disease. Atherosclerosis *205*, 1-8.

Fujita, H., Hamazaki, Y., Noda, Y., Oshima, M., and Minato, N. (2012). Claudin-4 deficiency results in urothelial hyperplasia and lethal hydronephrosis. PloS one *7*, e52272.

Gandhi, D., Molotkov, A., Batourina, E., Schneider, K., Dan, H., Reiley, M., Laufer, E., Metzger, D., Liang, F., Liao, Y.*, et al.* (2013). Retinoid signaling in progenitors controls specification and regeneration of the urothelium. Developmental cell *26*, 469-482.

Garcia-Espana, A., Chung, P.J., Zhao, X., Lee, A., Pellicer, A., Yu, J., Sun, T.T., and Desalle, R. (2006). Origin of the tetraspanin uroplakins and their co-evolution with associated proteins: implications for uroplakin structure and function. Molecular phylogenetics and evolution *41*, 355-367.

Gearing, K.L., Gottlicher, M., Teboul, M., Widmark, E., and Gustafsson, J.A. (1993). Interaction of the peroxisome-proliferator-activated receptor and retinoid X receptor. Proceedings of the National Academy of Sciences of the United States of America *90*, 1440-1444.

Goldstein, J.T., Berger, A.C., Shih, J., Duke, F.F., Furst, L., Kwiatkowski, D.J., Cherniack, A.D., Meyerson, M., and Strathdee, C.A. (2017). Genomic Activation of PPARG Reveals a Candidate Therapeutic Axis in Bladder Cancer. Cancer Res *77*, 6987-6998.

Green, H., and Kehinde, O. (1975). An established preadipose cell line and its differentiation in culture. II. Factors affecting the adipose conversion. Cell *5*, 19-27.

Green, H., and Meuth, M. (1974). An established pre-adipose cell line and its differentiation in culture. Cell *3*, 127-133.

Grygiel-Gorniak, B. (2014). Peroxisome proliferator-activated receptors and their ligands: nutritional and clinical implications--a review. Nutrition journal *13*, 17.

Hauser, S., Adelmant, G., Sarraf, P., Wright, H.M., Mueller, E., and Spiegelman, B.M. (2000). Degradation of the peroxisome proliferator-activated receptor gamma is linked to ligand-dependent activation. The Journal of biological chemistry *275*, 18527-18533.

Helsen, C., and Claessens, F. (2014). Looking at nuclear receptors from a new angle. Molecular and cellular endocrinology *382*, 97-106.

Hicks, R.M. (1975). The mammalian urinary bladder: an accommodating organ. Biological reviews of the Cambridge Philosophical Society *50*, 215-246.

Hu, E., Kim, J.B., Sarraf, P., and Spiegelman, B.M. (1996). Inhibition of adipogenesis through MAP kinase-mediated phosphorylation of PPARgamma. Science *274*, 2100-2103.

Hu, P., Deng, F.M., Liang, F.X., Hu, C.M., Auerbach, A., Shapiro, E., Wu, X.R., Kachar, B., and Sun, T.T. (2001). Ablation of uroplakin III gene results in small urothelial plaques, urothelial leakage, and vesicoureteral reflux. Urology *57*, 117.

Hummasti, S., and Tontonoz, P. (2006). The peroxisome proliferator-activated receptor N-terminal domain controls isotype-selective gene expression and adipogenesis. Molecular endocrinology *20*, 1261-1275.

Iborra, F.J., Jackson, D.A., and Cook, P.R. (2001). Coupled transcription and translation within nuclei of mammalian cells. Science *293*, 1139-1142.

Issemann, I., Prince, R.A., Tugwood, J.D., and Green, S. (1993). The retinoid X receptor enhances the function of the peroxisome proliferator activated receptor. Biochimie *75*, 251-256.

Jackson, A.R., Li, B., Cohen, S.H., Ching, C.B., McHugh, K.M., and Becknell, B. (2018). The uroplakin plaque promotes renal structural integrity during congenital and acquired urinary tract obstruction. American journal of physiology Renal physiology *315*, F1019-F1031.

Jones, J.C. (2001). Hemidesmosomes in bladder epithelial cells. Urology *57*, 103.

Jost, S.P., Gosling, J.A., and Dixon, J.S. (1989). The morphology of normal human bladder urothelium. Journal of anatomy *167*, 103-115.

Kaimal, R., Song, X., Yan, B., King, R., and Deng, R. (2009). Differential modulation of farnesoid X receptor signaling pathway by the thiazolidinediones. J Pharmacol Exp Ther *330*, 125-134.

Khandelwal, P., Abraham, S.N., and Apodaca, G. (2009). Cell biology and physiology of the uroepithelium. American journal of physiology Renal physiology *297*, F1477-1501.

Kilroy, G., Carter, L.E., Newman, S., Burk, D.H., Manuel, J., Moller, A., Bowtell, D.D., Mynatt, R.L., Ghosh, S., and Floyd, Z.E. (2015). The ubiquitin ligase Siah2 regulates obesity-induced adipose tissue inflammation. Obesity *23*, 2223-2232.

Kilroy, G., Kirk-Ballard, H., Carter, L.E., and Floyd, Z.E. (2012). The ubiquitin ligase Siah2 regulates PPARgamma activity in adipocytes. Endocrinology *153*, 1206-1218.

Kilroy, G.E., Zhang, X., and Floyd, Z.E. (2009). PPAR-gamma AF-2 domain functions as a component of a ubiquitin-dependent degradation signal. Obesity *17*, 665-673.

Kim, J.H., Park, K.W., Lee, E.W., Jang, W.S., Seo, J., Shin, S., Hwang, K.A., and Song, J. (2014). Suppression of PPARgamma through MKRN1-mediated ubiquitination and degradation prevents adipocyte differentiation. Cell death and differentiation *21*, 594-603.

Kreft, M.E., Sterle, M., Veranic, P., and Jezernik, K. (2005). Urothelial injuries and the early wound healing response: tight junctions and urothelial cytodifferentiation. Histochemistry and cell biology *123*, 529-539.

Kroker, A.J., and Bruning, J.B. (2015). Review of the Structural and Dynamic Mechanisms of PPARgamma Partial Agonism. PPAR research *2015*, 816856.

Kullmann, F.A., Clayton, D.R., Ruiz, W.G., Wolf-Johnston, A., Gauthier, C., Kanai, A., Birder, L.A., and Apodaca, G. (2017). Urothelial proliferation and regeneration after spinal cord injury. American journal of physiology Renal physiology *313*, F85-F102.

Kurzrock, E.A., Lieu, D.K., Degraffenried, L.A., Chan, C.W., and Isseroff, R.R. (2008). Label-retaining cells of the bladder: candidate urothelial stem cells. American journal of physiology Renal physiology *294*, F1415-1421.

Lamas Bervejillo, M., Bonanata, J., Franchini, G.R., Richeri, A., Marques, J.M., Freeman, B.A., Schopfer, F.J., Coitino, E.L., Corsico, B., Rubbo, H*., et al.* (2020). A FABP4-PPARgamma signaling axis regulates human monocyte responses to electrophilic fatty acid nitroalkenes. Redox Biol *29*, 101376.

Lavelle, J., Meyers, S., Ramage, R., Bastacky, S., Doty, D., Apodaca, G., and Zeidel, M.L. (2002). Bladder permeability barrier: recovery from selective injury of surface epithelial cells. American journal of physiology Renal physiology *283*, F242-253.

Lefterova, M.I., Haakonsson, A.K., Lazar, M.A., and Mandrup, S. (2014). PPARgamma and the global map of adipogenesis and beyond. Trends in endocrinology and metabolism: TEM *25*, 293-302.

Lefterova, M.I., and Lazar, M.A. (2009). New developments in adipogenesis. Trends in endocrinology and metabolism: TEM *20*, 107-114.

Lemberger, T., Desvergne, B., and Wahli, W. (1996). Peroxisome proliferator-activated receptors: a nuclear receptor signaling pathway in

lipid physiology. Annual review of cell and developmental biology *12*, 335-363.

Lewis, S.A., and Diamond, J.M. (1976). Na+ transport by rabbit urinary bladder, a tight epithelium. The Journal of membrane biology *28*, 1-40.

Lewis, S.A., Eaton, D.C., and Diamond, J.M. (1976). The mechanism of Na+ transport by rabbit urinary bladder. The Journal of membrane biology *28*, 41-70.

Li, Y., Fanning, A.S., Anderson, J.M., and Lavie, A. (2005). Structure of the conserved cytoplasmic C-terminal domain of occludin: identification of the ZO-1 binding surface. Journal of molecular biology *352*, 151-164.

Limas, C. (1993). Proliferative state of the urothelium with benign and atypical changes. Correlation with transferrin and epidermal growth factor receptors and blood group antigens. The Journal of pathology *171*, 39-47.

Liu, C., Tate, T., Batourina, E., Truschel, S.T., Potter, S., Adam, M., Xiang, T., Picard, M., Reiley, M., Schneider, K.*, et al.* (2019). Pparg promotes differentiation and regulates mitochondrial gene expression in bladder epithelial cells. Nature communications *10*, 4589.

Michikawa, H., Fujita-Yoshigaki, J., and Sugiya, H. (2008). Enhancement of barrier function by overexpression of claudin-4 in tight junctions of submandibular gland cells. Cell and tissue research *334*, 255-264.

Mota de Sa, P., Richard, A.J., Hang, H., and Stephens, J.M. (2017). Transcriptional Regulation of Adipogenesis. Comprehensive Physiology *7*, 635-674.

Nakanishi, K., Ogata, S., Hiroi, S., Tominaga, S., Aida, S., and Kawai, T. (2008). Expression of occludin and claudins 1, 3, 4, and 7 in urothelial carcinoma of the upper urinary tract. American journal of clinical pathology *130*, 43-49.

Negrete, H.O., Lavelle, J.P., Berg, J., Lewis, S.A., and Zeidel, M.L. (1996). Permeability properties of the intact mammalian bladder epithelium. The American journal of physiology *271*, F886-894.

Nemeth, A., Mozes, M.M., Calvier, L., Hansmann, G., and Kokeny, G. (2019). The PPARgamma agonist pioglitazone prevents TGF-beta induced renal fibrosis by repressing EGR-1 and STAT3. BMC nephrology *20*, 245.

Noruddin, N.A.A., Hamzah, M.F., Rosman, Z., Salin, N.H., Shu-Chien, A.C., and Muhammad, T.S.T. (2021). Natural Compound 3beta,7beta,25-trihydroxycucurbita-5,23(E)-dien-19-al from Momordica charantia Acts as PPARgamma Ligand. Molecules *26*.

Nuclear Receptors Nomenclature, C. (1999). A unified nomenclature system for the nuclear receptor superfamily. Cell *97*, 161-163.

Oettgen, P., Alani, R.M., Barcinski, M.A., Brown, L., Akbarali, Y., Boltax, J., Kunsch, C., Munger, K., and Libermann, T.A. (1997). Isolation and characterization of a novel epithelium-specific transcription factor, ESE-1,

a member of the ets family. Molecular and cellular biology *17*, 4419-4433.

Omi, T., Brenig, B., Spilar Kramer, S., Iwamoto, S., Stranzinger, G., and Neuenschwander, S. (2005). Identification and characterization of novel peroxisome proliferator-activated receptor-gamma (PPAR-gamma) transcriptional variants in pig and human. Journal of animal breeding and genetics = Zeitschrift fur Tierzuchtung und Zuchtungsbiologie *122 Suppl 1*, 45-53.

Oottamasathien, S., Wang, Y., Williams, K., Franco, O.E., Wills, M.L., Thomas, J.C., Saba, K., Sharif-Afshar, A.R., Makari, J.H., Bhowmick, N.A.*, et al.* (2007). Directed differentiation of embryonic stem cells into bladder tissue. Developmental biology *304*, 556-566.

Pinton, P., Braicu, C., Nougayrede, J.P., Laffitte, J., Taranu, I., and Oswald, I.P. (2010). Deoxynivalenol impairs porcine intestinal barrier function and decreases the protein expression of claudin-4 through a mitogen-activated protein kinase-dependent mechanism. The Journal of nutrition *140*, 1956-1962.

Porter, K.R., Kenyon, K., and Badenhausen, S. (1967). Specializations of the unit membrane. Protoplasma *63*, 262-274.

Powell, D.W. (1981). Barrier function of epithelia. The American journal of physiology *241*, G275-288.

Pust, R., Butz, M., Rost, A., Ogbuihi, S., and Riedel, B. (1976). Denudation of the urinary bladder mucosa in the cat by formaldehyde. Urological research *4*, 55-61.

Reddy, O.L., Cates, J.M., Gellert, L.L., Crist, H.S., Yang, Z., Yamashita, H., Taylor, J.A., 3rd, Smith, J.A., Jr., Chang, S.S., Cookson, M.S.*, et al.* (2015). Loss of FOXA1 Drives Sexually Dimorphic Changes in Urothelial Differentiation and Is an Independent Predictor of Poor Prognosis in Bladder Cancer. The American journal of pathology *185*, 1385-1395.

Ren, D., Collingwood, T.N., Rebar, E.J., Wolffe, A.P., and Camp, H.S. (2002). PPARgamma knockdown by engineered transcription factors: exogenous PPARgamma2 but not PPARgamma1 reactivates adipogenesis. Genes & development *16*, 27-32.

Robino, L., Scavone, P., Araujo, L., Algorta, G., Zunino, P., Pirez, M.C., and Vignoli, R. (2014). Intracellular bacteria in the pathogenesis of Escherichia coli urinary tract infection in children. Clinical infectious diseases : an official publication of the Infectious Diseases Society of America *59*, e158-164.

Rochel, N., Krucker, C., Coutos-Thevenot, L., Osz, J., Zhang, R., Guyon, E., Zita, W., Vanthong, S., Hernandez, O.A., Bourguet, M.*, et al.* (2019). Recurrent activating mutations of PPARgamma associated with luminal bladder tumors. Nat Commun *10*, 253.

Rotterud, R., Nesland, J.M., Berner, A., and Fossa, S.D. (2005). Expression of the epidermal growth factor receptor family in normal and malignant urothelium. BJU international *95*, 1344-1350.

Rudat, C., Grieskamp, T., Rohr, C., Airik, R., Wrede, C., Hegermann, J., Herrmann, B.G., Schuster-Gossler, K., and Kispert, A. (2014). Upk3b is dispensable for development and integrity of urothelium and mesothelium. PloS one *9*, e112112.

Saladin, R., Fajas, L., Dana, S., Halvorsen, Y.D., Auwerx, J., and Briggs, M. (1999). Differential regulation of peroxisome proliferator activated receptor gamma1 (PPARgamma1) and PPARgamma2 messenger RNA expression in the early stages of adipogenesis. Cell growth & differentiation : the molecular biology journal of the American Association for Cancer Research *10*, 43-48.

Seedorf, U., and Aberle, J. (2007). Emerging roles of PPARdelta in metabolism. Biochimica et biophysica acta *1771*, 1125-1131.

Shabir, S., and Southgate, J. (2008). Calcium signalling in wound-responsive normal human urothelial cell monolayers. Cell calcium *44*, 453-464.

Shao, D., Rangwala, S.M., Bailey, S.T., Krakow, S.L., Reginato, M.J., and Lazar, M.A. (1998). Interdomain communication regulating ligand binding by PPAR-gamma. Nature *396*, 377-380.

Shi, J., Zhang, W., You, M., Xu, Y., Hou, Y., and Jin, J. (2016). Pioglitazone inhibits EGFR/MDM2 signaling-mediated PPARgamma degradation. European journal of pharmacology *791*, 316-321.

Shinohara, S., and Fujimori, K. (2020). Promotion of lipogenesis by PPARgamma-activated FXR expression in adipocytes. Biochem Biophys Res Commun *527*, 49-55.

Siegel, R.L., Miller, K.D., and Jemal, A. (2016). Cancer statistics, 2016. CA: a cancer journal for clinicians *66*, 7-30.

Siersbaek, R., Nielsen, R., and Mandrup, S. (2010). PPARgamma in adipocyte differentiation and metabolism--novel insights from genome-wide studies. FEBS letters *584*, 3242-3249.

Siersbaek, R., Nielsen, R., and Mandrup, S. (2012). Transcriptional networks and chromatin remodeling controlling adipogenesis. Trends in endocrinology and metabolism: TEM *23*, 56-64.

Smith, N.J., Hinley, J., Varley, C.L., Eardley, I., Trejdosiewicz, L.K., and Southgate, J. (2015). The human urothelial tight junction: claudin 3 and the ZO-1alpha(+) switch. Bladder *2*, e9.

Southgate, J., Hutton, K.A., Thomas, D.F., and Trejdosiewicz, L.K. (1994). Normal human urothelial cells *in vitro*: proliferation and induction of stratification. Laboratory investigation; a journal of technical methods and pathology *71*, 583-594.

Staack, A., Hayward, S.W., Baskin, L.S., and Cunha, G.R. (2005). Molecular, cellular and developmental biology of urothelium as a basis of bladder regeneration. Differentiation; research in biological diversity *73*, 121-133.

Steger, D.J., Grant, G.R., Schupp, M., Tomaru, T., Lefterova, M.I., Schug, J., Manduchi, E., Stoeckert, C.J., Jr., and Lazar, M.A. (2010). Propagation of adipogenic signals through an epigenomic transition state. Genes & development *24*, 1035-1044.

Strand, D.W., Jiang, M., Murphy, T.A., Yi, Y., Konvinse, K.C., Franco, O.E., Wang, Y., Young, J.D., and Hayward, S.W. (2012). PPARgamma isoforms differentially regulate metabolic networks to mediate mouse prostatic epithelial differentiation. Cell death & disease *3*, e361.

Sugasi, S., Lesbros, Y., Bisson, I., Zhang, Y.Y., Kucera, P., and Frey, P. (2000). *In vitro* engineering of human stratified urothelium: analysis of its morphology and function. The Journal of urology *164*, 951-957.

Sun, K., Wang, Q., and Huang, X.H. (2006). PPAR gamma inhibits growth of rat hepatic stellate cells and TGF beta-induced connective tissue growth factor expression. Acta pharmacologica Sinica *27*, 715-723.

Takada, I., and Makishima, M. (2020). Peroxisome proliferator-activated receptor agonists and antagonists: a patent review (2014-present). Expert Opin Ther Pat *30*, 1-13.

Takenaka, Y., Inoue, I., Nakano, T., Shinoda, Y., Ikeda, M., Awata, T., and Katayama, S. (2013). A Novel Splicing Variant of Peroxisome Proliferator-Activated Receptor-gamma (Ppargamma1sv) Cooperatively Regulates Adipocyte Differentiation with Ppargamma2. PloS one *8*, e65583.

Tan, X., Dagher, H., Hutton, C.A., and Bourke, J.E. (2010). Effects of PPAR gamma ligands on TGF-beta1-induced epithelial-mesenchymal transition in alveolar epithelial cells. Respiratory research *11*, 21.

Tontonoz, P., Graves, R.A., Budavari, A.I., Erdjument-Bromage, H., Lui, M., Hu, E., Tempst, P., and Spiegelman, B.M. (1994a). Adipocyte-specific transcription factor ARF6 is a heterodimeric complex of two nuclear hormone receptors, PPAR gamma and RXR alpha. Nucleic acids research *22*, 5628-5634.

Tontonoz, P., Hu, E., Graves, R.A., Budavari, A.I., and Spiegelman, B.M. (1994b). mPPAR gamma 2: tissue-specific regulator of an adipocyte enhancer. Genes & development *8*, 1224-1234.

Tontonoz, P., Hu, E., and Spiegelman, B.M. (1994c). Stimulation of adipogenesis in fibroblasts by PPAR gamma 2, a lipid-activated transcription factor. Cell *79*, 1147-1156.

Van Itallie, C.M., and Anderson, J.M. (2014). Architecture of tight junctions and principles of molecular composition. Seminars in cell & developmental biology *36*, 157-165.

Varley, C., Hill, G., Pellegrin, S., Shaw, N.J., Selby, P.J., Trejdosiewicz, L.K., and Southgate, J. (2005). Autocrine regulation of human urothelial cell proliferation and migration during regenerative responses *in vitro*. Experimental cell research *306*, 216-229.

Varley, C.L., Bacon, E.J., Holder, J.C., and Southgate, J. (2009). FOXA1 and IRF-1 intermediary transcriptional regulators of PPARgamma-induced urothelial cytodifferentiation. Cell death and differentiation *16*, 103-114.

Varley, C.L., Garthwaite, M.A., Cross, W., Hinley, J., Trejdosiewicz, L.K., and Southgate, J. (2006). PPARgamma-regulated tight junction development during human urothelial cytodifferentiation. Journal of cellular physiology *208*, 407-417.

Varley, C.L., Stahlschmidt, J., Lee, W.C., Holder, J., Diggle, C., Selby, P.J., Trejdosiewicz, L.K., and Southgate, J. (2004). Role of PPARgamma and EGFR signalling in the urothelial terminal differentiation programme. J Cell Sci *117*, 2029-2036.

Waite, K.J., Floyd, Z.E., Arbour-Reily, P., and Stephens, J.M. (2001). Interferon-gamma-induced regulation of peroxisome proliferator-activated receptor gamma and STATs in adipocytes. The Journal of biological chemistry *276*, 7062-7068.

Walker, B.E. (1960). Renewal of cell populations in the female mouse. The American journal of anatomy *107*, 95-105.

Wang, F., Mullican, S.E., DiSpirito, J.R., Peed, L.C., and Lazar, M.A. (2013). Lipoatrophy and severe metabolic disturbance in mice with fat-specific deletion of PPARgamma. Proceedings of the National Academy of Sciences of the United States of America *110*, 18656-18661.

Wang, J., Batourina, E., Schneider, K., Souza, S., Swayne, T., Liu, C., George, C.D., Tate, T., Dan, H., Wiessner, G*., et al.* (2018). Polyploid Superficial Cells that Maintain the Urothelial Barrier Are Produced via Incomplete Cytokinesis and Endoreplication. Cell reports *25*, 464-477 e464.

Wezel, F., Pearson, J., and Southgate, J. (2014). Plasticity of *in vitro*-generated urothelial cells for functional tissue formation. Tissue engineering Part A *20*, 1358-1368.

Wu, X.R., Kong, X.P., Pellicer, A., Kreibich, G., and Sun, T.T. (2009). Uroplakins in urothelial biology, function, and disease. Kidney international *75*, 1153-1165.

Wu, X.R., Lin, J.H., Walz, T., Haner, M., Yu, J., Aebi, U., and Sun, T.T. (1994). Mammalian uroplakins. A group of highly conserved urothelial differentiation-related membrane proteins. The Journal of biological chemistry *269*, 13716-13724.

Wu, X.R., and Sun, T.T. (1993). Molecular cloning of a 47 kDa tissue-specific and differentiation-dependent urothelial cell surface glycoprotein. Journal of cell science *106 (Pt 1)*, 31-43.

Xu, J., Kausalya, P.J., Phua, D.C., Ali, S.M., Hossain, Z., and Hunziker, W. (2008). Early embryonic lethality of mice lacking ZO-2, but Not ZO-3, reveals critical and nonredundant roles for individual zonula occludens proteins in mammalian development. Molecular and cellular biology *28*, 1669-1678.

Xu, Y., Jin, J., Zhang, W., Zhang, Z., Gao, J., Liu, Q., Zhou, C., Xu, Q., Shi, H., Hou, Y.*, et al.* (2016). EGFR/MDM2 signaling promotes NF-kappaB activation via PPARgamma degradation. Carcinogenesis *37*, 215-222.

Xue, P., Hou, Y., Zuo, Z., Wang, Z., Ren, S., Dong, J., Fu, J., Wang, H., Andersen, M.E., Zhang, Q.*, et al.* (2020). Long isoforms of NRF1 negatively regulate adipogenesis via suppression of PPARgamma expression. Redox biology *30*, 101414.

Yamashita, D., Yamaguchi, T., Shimizu, M., Nakata, N., Hirose, F., and Osumi, T. (2004). The transactivating function of peroxisome proliferator-activated receptor gamma is negatively regulated by SUMO conjugation in the amino-terminal domain. Genes to cells : devoted to molecular & cellular mechanisms *9*, 1017-1029.

Yang, D.R., Lin, S.J., Ding, X.F., Miyamoto, H., Messing, E., Li, L.Q., Wang, N., and Chang, C. (2013). Higher expression of peroxisome proliferator-activated receptor gamma or its activation by agonist thiazolidinedione-rosiglitazone promotes bladder cancer cell migration and invasion. Urology *81*, 1109 e1101-1106.

Yu, J., Lin, J.H., Wu, X.R., and Sun, T.T. (1994). Uroplakins Ia and Ib, two major differentiation products of bladder epithelium, belong to a family of four transmembrane domain (4TM) proteins. The Journal of cell biology *125*, 171-182.

Yu, S., and Reddy, J.K. (2007). Transcription coactivators for peroxisome proliferator-activated receptors. Biochimica et biophysica acta *1771*, 936-951.

Zhang, Y., Dallner, O.S., Nakadai, T., Fayzikhodjaeva, G., Lu, Y.H., Lazar, M.A., Roeder, R.G., and Friedman, J.M. (2018). A noncanonical PPARgamma/RXRalpha-binding sequence regulates leptin expression in response to changes in adipose tissue mass. Proceedings of the National Academy of Sciences of the United States of America *115*, E6039-E6047.

Zhang, Y., Zheng, Y., Wang, X., Qiu, J., Liang, C., Cheng, G., Wang, H., Zhao, C., Yang, W., Zan, L*., et al.* (2020). Bovine Stearoyl-CoA Desaturase 1 Promotes Adipogenesis by Activating the PPARgamma Receptor. Journal of agricultural and food chemistry *68*, 12058-12066.